



Searching for new physics in $2\nu\beta\beta$ with scintillating cryogenic calorimeters

Ph.D. thesis defence XXXV cycle — 16/05/2024

Candidate: Emanuela Celi

Advisors: Prof. Fernando Ferroni
Prof. Lorenzo Pagnanini

Outline

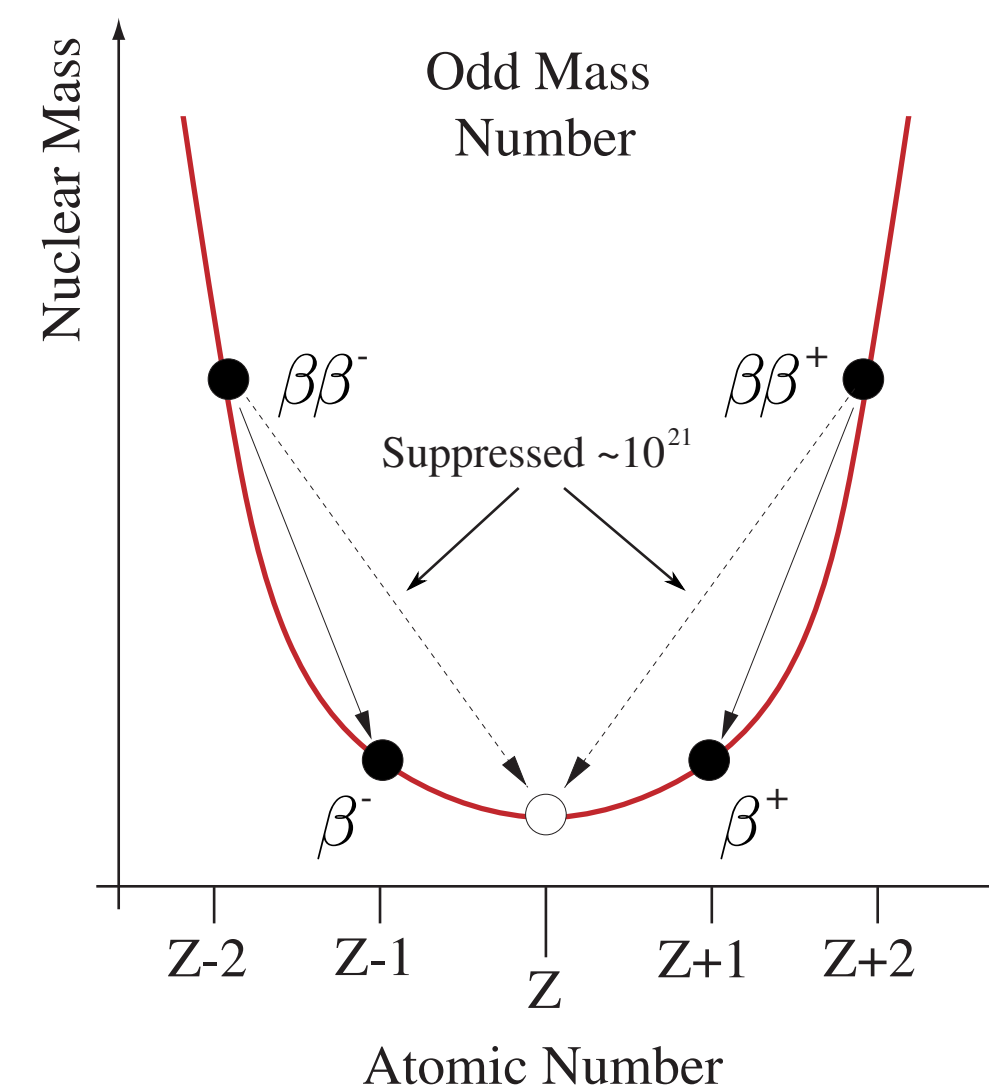
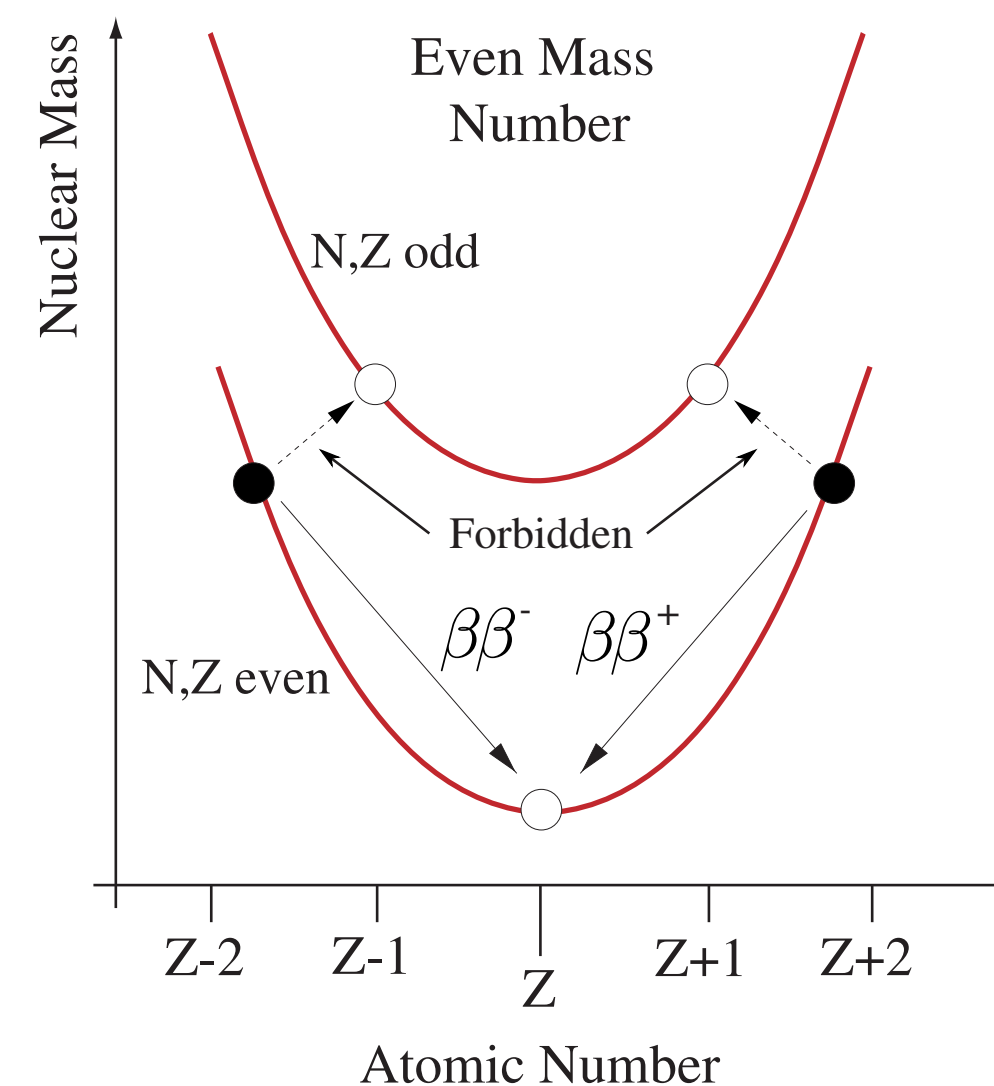
- 1 Double- β decays
- 2 Scintillating cryogenic calorimeters
- 3 CUPID-0 combined background model
- 4 CUPID-Mo BSM studies
- 5 CUPID sensitivity
- 6 Conclusion and outlook

Double- β decays

In nature, only a subset of even-even nuclei could decay through double- β decay.

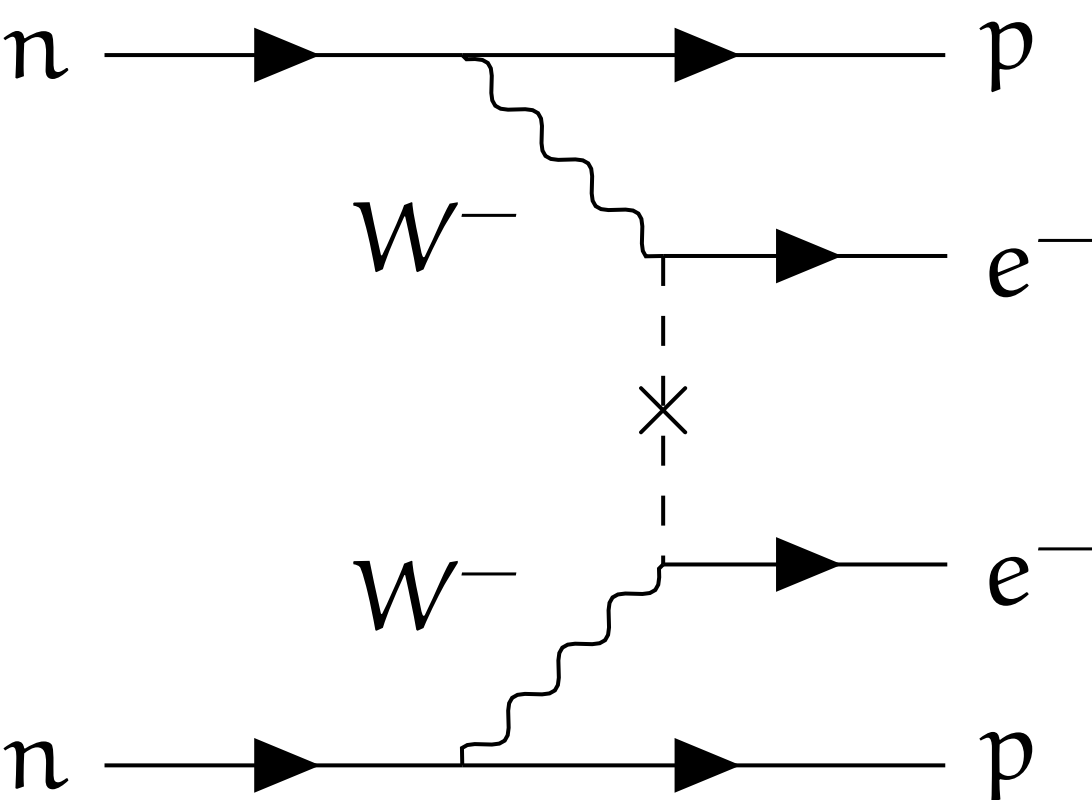
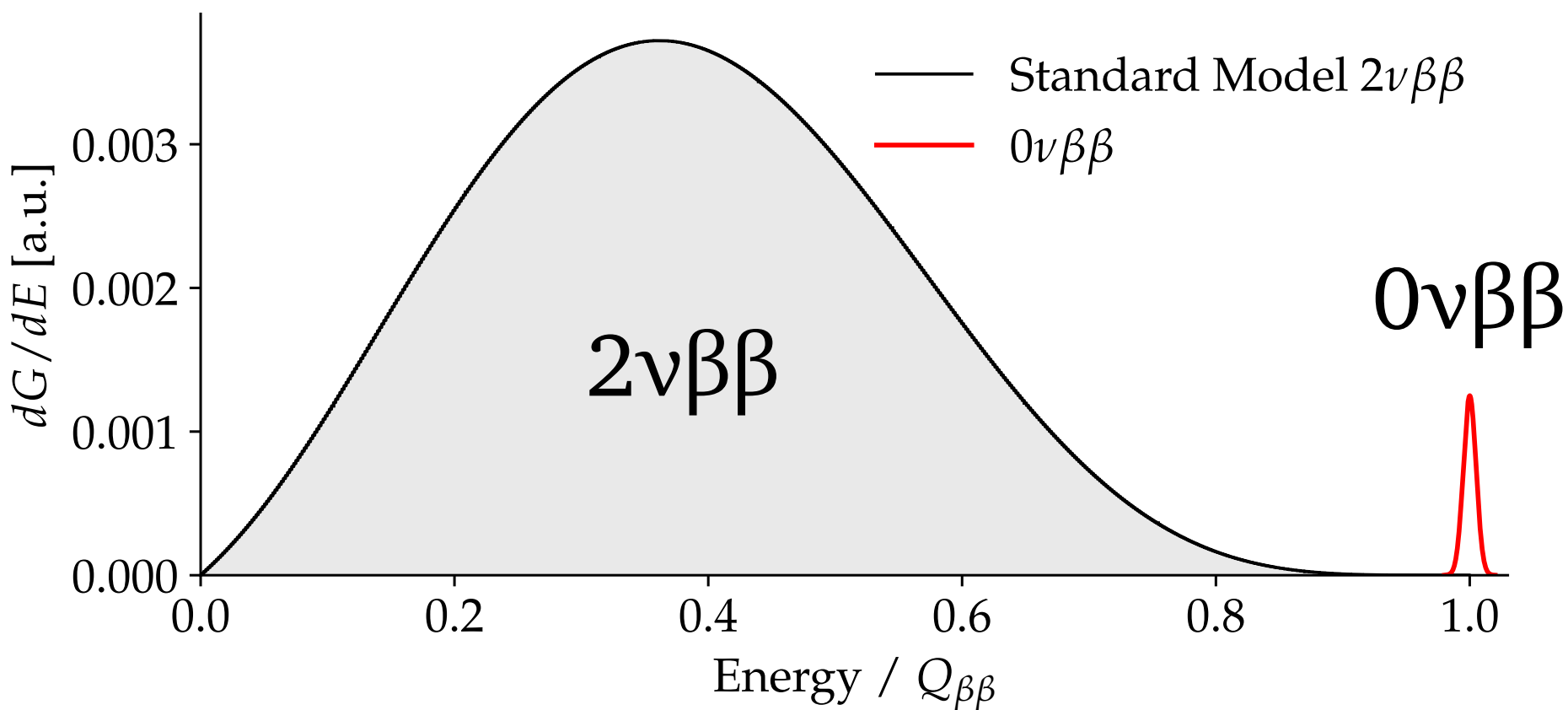
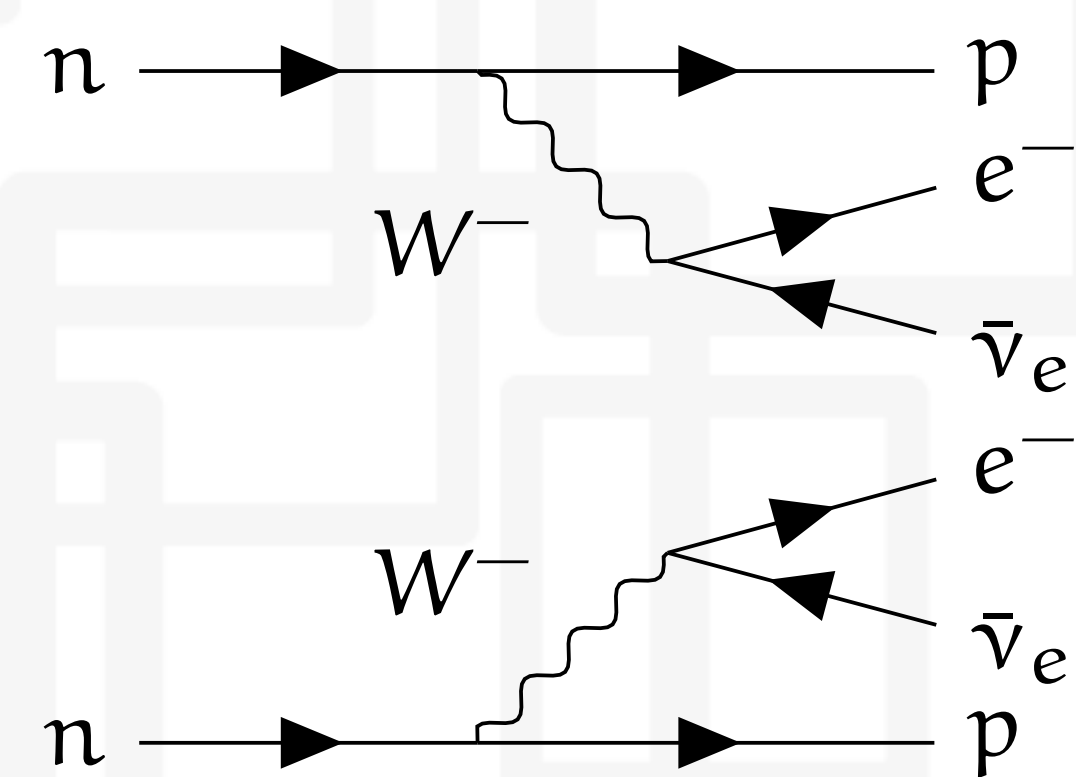
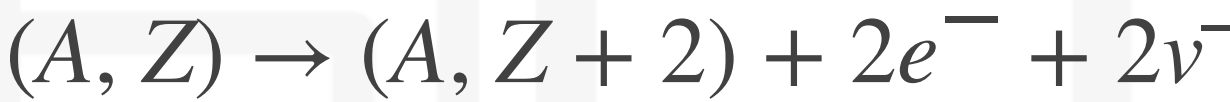
This can happen when the attractive nuclear pairing interaction adds binding energy to nuclei with even numbers of protons and neutrons.

Isotope	Isotopic abundance (%)	Enrichment (%)
^{48}Ca	0.187	16
^{76}Ge	7.8	92
^{82}Se	8.7	96
^{96}Zr	2.8	86
^{100}Mo	9.8	99
^{116}Cd	7.5	82
^{130}Te	34.08	92
^{136}Xe	8.9	90
^{150}Nd	5.6	91



Double- β decays

$$Q_{\beta\beta} = m_f - m_i$$



Half-life from 10^{18} — 10^{21} yr

Isotope	$Q_{\beta\beta}$ [MeV]	$T_{1/2}^{2\nu}$ [yr]
^{48}Ca	4.263	$6.4_{-0.6}^{+0.7} \text{ (stat.) }_{-0.9}^{+1.2} \text{ (syst.)} \times 10^{19}$
^{76}Ge	2.039	$2.022 \pm 0.018 \text{ (stat.)} \pm 0.038 \text{ (syst.)} \times 10^{21}$
^{82}Se	2.998	$8.69 \pm 0.05 \text{ (stat.) }_{-0.06}^{+0.09} \text{ (syst.)} \times 10^{19}$
^{96}Zr	3.348	$2.35 \pm 0.14 \text{ (stat.)} \pm 0.16 \text{ (syst.)} \times 10^{19}$
^{100}Mo	3.035	$7.07 \pm 0.02 \text{ (stat.)} \pm 0.11 \text{ (syst.)} \times 10^{18}$
^{116}Cd	2.813	$2.63 \pm 0.01 \text{ (stat.) }_{-0.13}^{+0.11} \text{ (syst.)} \times 10^{19}$
^{130}Te	2.527	$8.76_{-0.07}^{+0.09} \text{ (stat.) }_{-0.17}^{+0.14} \text{ (syst.)} \times 10^{20}$
^{136}Xe	2.459	$2.165 \pm 0.016 \text{ (stat.)} \pm 0.059 \text{ (syst.)} \times 10^{21}$
^{150}Nd	3.371	$9.34 \pm 0.22 \text{ (stat.) }_{-0.60}^{+0.62} \text{ (syst.)} \times 10^{18}$

- ❖ Lepton number violating process not conserving the B-L symmetry of the SM
- ❖ Only practical way to probe that neutrinos are Majorana particles, validating the so called “see-saw” mechanism

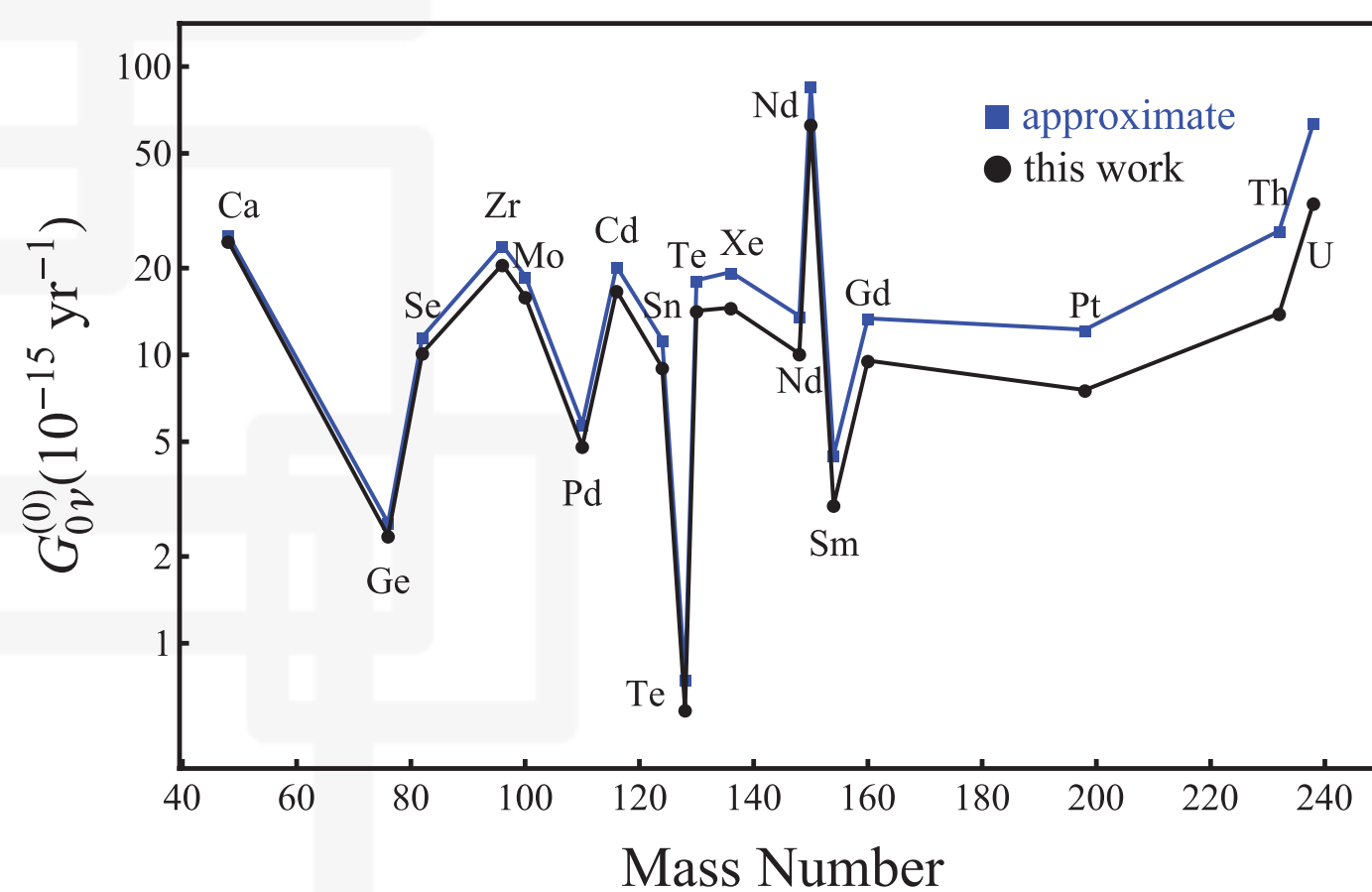
Isotope	$T_{1/2}^{0\nu}$ [y]
^{76}Ge	$> 1.8 \times 10^{26}$
^{82}Se	$> 4.6 \times 10^{24}$
^{100}Mo	$> 1.8 \times 10^{24}$
^{116}Cd	$> 2.2 \times 10^{23}$
^{130}Te	$> 2.2 \times 10^{25}$
^{136}Xe	$> 2.3 \times 10^{26}$

$0\nu\beta\beta$ inverse half-life

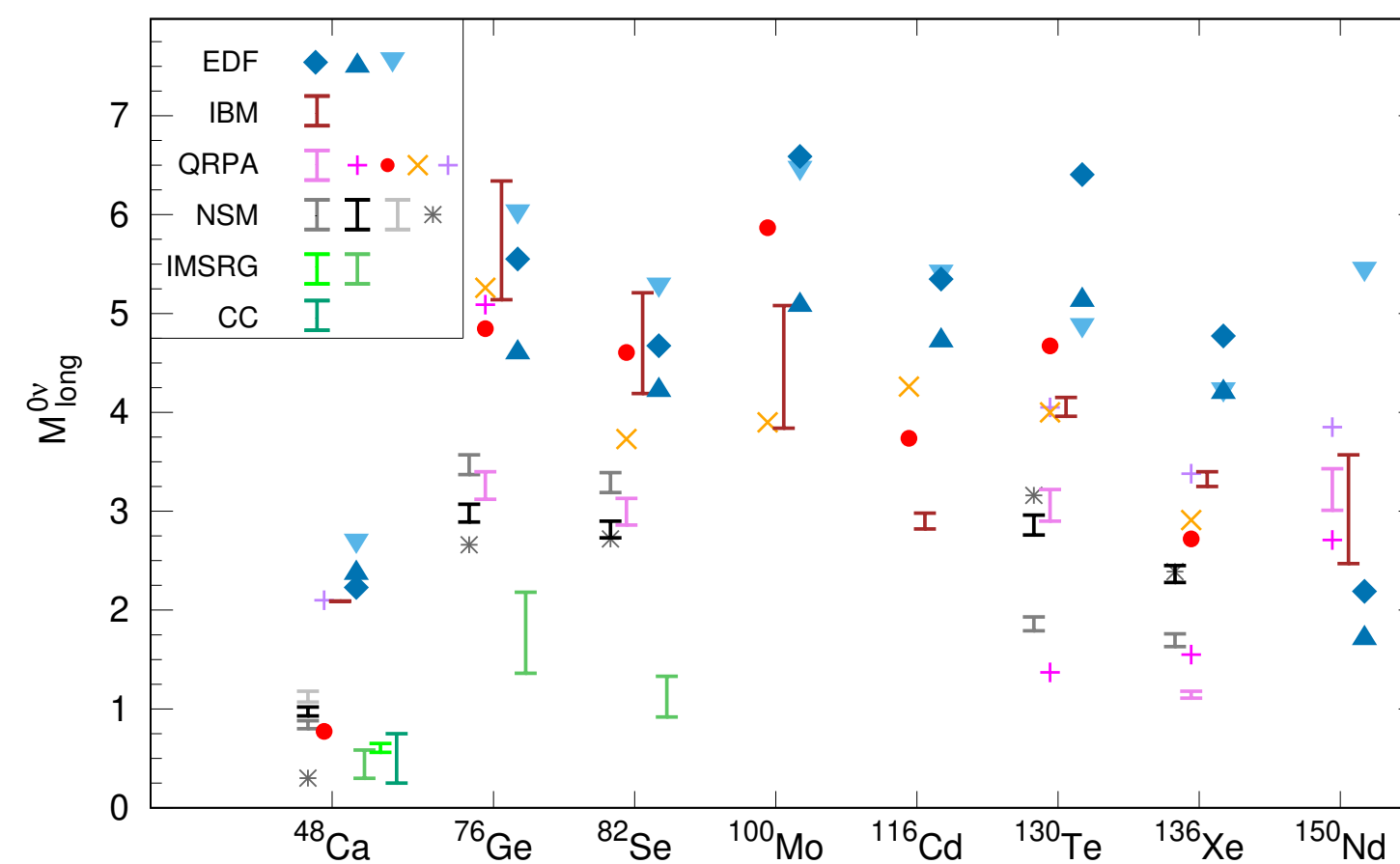
$$[T_{1/2}^{0\nu}]^{-1} = G_{0\nu} |M_{0\nu}|^2 \left(\frac{m_{\beta\beta}}{m_e} \right)^2$$

Phase Space Factor

$$G_{0\nu} \propto Q_{\beta\beta}^5$$



Nuclear Matrix Element
depends on nuclear models.
Still a source of uncertainty



Effective Majorana Mass,
the parameter of interest

$$m_{\beta\beta} = \left| \sum_{j=1}^3 U_{ej}^2 m_j \right| = \left| U_{e1}^2 m_1 + U_{e2}^2 e^{i\beta_1} m_2 + U_{e3}^2 e^{i\beta_2} m_3 \right|$$

Isotope	$T_{1/2}^{0\nu}$ [y]	$m_{\beta\beta}$ [eV]
^{76}Ge	$> 1.8 \times 10^{26}$	$< (0.079 - 0.180)$
^{82}Se	$> 4.6 \times 10^{24}$	$< (0.263 - 0.545)$
^{100}Mo	$> 1.8 \times 10^{24}$	$< (0.280 - 0.490)$
^{116}Cd	$> 2.2 \times 10^{23}$	$< (1.0 - 1.7)$
^{130}Te	$> 2.2 \times 10^{25}$	$< (0.090 - 0.305)$
^{136}Xe	$> 2.3 \times 10^{26}$	$< (0.036 - 0.156)$



What about $2\nu\beta\beta$?
Can we use it to search for new physics?

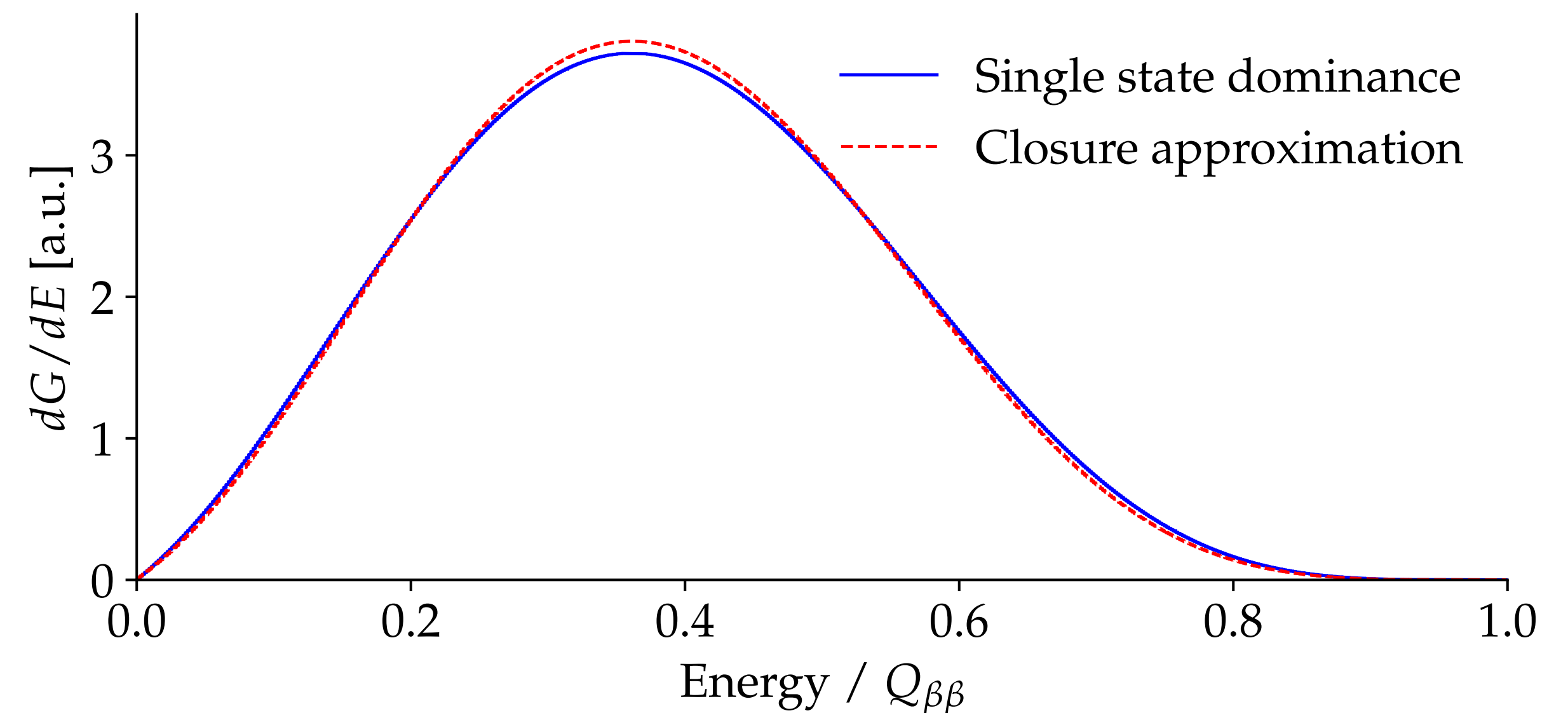
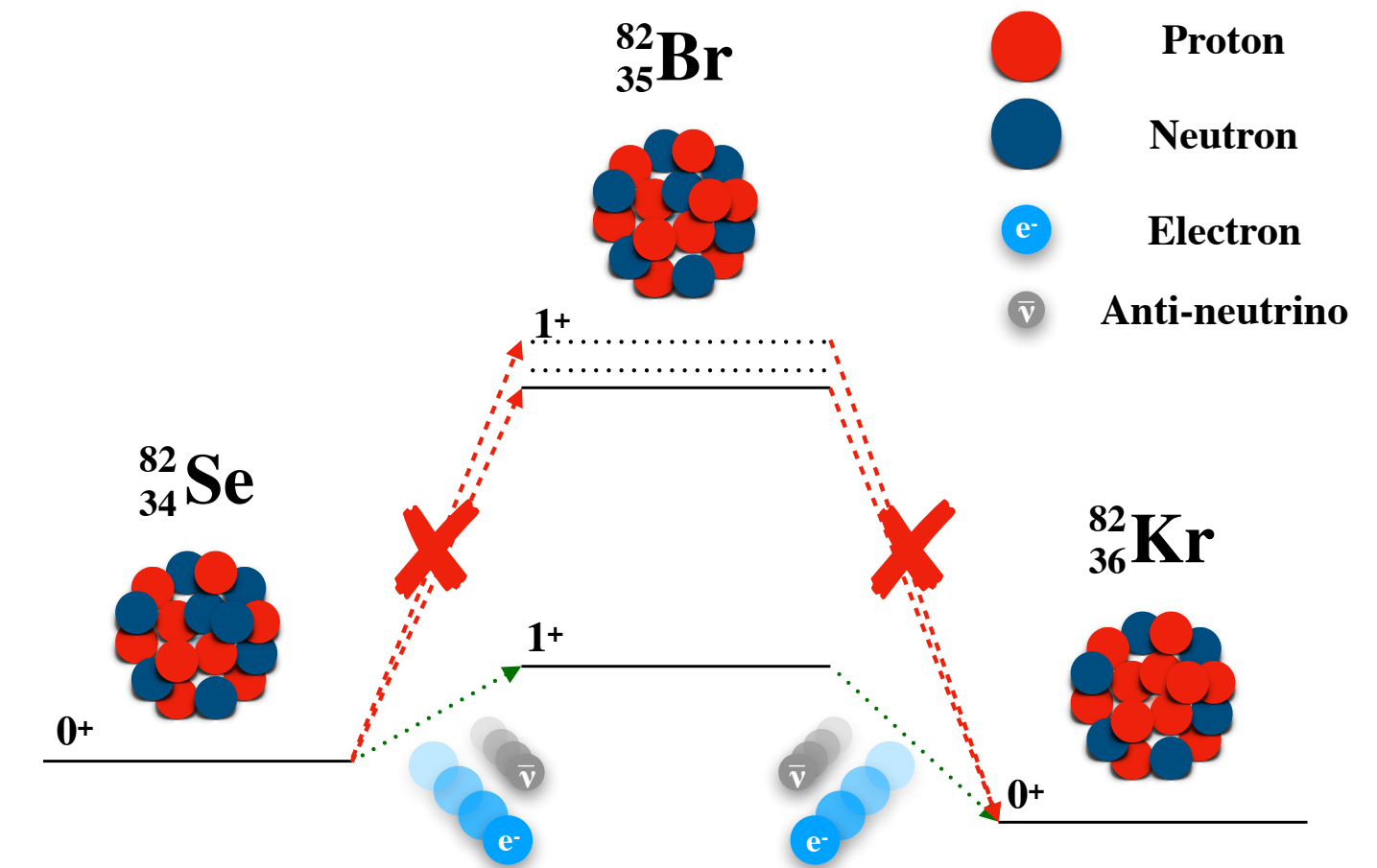
$2\nu\beta\beta$ spectrum: HSD vs. SSD

$$\frac{\Gamma_{2\nu}}{\ln 2} = [T_{1/2}^{2\nu}]^{-1} = G_{2\nu} |M_{2\nu}|^2$$

- ❖ $G_{2\nu}$ is the Phase Space Factor (PSF)
- ❖ $M_{2\nu}$ is the Nuclear Matrix Element (NME)

Assumptions on the energy of the intermediate nuclear state:

- ❖ Single-state dominance (SSD) \rightarrow ^{100}Mo and ^{82}Se
- ❖ Higher-state dominance (HSD) or Closure approximation (CA)



$2\nu\beta\beta$ improved description

Instead of approximating SSD or HSD, the $2\nu\beta\beta$ PSF is written as a sum of components representing a Taylor expansion in terms of the lepton energies:

$$\Gamma_{2\nu} = \left| M_1^{2\nu} \right|^2 \left\{ G_0^{2\nu} + \xi_{31}^{2\nu} G_2^{2\nu} + \frac{1}{3} \left(\xi_{31}^{2\nu} \right)^2 G_{22}^{2\nu} + \left[\frac{1}{3} \left(\xi_{31}^{2\nu} \right)^2 + \xi_{51}^{2\nu} \right] G_4^{2\nu} \right\}$$

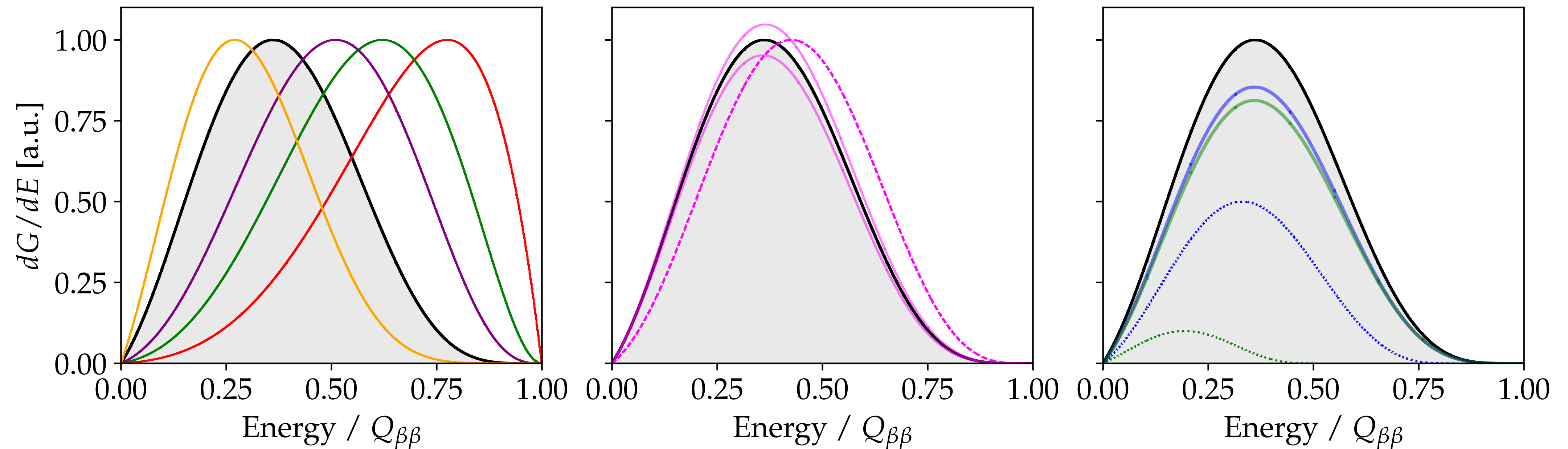
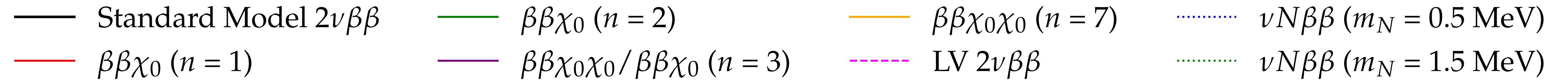
$\xi_{31}^{2\nu}$ and $\xi_{51}^{2\nu}$ determine the shape of the spectrum

When $\xi_{31}^{2\nu}, \xi_{51}^{2\nu} = 0 \rightarrow$ HSD

Or $\xi_{31}^{2\nu}, \xi_{51}^{2\nu} \neq 0 \rightarrow$ SSD (the values depend on the nucleus)

Instead of making assumptions, the values of $\xi_{31}^{2\nu}, \xi_{51}^{2\nu}$ can be measured

Exotic double- β decays



Majoron emitting modes

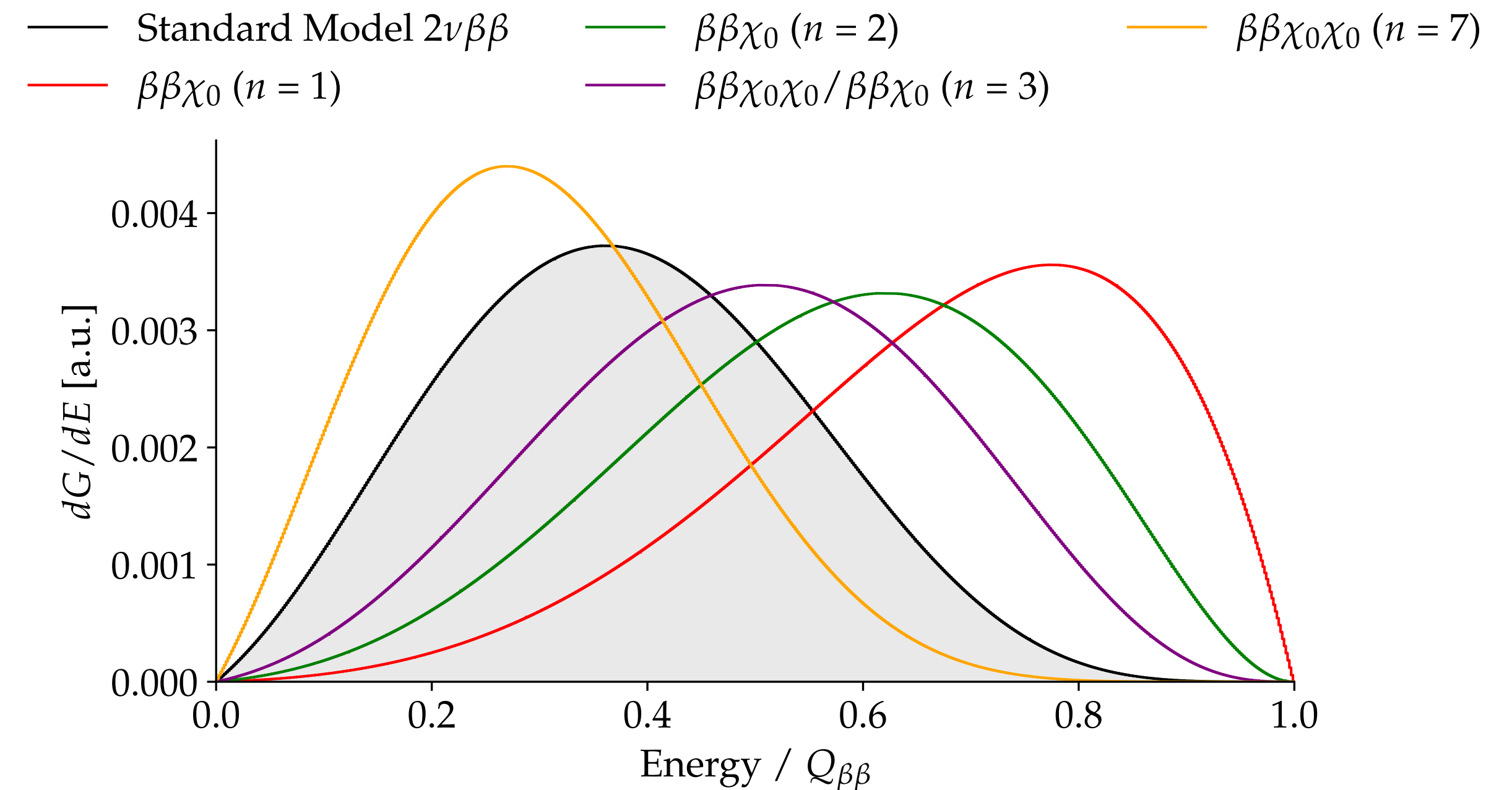
Majorons are massless bosons resulting from the spontaneous B–L symmetry breaking in the low-energy regime.

One ($\beta\beta\chi_0$) or two ($\beta\beta\chi_0\chi_0$) Majorons can be emitted according to the different models

The parameter of interest is the neutrino-Majoron coupling:

$$[T_{0\nu M}^{1/2}]^{-1} = G_{0\nu M} \left| \langle g_{ee}^M \rangle \right|^{2m} \left| M_{0\nu M} \right|^2$$

$$\frac{d\Gamma}{dT} \propto (Q_{\beta\beta} - T)^n$$



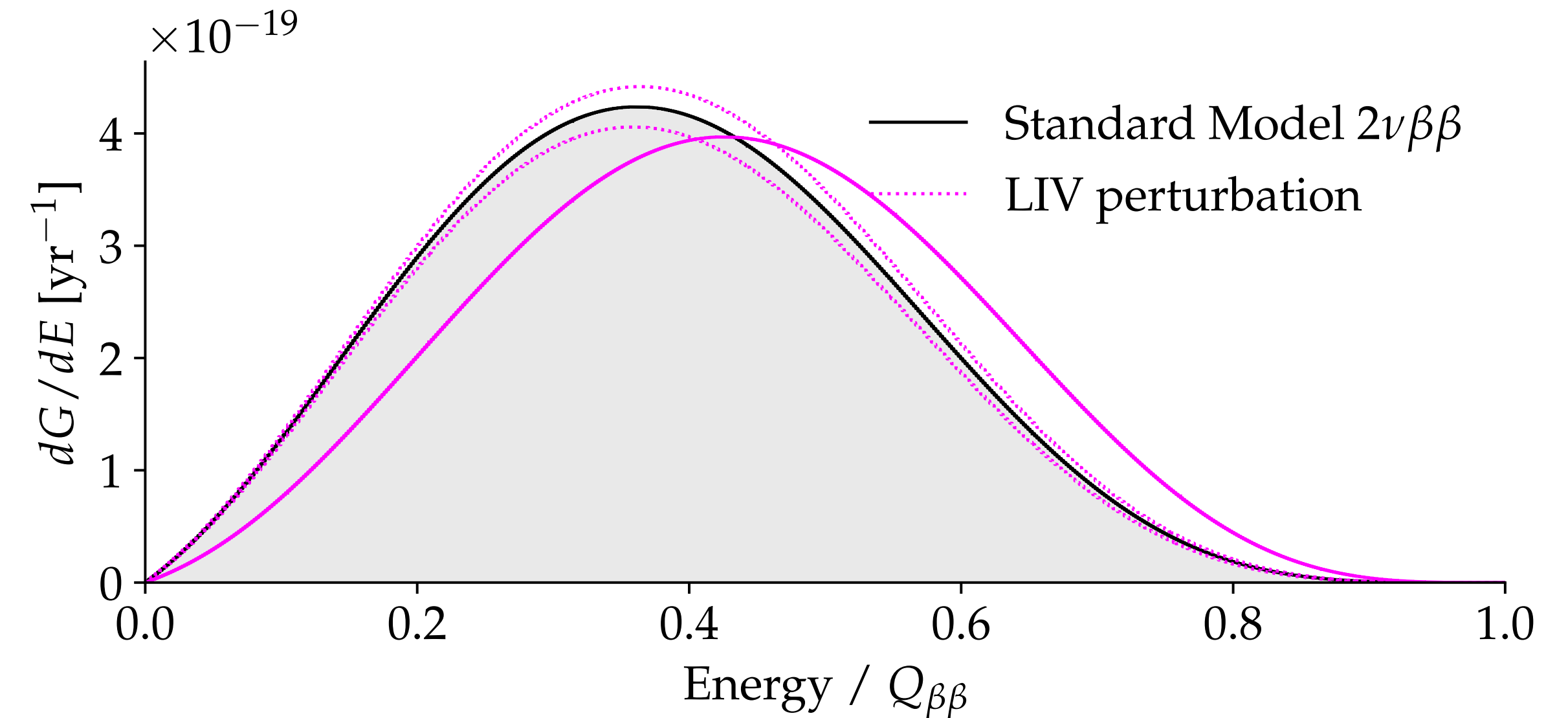
Lorentz violating $2\nu\beta\beta$

The Standard Model Extension predicts the existence of Lorentz Violating (LV) fields.

In the neutrino sector it can modify the decay rate of $2\nu\beta\beta$

$$\Gamma = \Gamma_{SM} + 10 \cdot \dot{a}_{of}^{(3)} \cdot \Gamma_{LV}$$

$\dot{a}_{of}^{(3)}$ is the *countershaded operator* and determines the strength of the Lorentz violating effect.



Isotope	Limit on $\dot{a}_{of}^{(3)}$ [GeV]
^{76}Ge	$(-2.7 < \dot{a}_{of}^{(3)} < 6.2) \cdot 10^{-6}$
^{82}Se	$\dot{a}_{of}^{(3)} < 4.1 \cdot 10^{-6}$
^{136}Xe	$-2.65 \cdot 10^{-5} < \dot{a}_{of}^{(3)} < 7.6 \cdot 10^{-6}$
^{116}Cd	$\dot{a}_{of}^{(3)} < 4.0 \cdot 10^{-6}$
^{100}Mo	$(-4.2 < \dot{a}_{of}^{(3)} < 3.5) \cdot 10^{-7}$
^3H	$ \dot{a}_{of}^{(3)} < 3.0 \cdot 10^{-8}$

Sterile neutrino emission

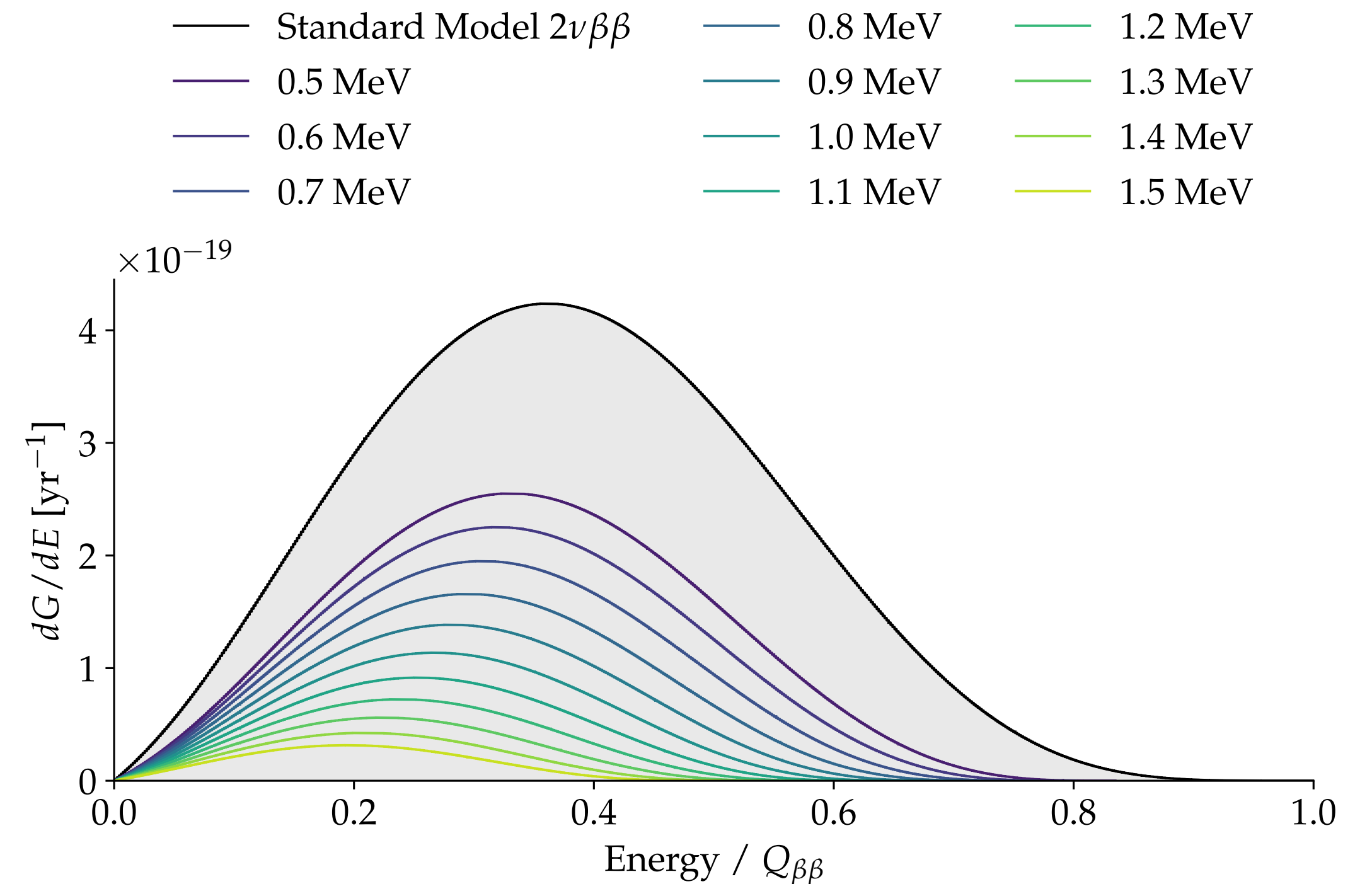
If the sterile neutrino N has a mass $m_N < Q_{\beta\beta}$, it can be emitted instead of an antineutrinos in the $2\nu\beta\beta$ ($\nu N\beta\beta$):

$$(A, Z) \rightarrow (A, Z + 2) + 2e^- + \bar{\nu} + N$$

The effect on the total decay rate is:

$$\Gamma = \cos^4 \theta \Gamma_{SM} + 2 \cos^2 \theta \sin^2 \theta \Gamma_{\nu N}$$

Where $\sin^2 \theta$ is called active-sterile mixing strength



Outline

1

Double- β decays

2

Scintillating cryogenic calorimeters

3

CUPID-0 combined background model

4

CUPID-Mo BSM studies

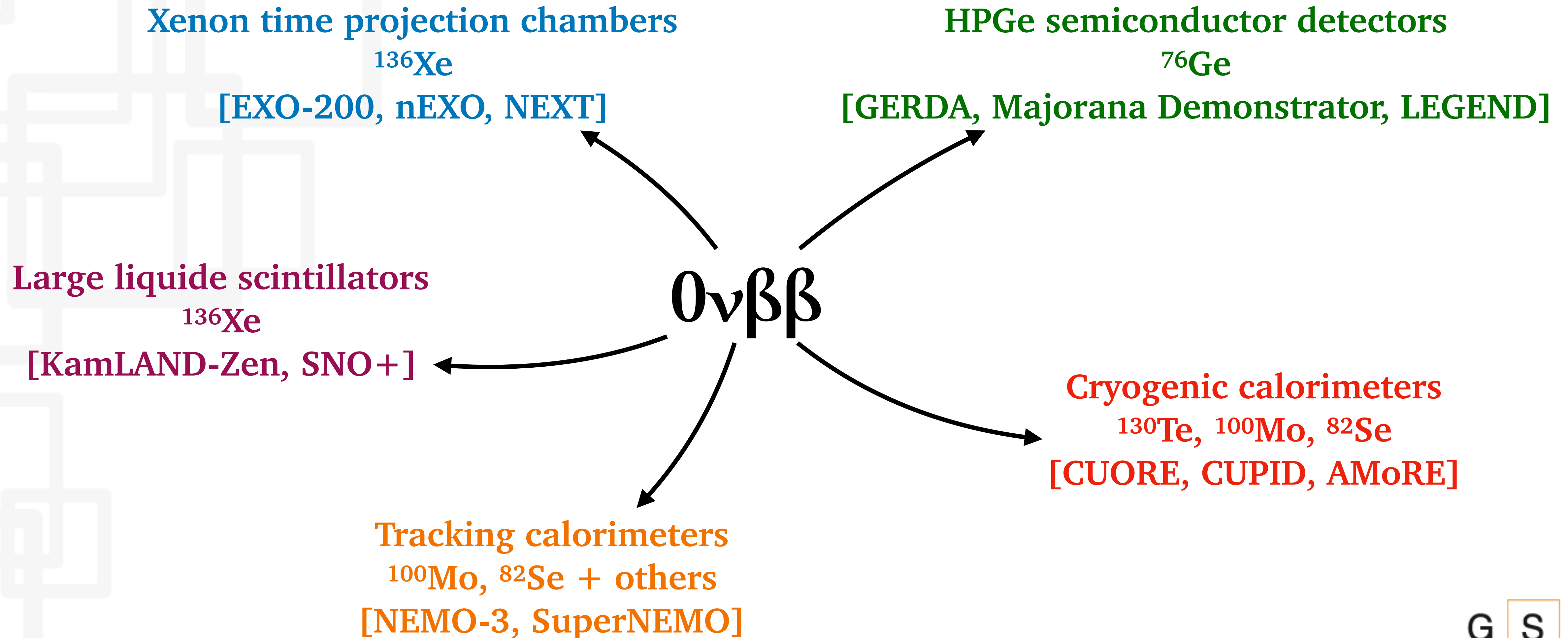
5

CUPID sensitivity

6

Conclusion and outlook

Plenty of experimental techniques



+ many others

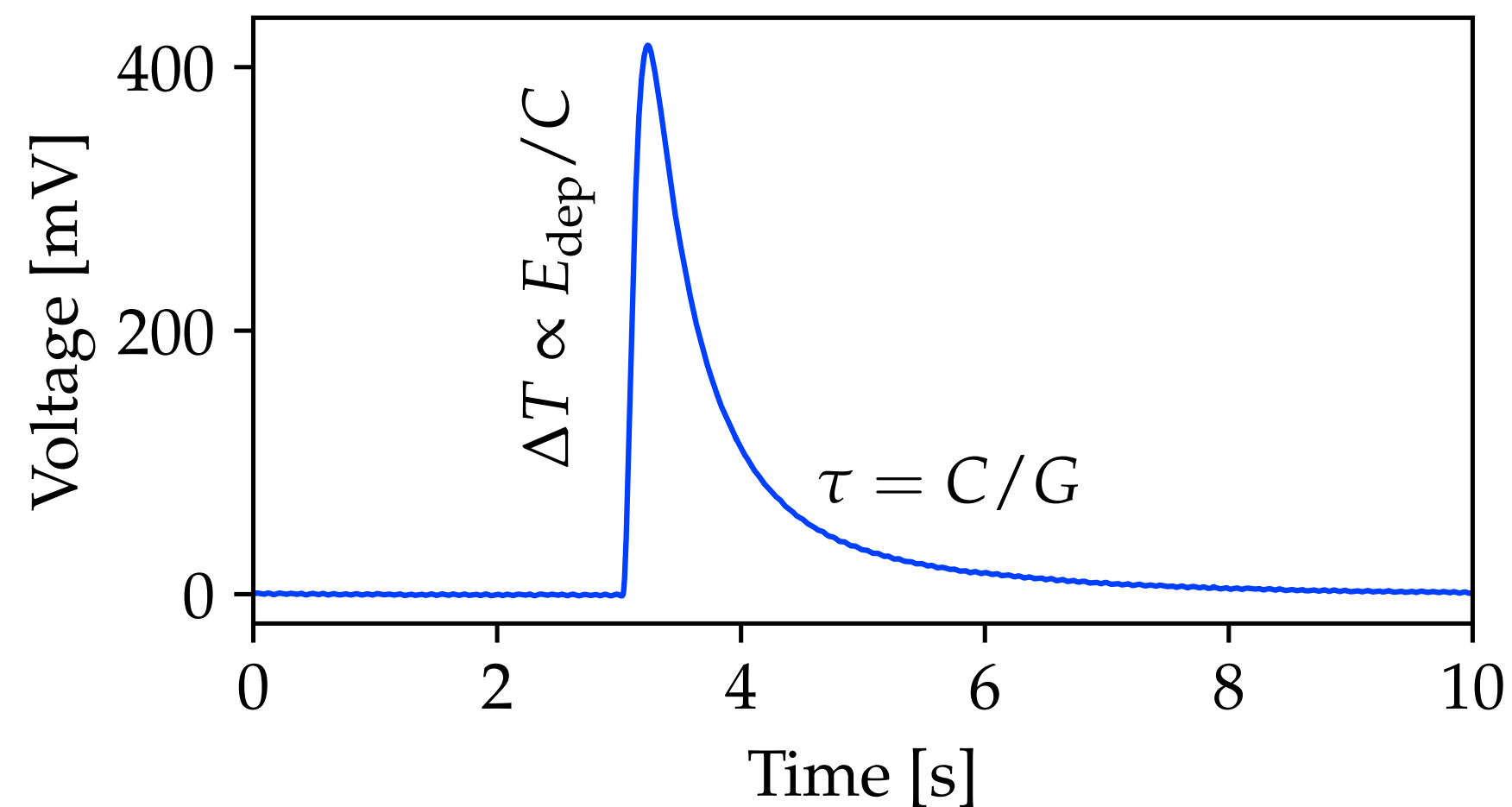


Cryogenic calorimeters for $0\nu\beta\beta$ searches

Highly sensitive calorimeters operated at cryogenic temperature (~ 10 mK)

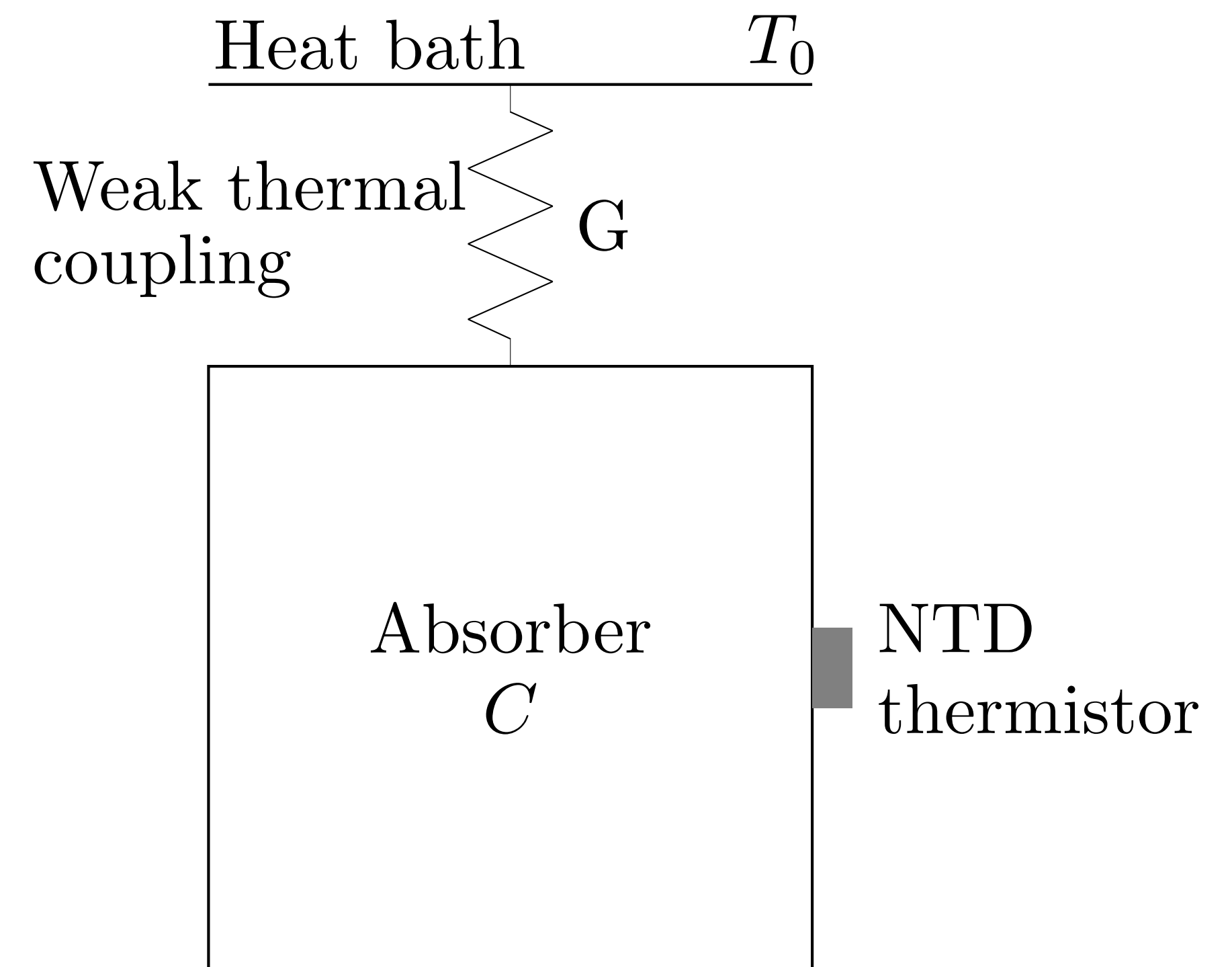
$$\Delta T(t) = \frac{\Delta E}{C} \exp\left(-\frac{t}{\tau}\right) \text{ where } \tau = \frac{C}{G}$$

From Debye law $C \propto T^3$



$$C = 10^{-9} \text{ J/K}$$

$$\Delta T = 0.1 \frac{\text{mK}}{\text{MeV}} \text{ at } 10\text{mK}$$



C = heat capacity

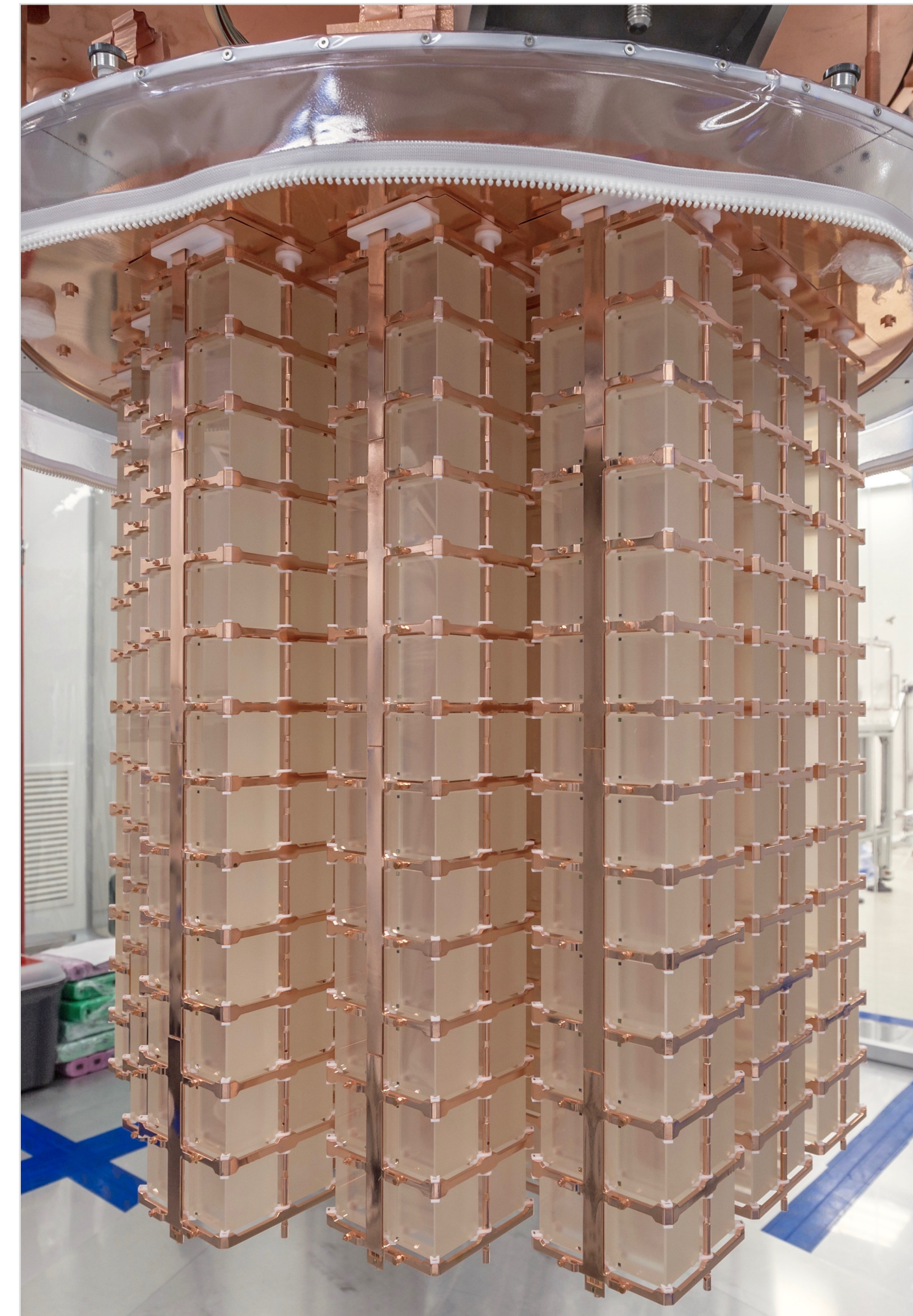
G = thermal conductance

Performances

- ❖ Excellent energy resolution ($<1\%$ at 3 MeV)
- ❖ High detection efficiency, the emitting isotope is embedded in the detector
- ❖ Possibility to study **different $\beta\beta$ emitters** (and take those with higher $Q_{\beta\beta}$)
- ❖ Radio-pure materials
- ❖ Mass scalability

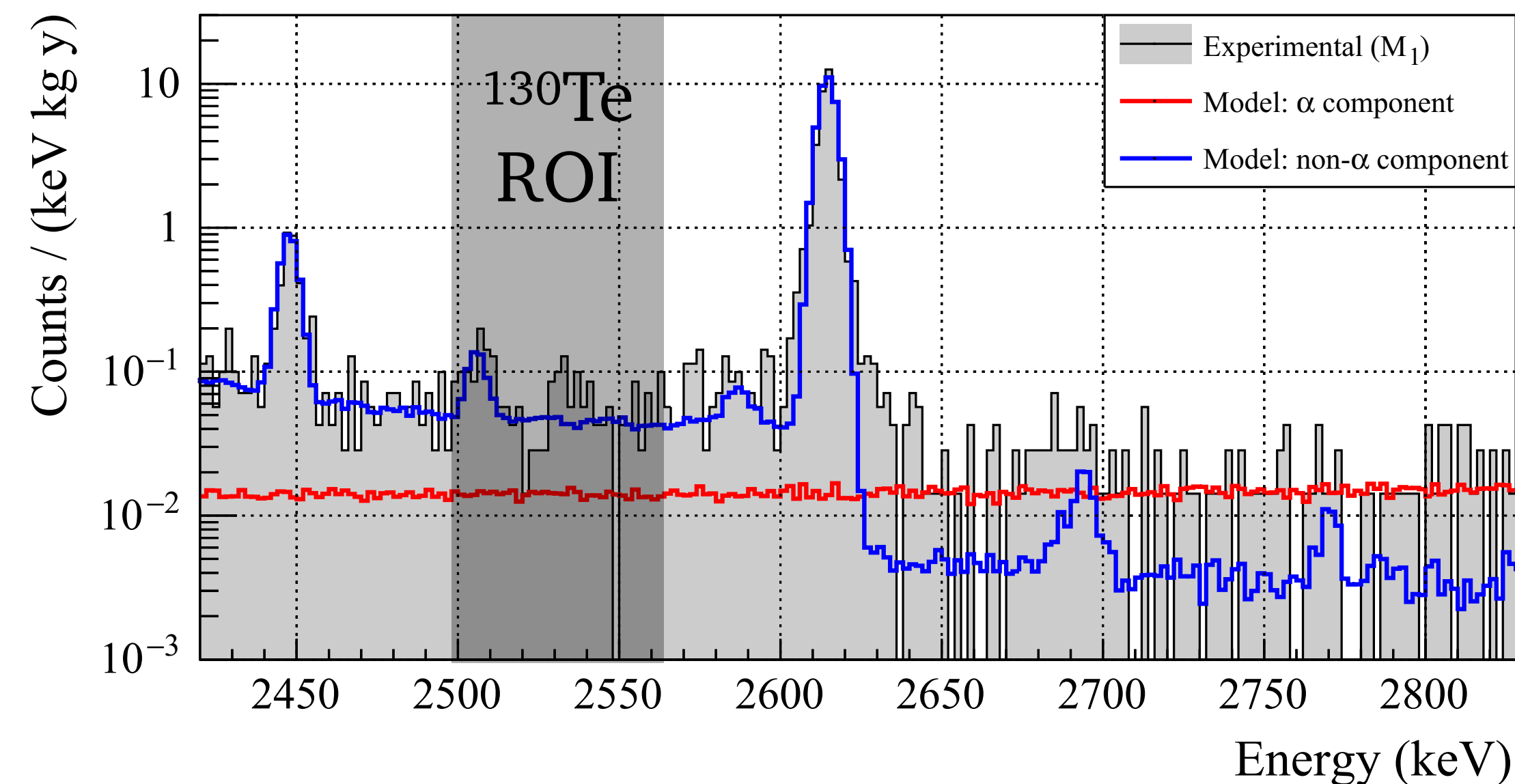
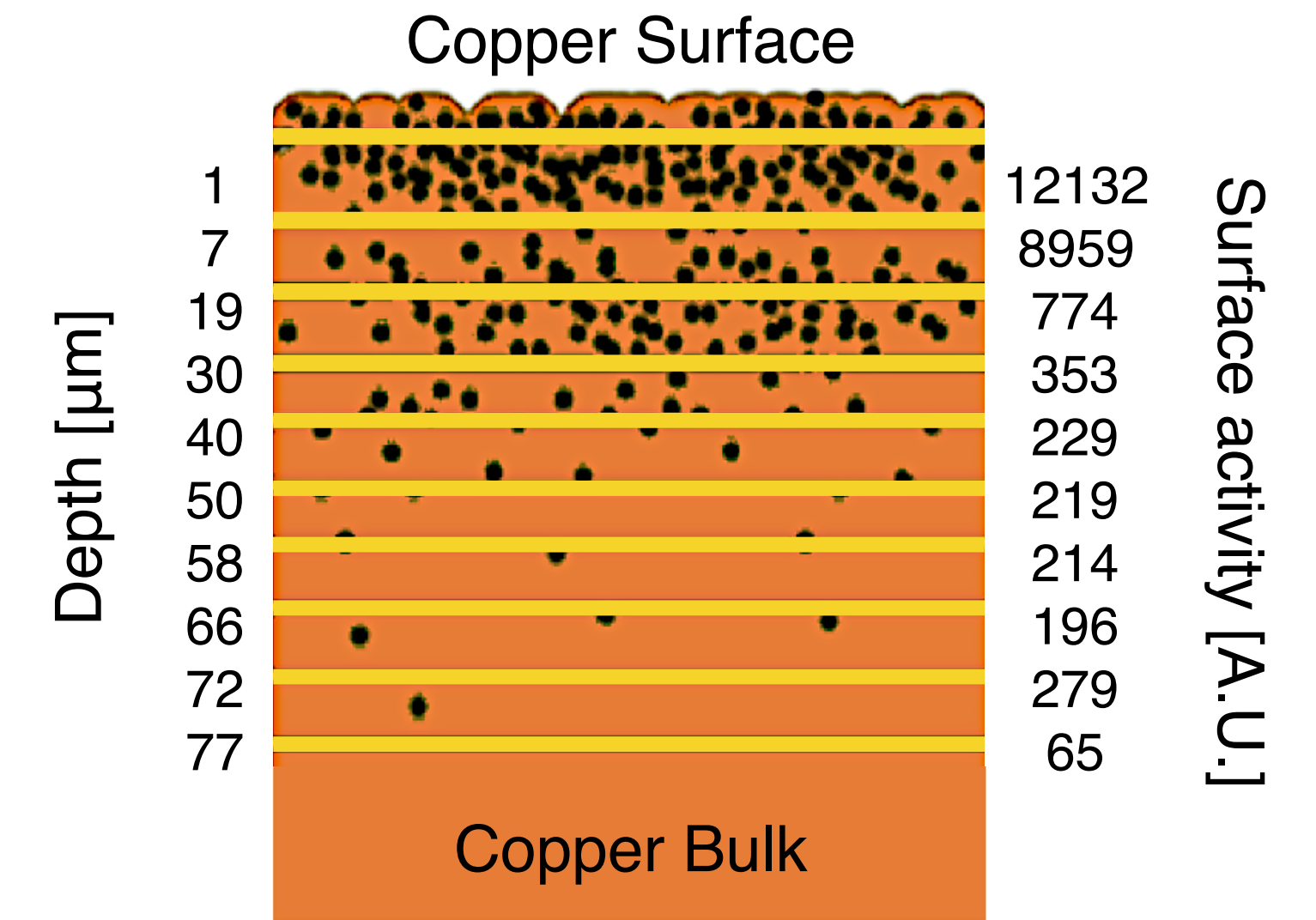


CUORE
experiment



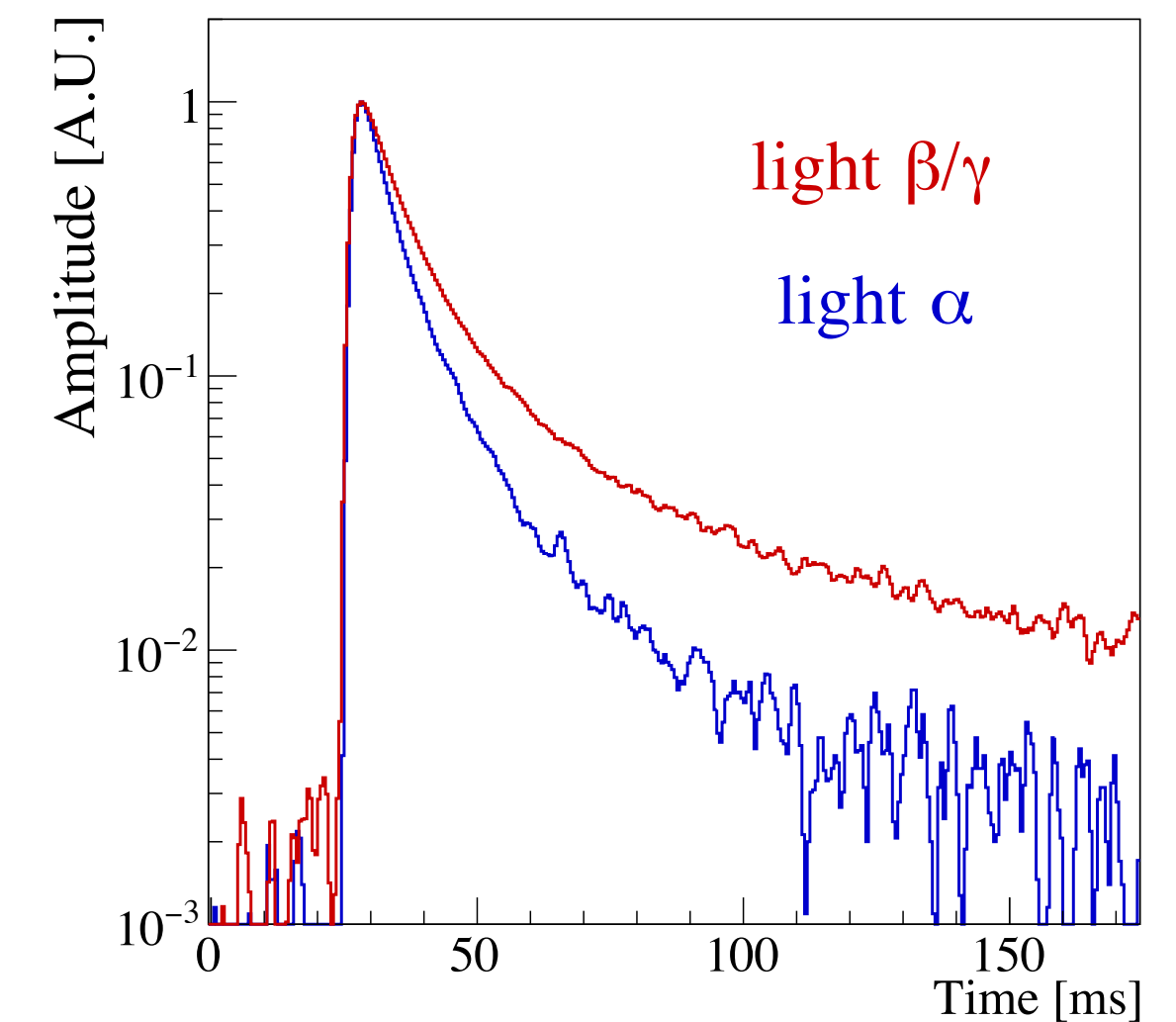
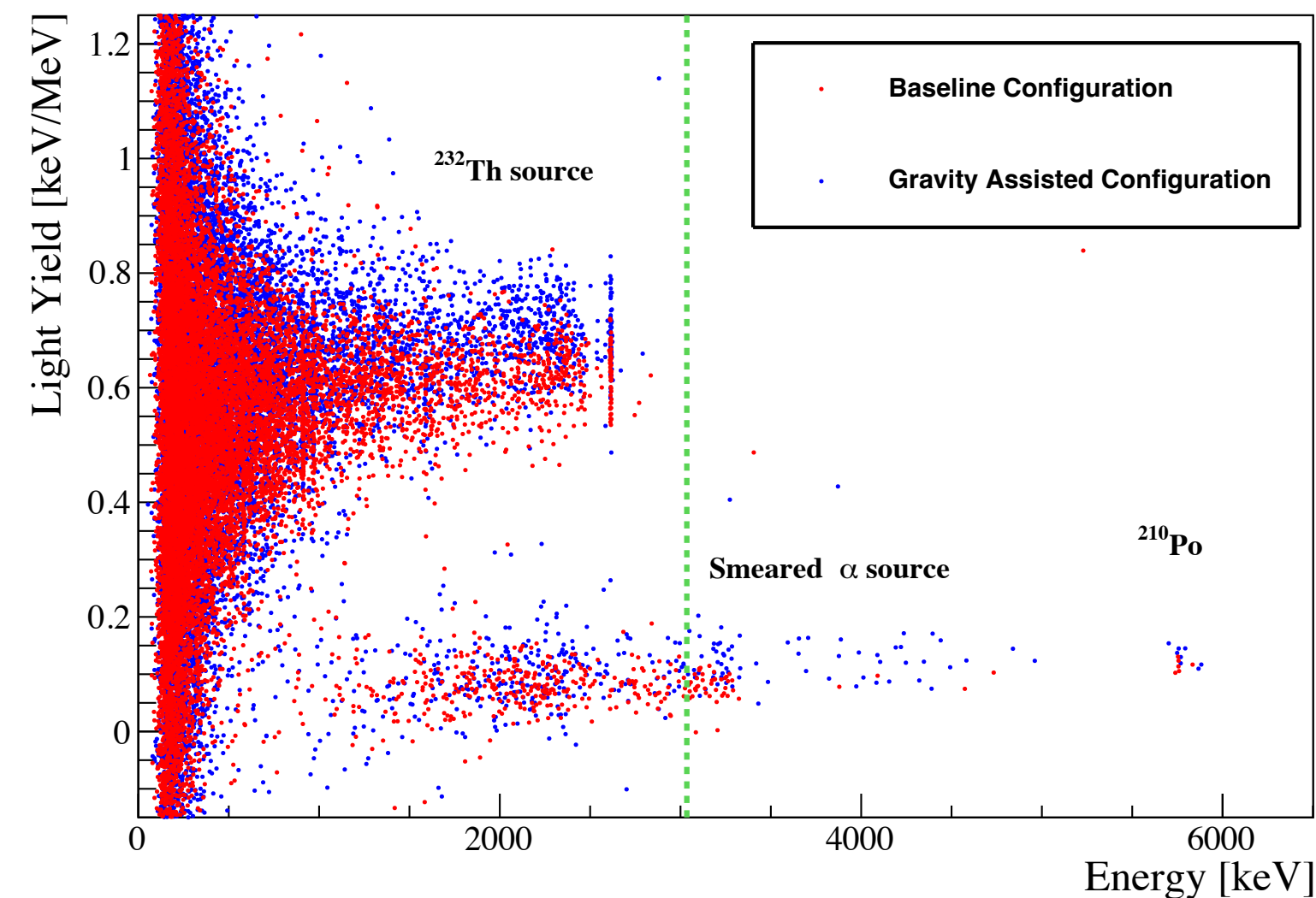
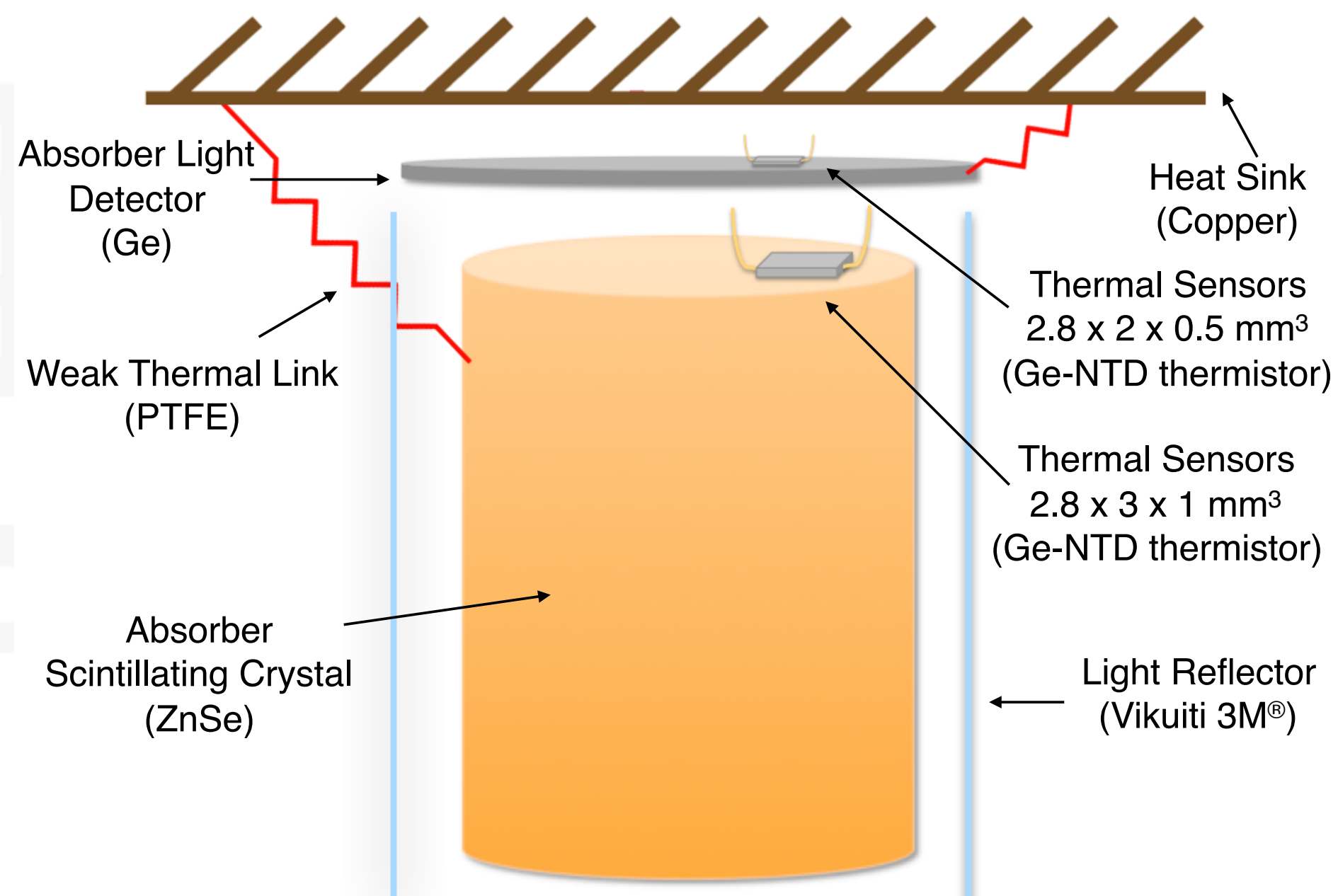
Degraded α -particles

- ❖ A significant background come from degraded α -particles from contamination in passive material
- ❖ Needs for a technique able to **distinguish α -particles from β/γ radiation**
- ❖ Further background reduction with high Q-value isotopes



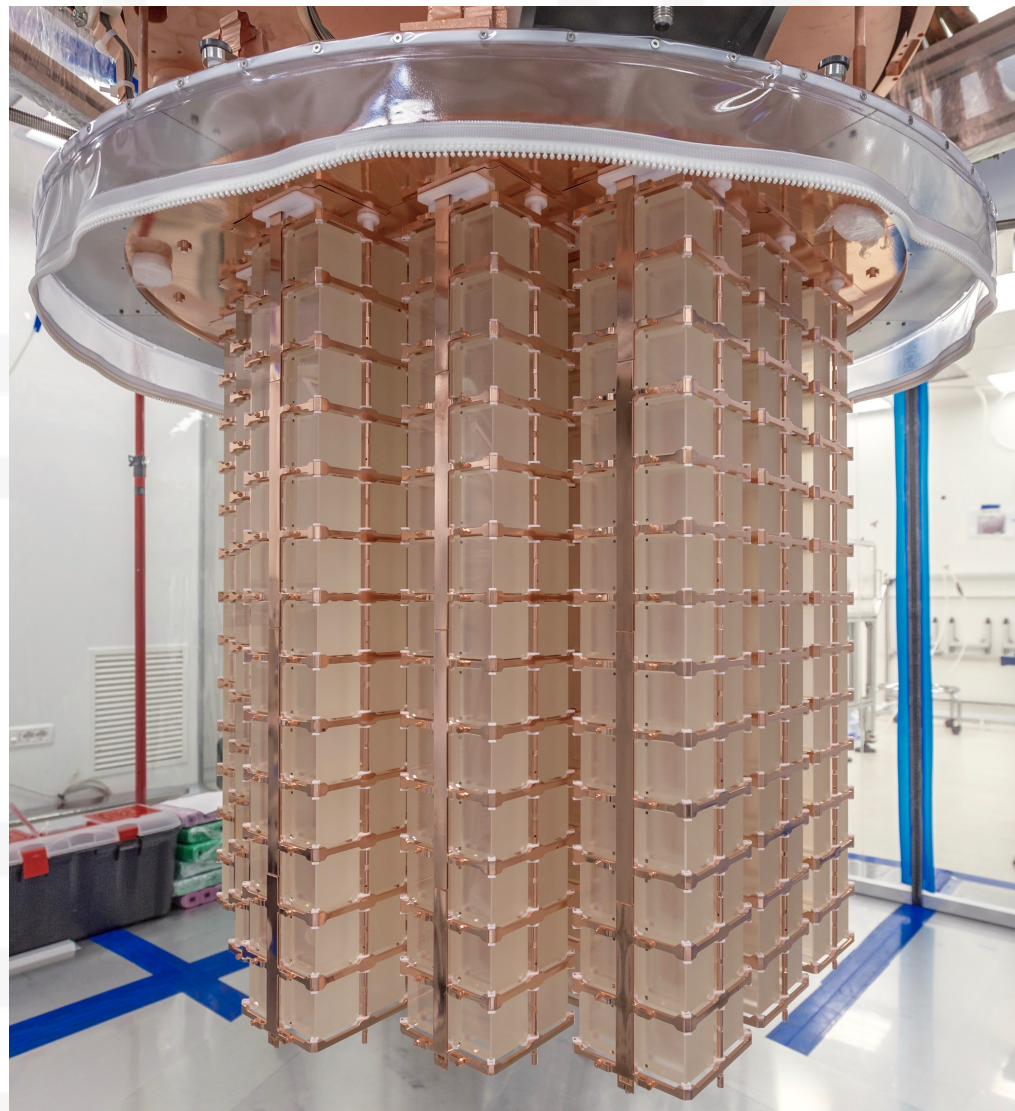
Scintillating cryogenic calorimeters

- ❖ Absorber: scintillating crystals at cryogenic temperatures (ZnSe, Li₂MoO₄, etc...)
- ❖ Light Detector: thin Germanium wafer coupled to the absorber working as a cryogenic calorimeter
- ❖ The particle identification can be done with by detecting the amount of light emitted (Light Yield) or the pulse shape of light signals

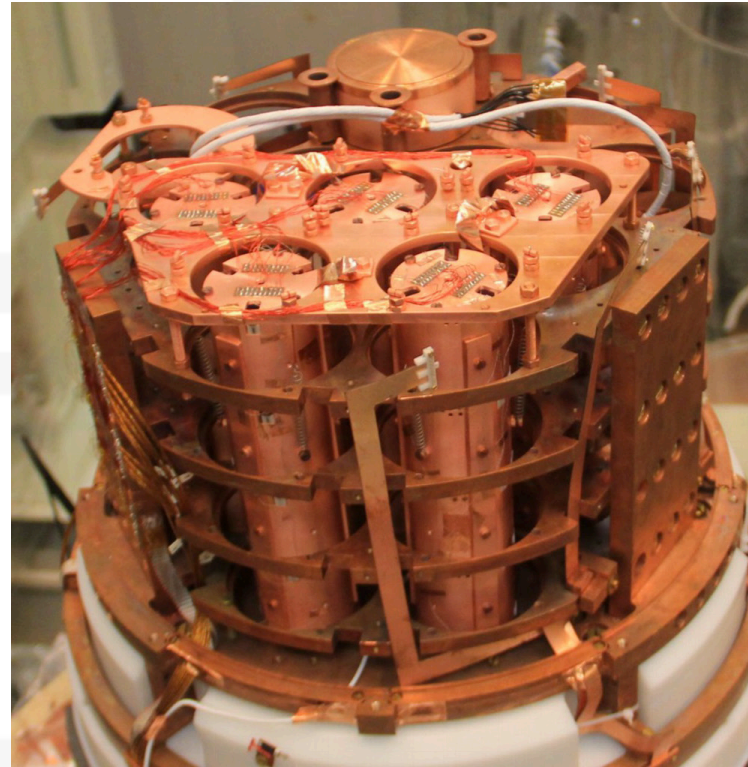


From CUORE to CUPID

CUORE

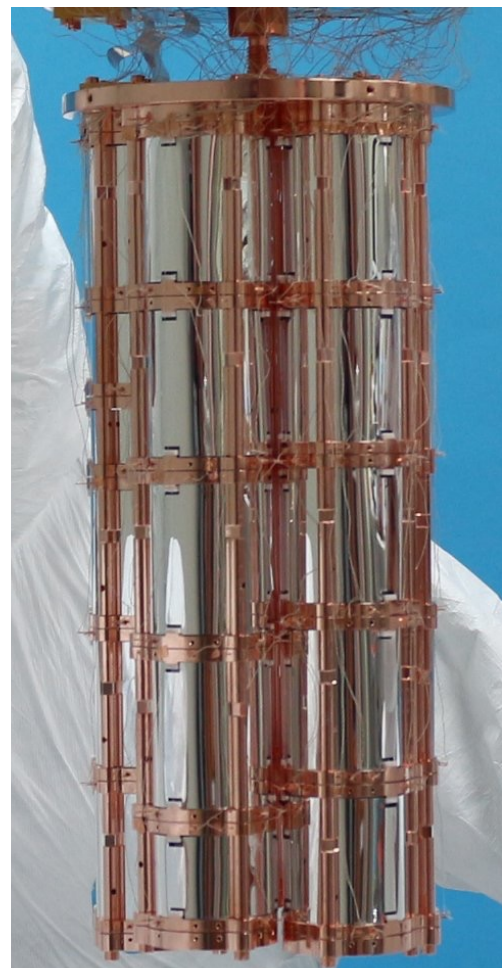


- ❖ 988 TeO_2 crystals
- ❖ 206 kg of ^{130}Te
- ❖ Largest cryogenic facility in the world
- ❖ $\text{BI} \sim 1.5 \times 10^{-2} \text{ ckky}$
- ❖ No particle identification



CUPID-Mo

- ❖ 20 Li_2MoO_4 crystals
- ❖ 20 Ge light detectors
- ❖ 2.3 kg of ^{100}Mo
- ❖ $\text{BI} \sim 3.9 \times 10^{-3} \text{ ckky}$



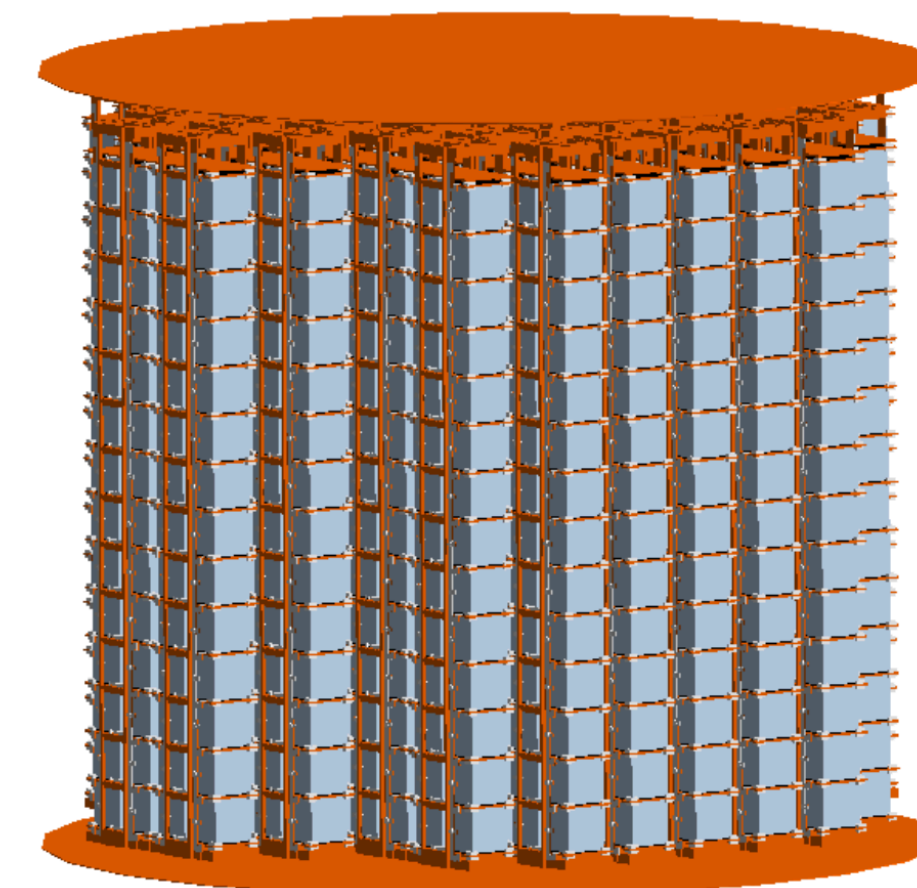
CUPID-0

- ❖ 26 ZnSe crystals
- ❖ 31 Ge light detectors
- ❖ 5.2 kg of ^{82}Se
- ❖ $\text{BI} \sim 4.0 \times 10^{-3} \text{ ckky}$



CUPID - next generation

- ❖ 1596 Li_2MoO_4 crystals
- ❖ 1710 Ge light detectors
- ❖ 240 kg of ^{100}Mo
- ❖ **Target BI $\sim 10^{-4} \text{ ckky}$**
- ❖ Re-use of CUORE cryogenic facility



Outline

1

Double- β decays

2

Scintillating cryogenic calorimeters

3

CUPID-0 combined background model

4

CUPID-Mo BSM studies

5

CUPID sensitivity

6

Conclusion and outlook

The CUPID-0 detector

- ❖ 24 ZnSe crystals enriched at $>95\%$ of ^{82}Se + two natural ones + 31 Ge Light detectors
- ❖ Located at LNGS
- ❖ $Q_{\beta\beta}(^{82}\text{Se}) = \sim 2998 \text{ keV} \rightarrow$ low background region
- ❖ NTD-Ge thermistors as temperature sensors
- ❖ Total mass: 10.5 kg ZnSe

In Jan 2019 the CUPID-0 collaboration has made an upgrade of the detector, starting the so-called “Phase II” of the experiment.

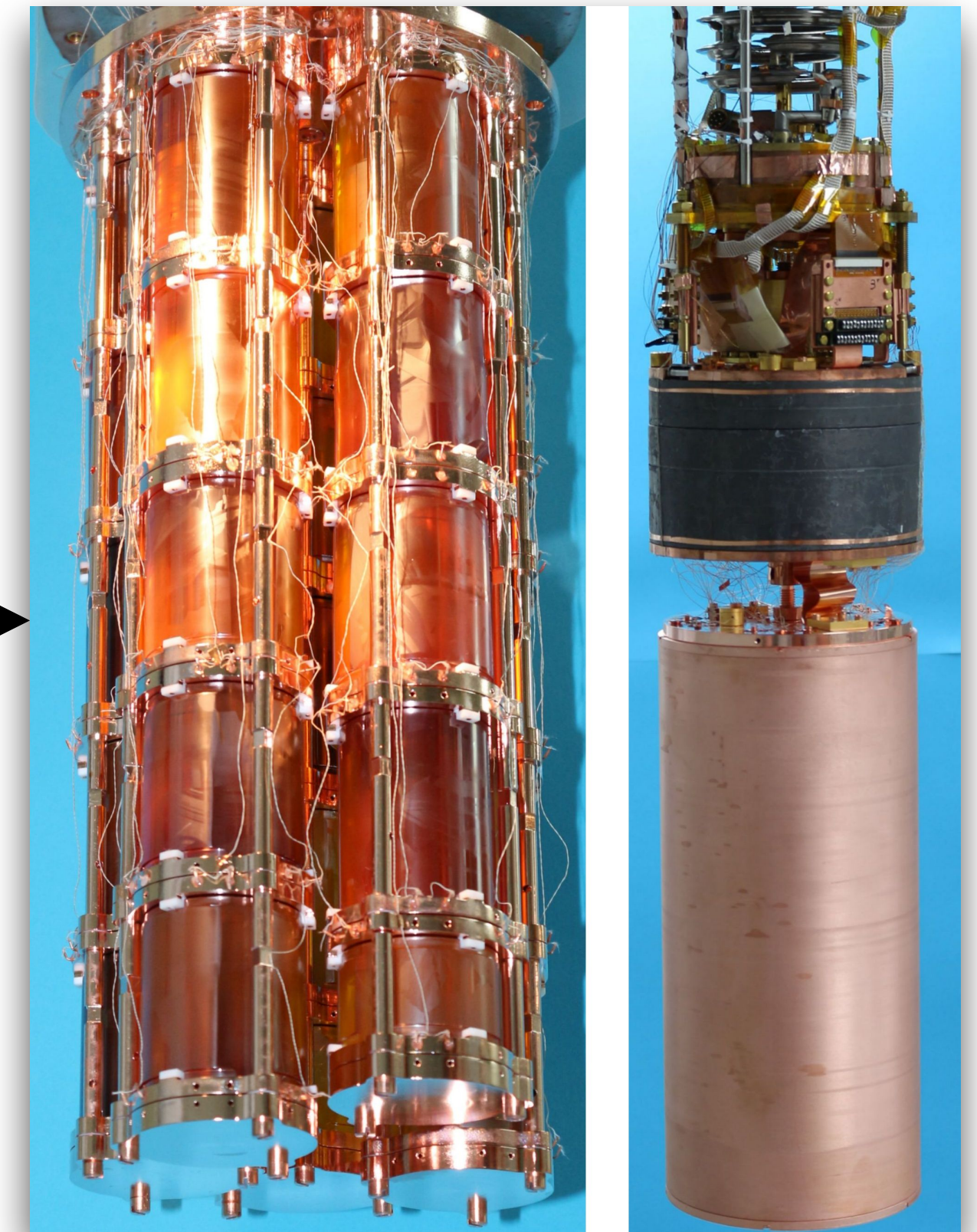
Phase I

9.99 kg×y

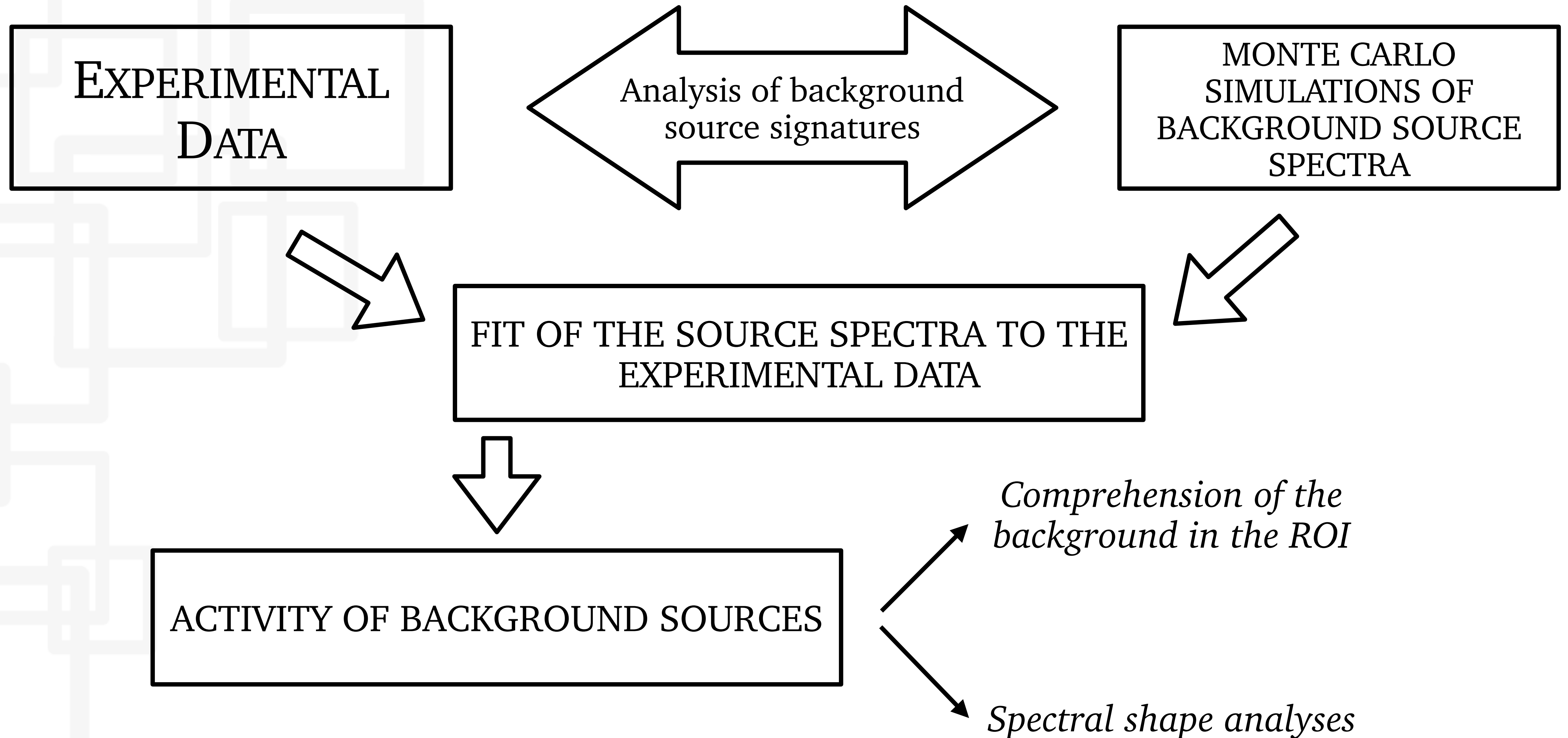


Phase II

5.74 kg×y

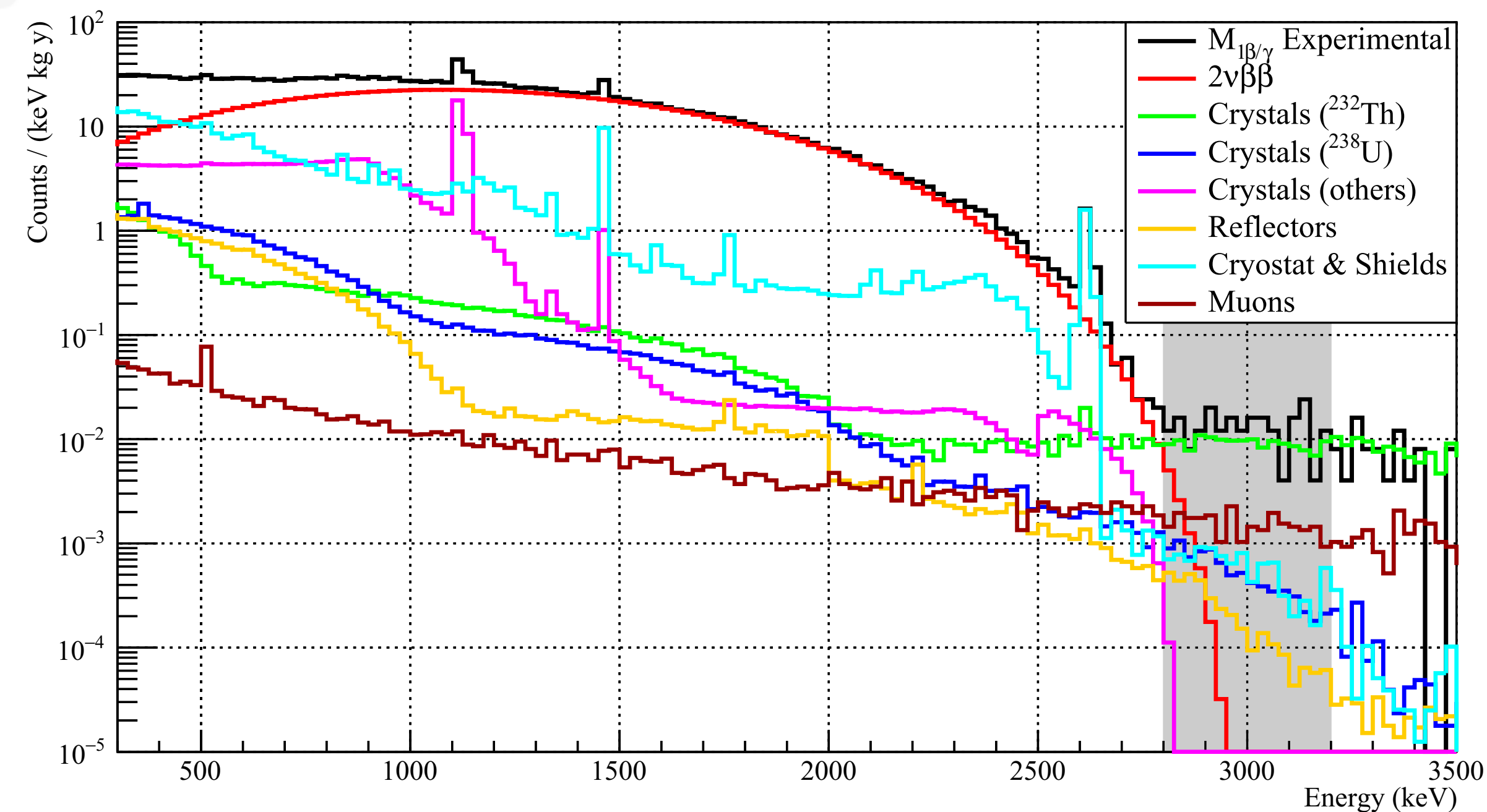


Background model



Phase I background model

- ❖ Fundamental for the spectral shape reconstruction and identify dominant background sources
- ❖ Further precision with the integration of Phase II data

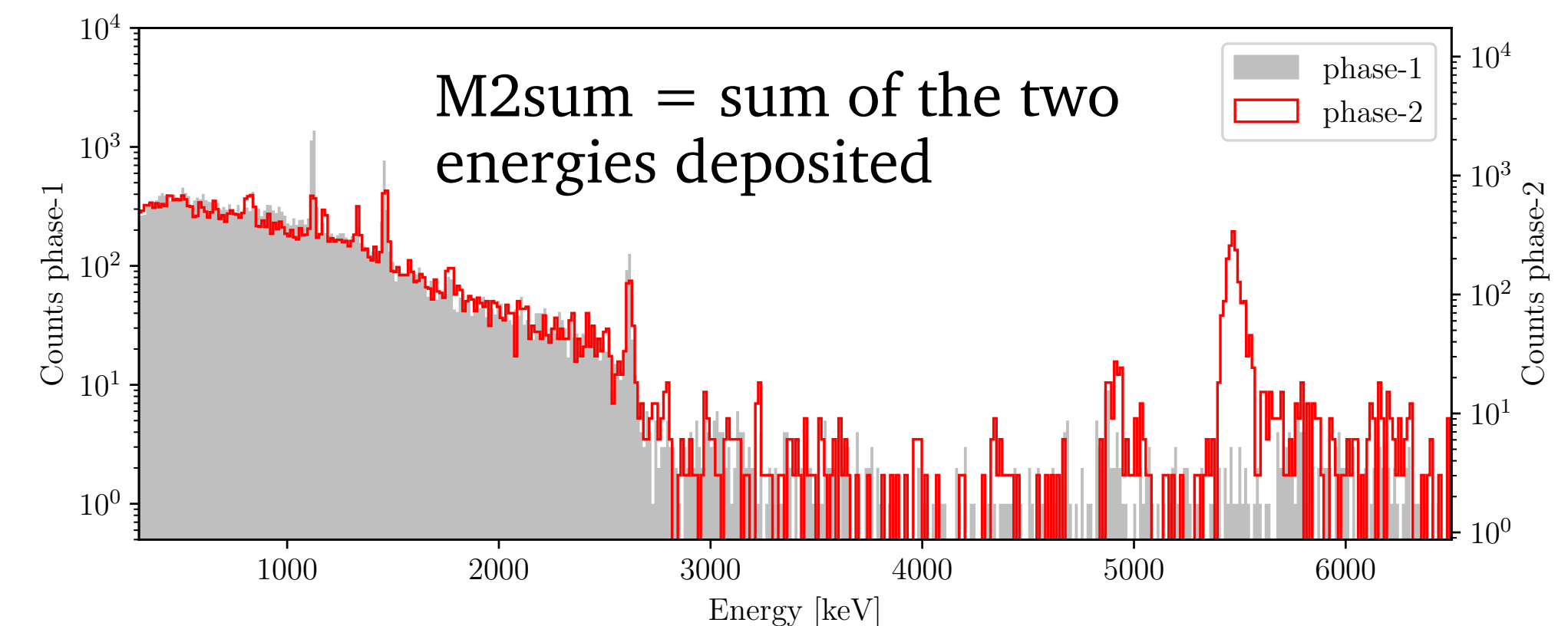
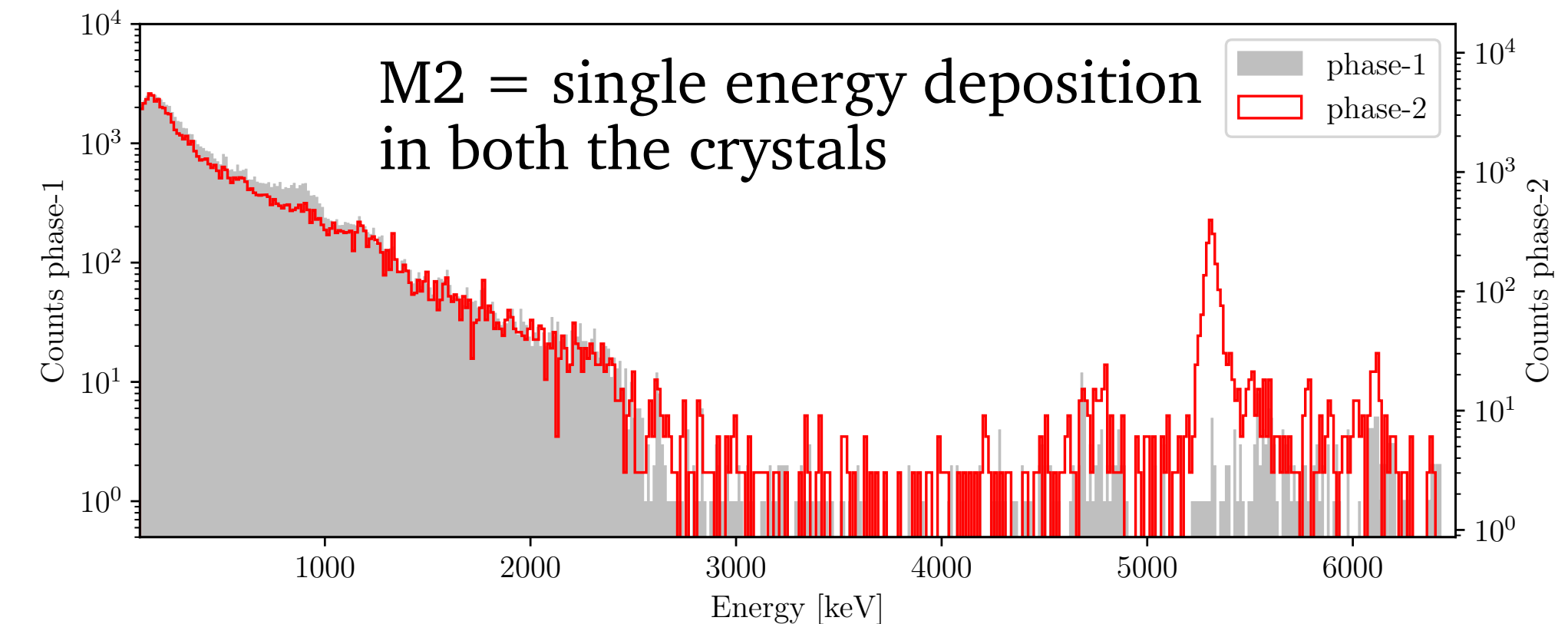
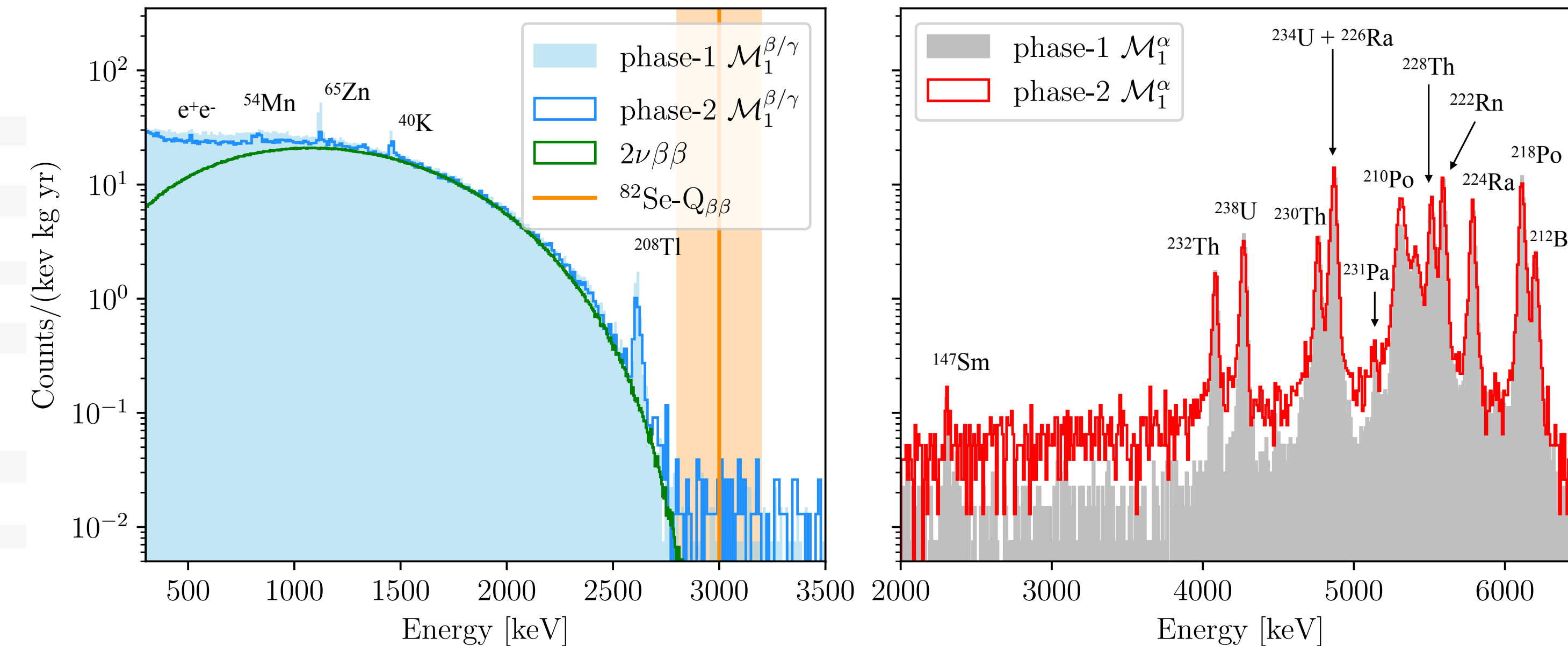
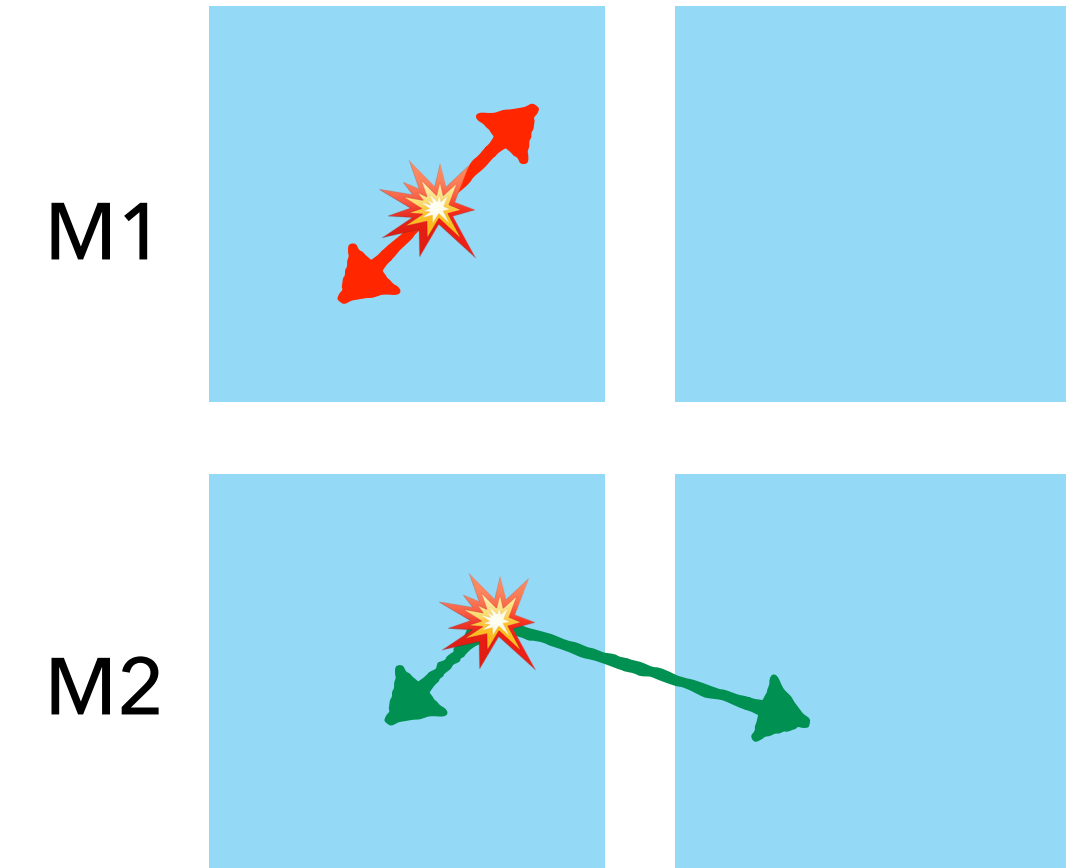


Eur. Phys. J. C 79, 583 (2019)

Experimental spectra

Data selection based on time coincidences and particle identification.

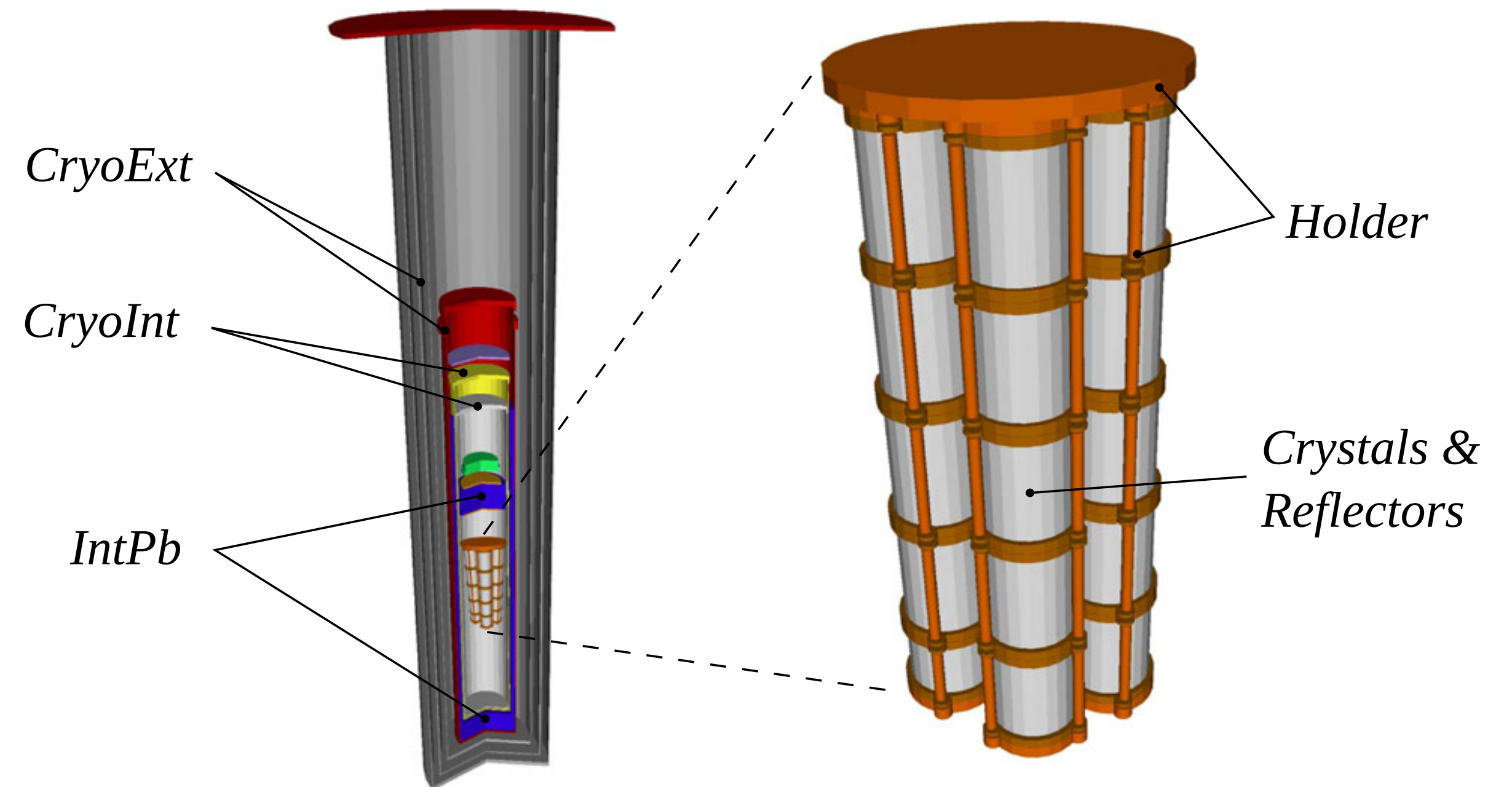
- ❖ α -contaminations have the same activity in phase-I and phase-II
- ❖ Higher alpha continuum from close component contaminations (10 mK)
- ❖ $2\nu\beta\beta$ is dominant up to 3 MeV



Background model - simulations

- ❖ A GEANT4 based software taking into account the detector geometry generates a **series on Monte Carlo spectra**
- ❖ The simulations are processed with a **custom software to implement experimental features** on simulated data (energy and time resolution, coincidences, particle identification...)

The background sources included follows the material components and the geometry. Degenerate spectra are grouped together in a single simulation



+ PbExt

Phase-I → Reflectors + Holders

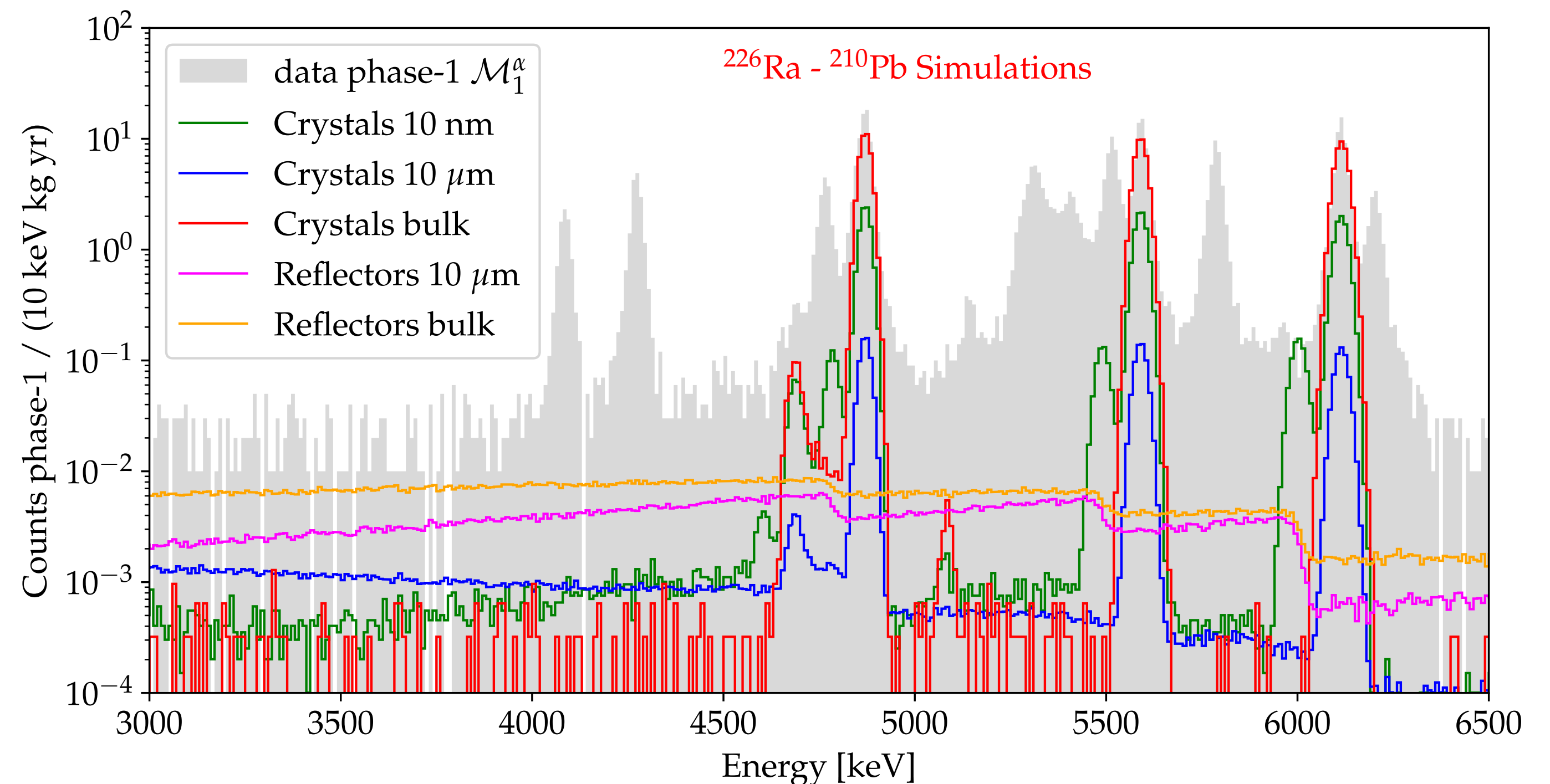
Phase-II → Holders + 10mK

Background model - sources

- ❖ Long-living radioisotope (^{232}Th , ^{238}U , ^{235}U , ^{40}K) with the possible breaks of the chains → Crystals, Holders and Cryostat
- ❖ Cosmogenic activation products of Copper and ZnSe (^{65}Zn , ^{60}Co , ^{54}Mn) → Crystals and Holders
- ❖ Muons → Environment
- ❖ $2\nu\beta\beta$ using SSD approximation

Crystal contaminants are modeled with different depth profiles $e^{-x/\lambda}$

λ = depth parameter assumed to be 10nm or $10\mu\text{m}$



Background model - Fit

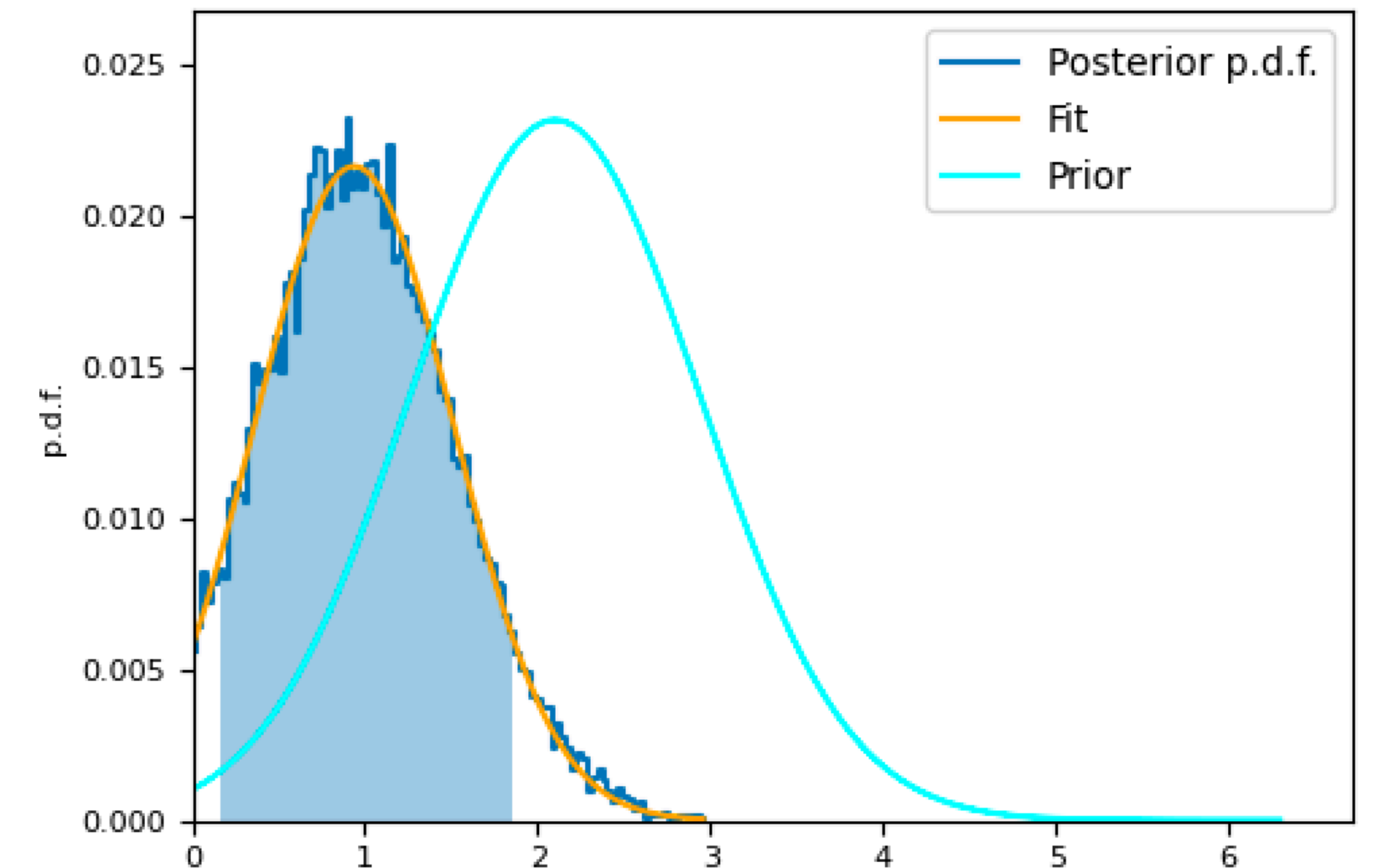
Binned simultaneous Maximum Likelihood fit using a Bayesian framework with a Markov Chain Monte Carlo (MCMC) approach.

We model the spectra i and energy bin b as $f_i(E_b; \vec{N}) = \sum_{j=1}^{N_s} N_j \cdot f_{j,i}(E_b)$

$$\text{Activity} \left[\frac{\text{Bq}}{\text{kg}} \right] = \frac{N_j \cdot N^{MC}}{\text{Mass}[\text{kg}] \times \text{lifetime}[\text{s}]}$$

From the Bayes theorem the *joint posterior pdf* is

$$\text{Posterior}(\vec{N} \mid \text{data}) \propto \prod_{i,b} \text{Pois} \left(n_{i,b} \mid f_i(E_b; \vec{N}) \right) \times \text{Prior}(\vec{N})$$



Background model - Fit

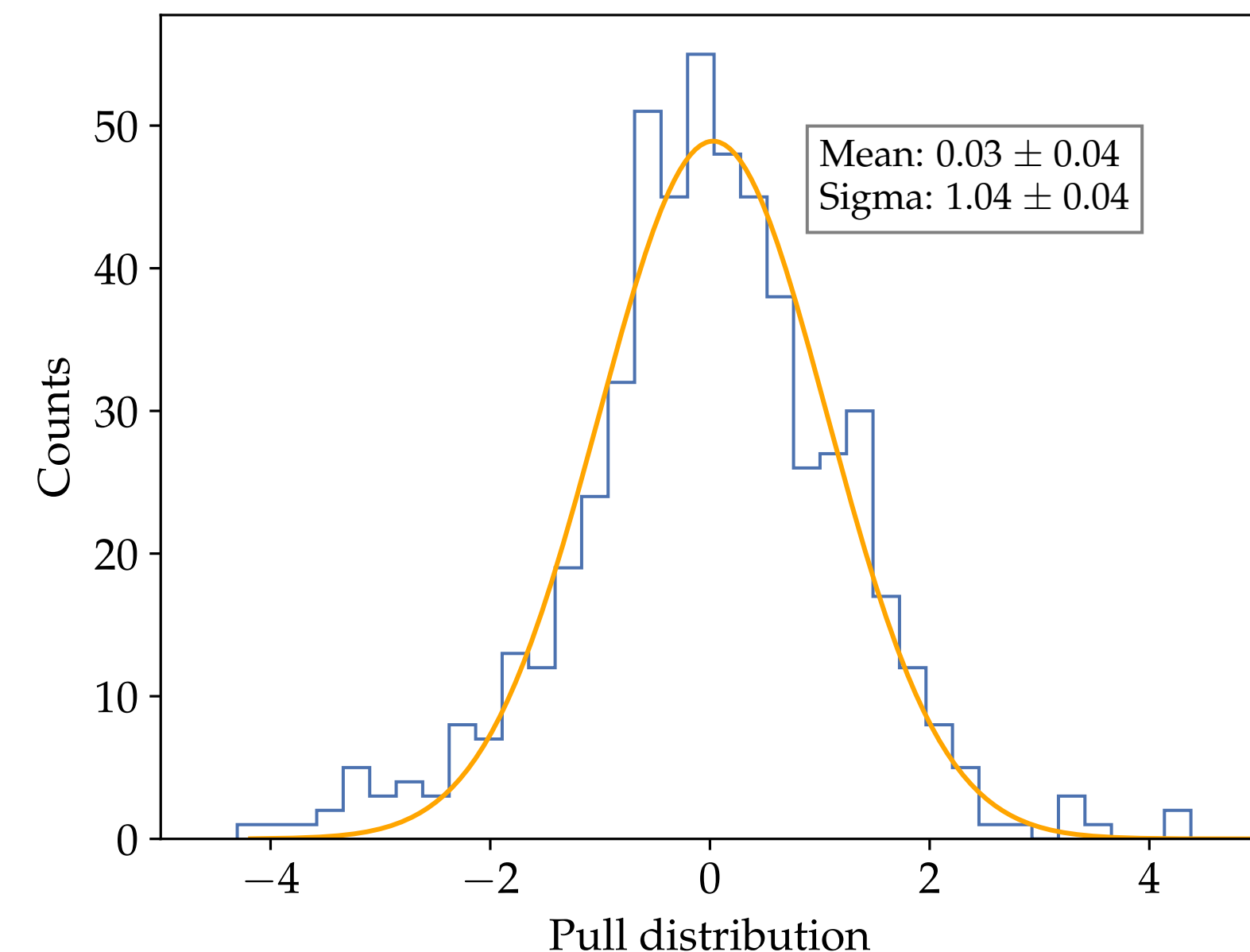
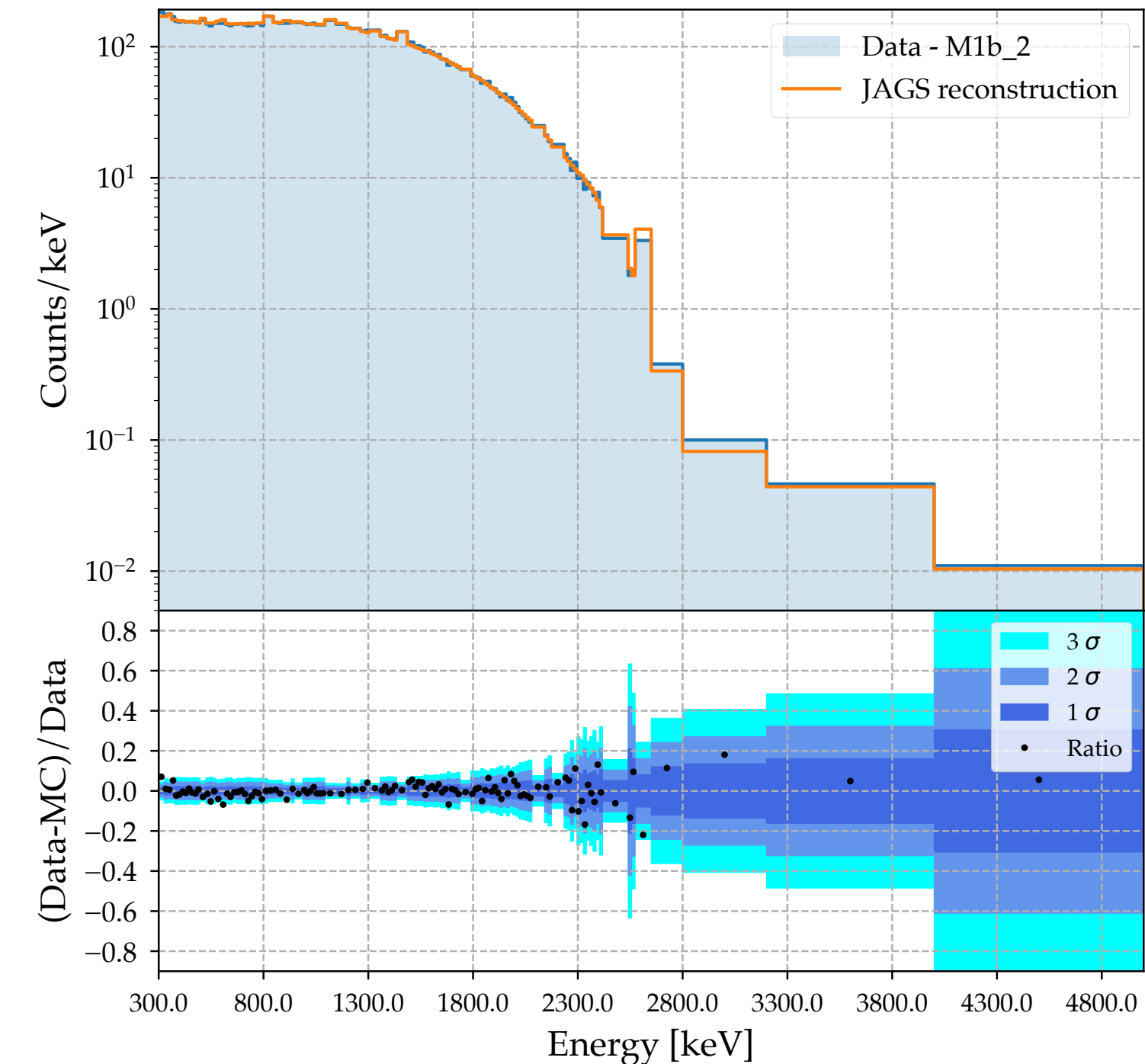
Variable binning for low counts regions and peaks

Constraints on all the long living isotopes to have the same activity between phase-I and phase-II

+ priors based on previous experiments results and measured muon flux

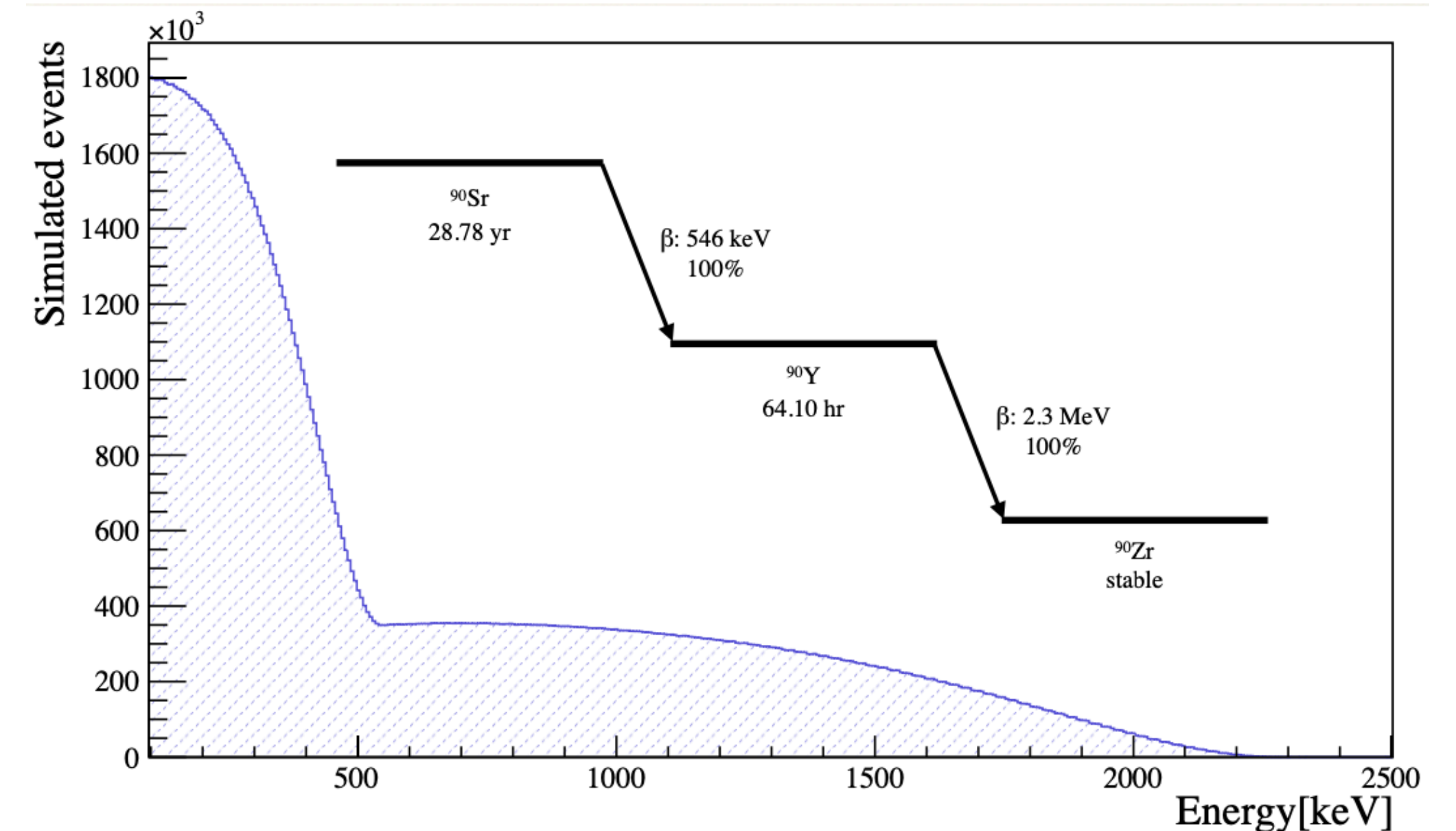
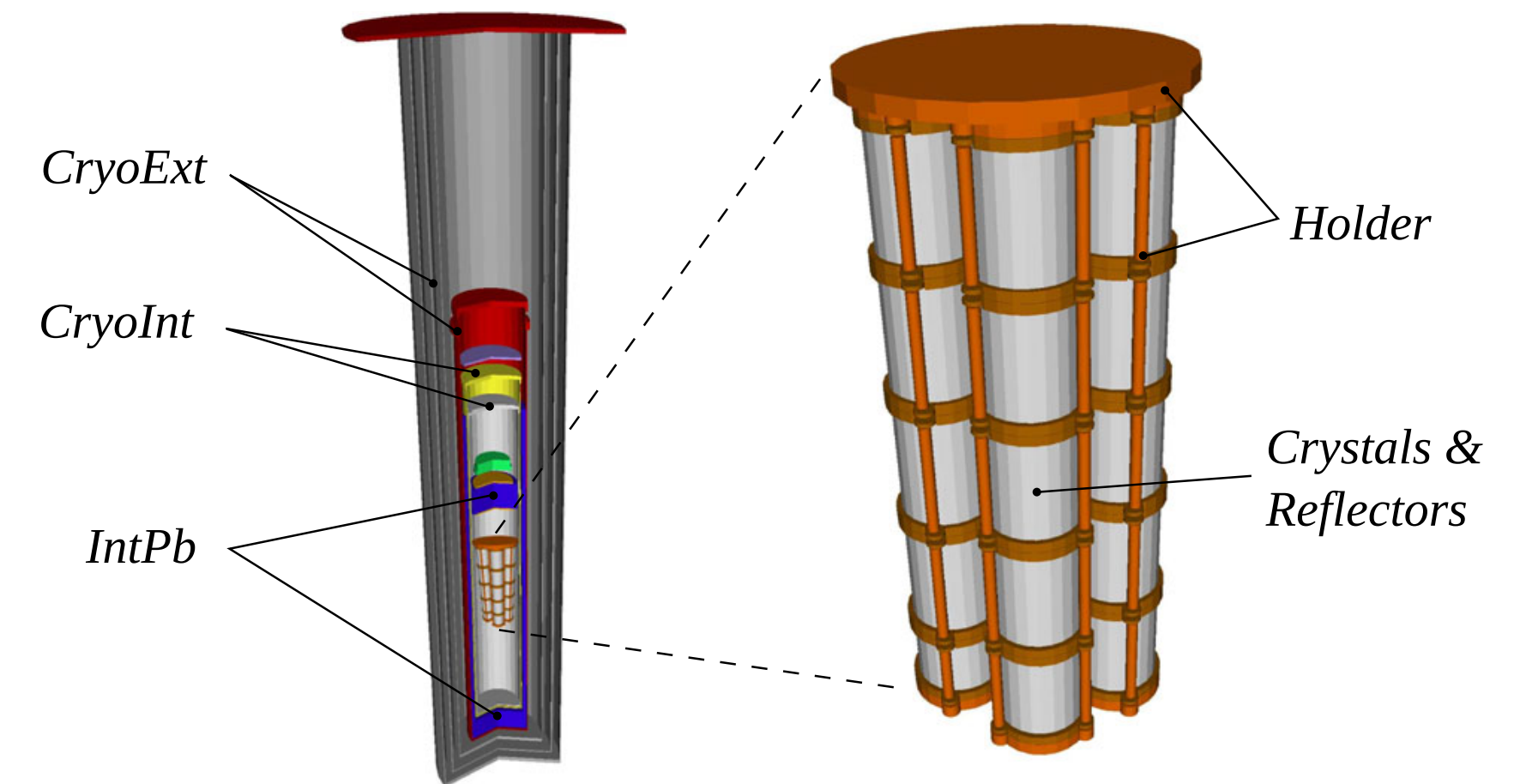
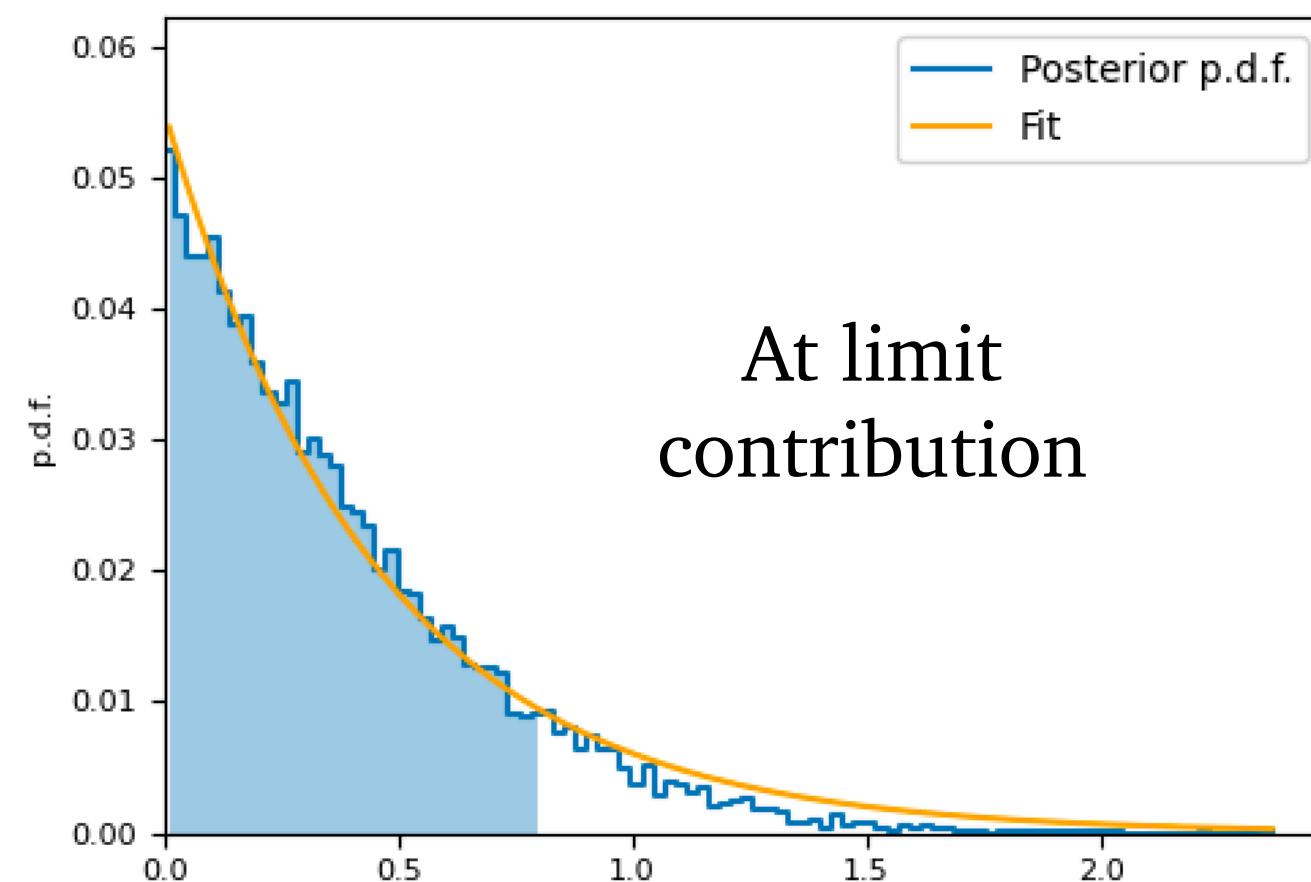
Simultaneous fit on 8 experimental experimental spectra using **JAGS**, 78 simulations, with 17 couples of them constrained

This list of sources and this configuration of the parameters define the *Reference* fit



Fit systematics

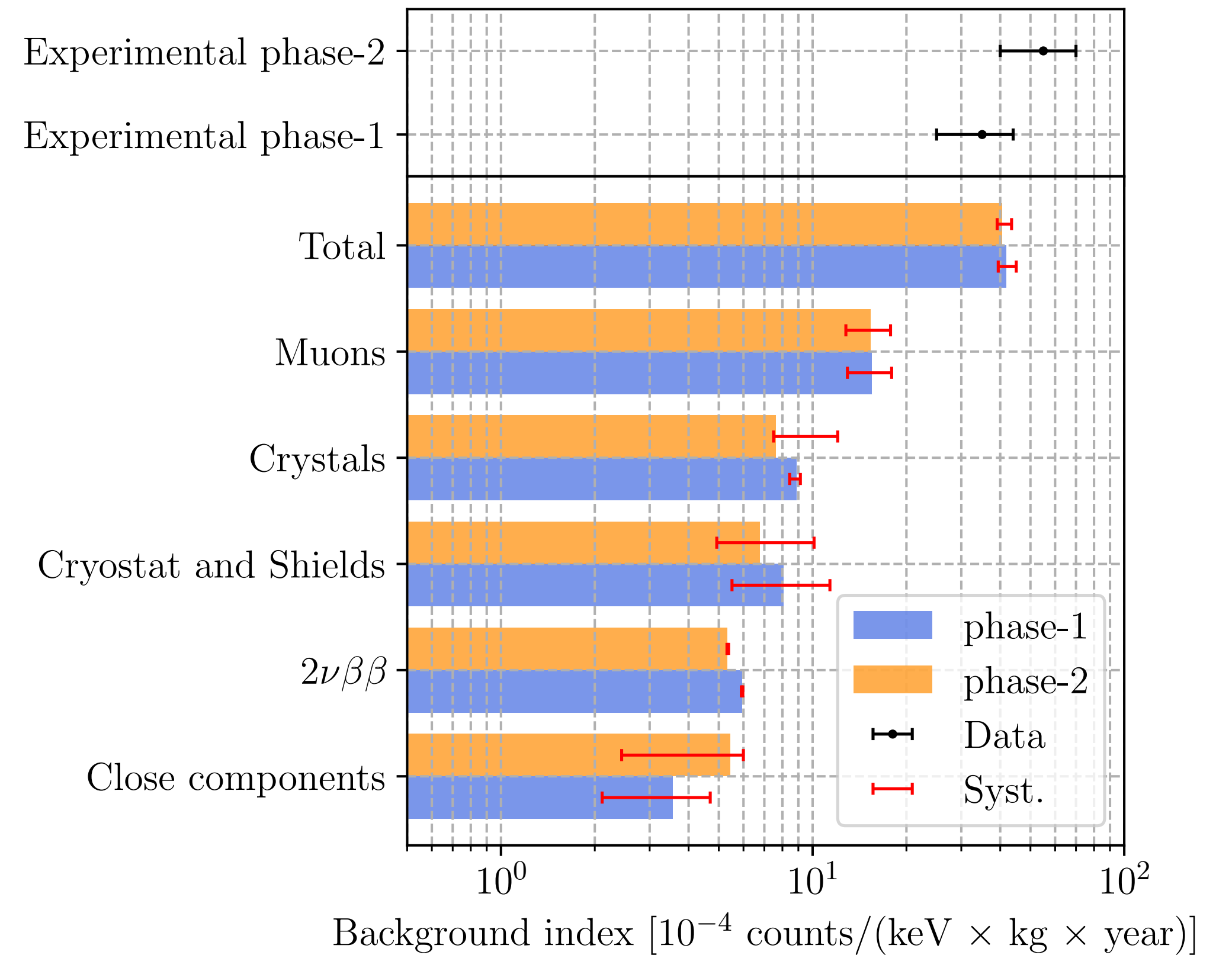
- ❖ Energy **calibration**: alternative energy scale corrected for the ^{56}Co calibration residuals
- ❖ $^{90}\text{Sr}/^{90}\text{Y}$
- ❖ **Source location** effects
- ❖ **Reduced list** of sources: remove sources which posterior p.d.f. is compatible with 0
- ❖ Others...



Background in the ROI

- ❖ Simulations can reproduce the background in the $0\nu\beta\beta$ ROI applying the same cuts used in experimental data
- ❖ The higher background in phase II is explained as an over-fluctuation

Component	ROI _{bkg} rate [10^{-4} counts/keV/kg/yr]		
	phase-I (only)	phase-I (comb.)	phase-II (comb.)
<i>Crystals</i>	$11.7 \pm 0.6^{+1.6}_{-0.8}$	$8.9 \pm 0.5^{+0.3}_{-0.4}$	$7.6 \pm 0.4^{+4.4}_{-0.1}$
<i>Near Components</i>	$2.1 \pm 0.3^{+2.2}_{-1.0}$	$3.6 \pm 0.3^{+1.1}_{-1.4}$	$5.4 \pm 0.9^{+0.6}_{-3.0}$
<i>Cryostat & Shields</i>	$5.9 \pm 1.3^{+7.2}_{-2.9}$	$8.0 \pm 1.5^{+3.3}_{-2.5}$	$6.8 \pm 1.0^{+3.3}_{-1.8}$
Muons	$15.3 \pm 1.3 \pm 2.5$	$15.4 \pm 0.7 \pm 2.5$	$15.3 \pm 0.7 \pm 2.5$
$2\nu\beta\beta$	$6.0 \pm 0.02^{+0.13}_{-0.09}$	$5.93 \pm 0.03^{+0.04}_{-0.02}$	$5.31 \pm 0.03^{+0.06}_{-0.04}$
Total	$41 \pm 2^{+9}_{-4}$	$42 \pm 2^{+4}_{-4}$	$40 \pm 2^{+4}_{-2}$
Experimental	35^{+10}_{-9}	35^{+10}_{-9}	55^{+15}_{-15}



$2\nu\beta\beta$ half-life measurement

Fit systematics combined with the 68% difference between the *Reference*

+Fit systematics (+1.0%)(−0.7%)
 +Stat. uncertainty ($\pm 0.6\%$) (including efficiency and enrichment uncertainty)
 +Theoretical uncertainty ($\pm 0.3\%$) (SSD vs. HSD)
 = (+1.2%)(−0.9%)

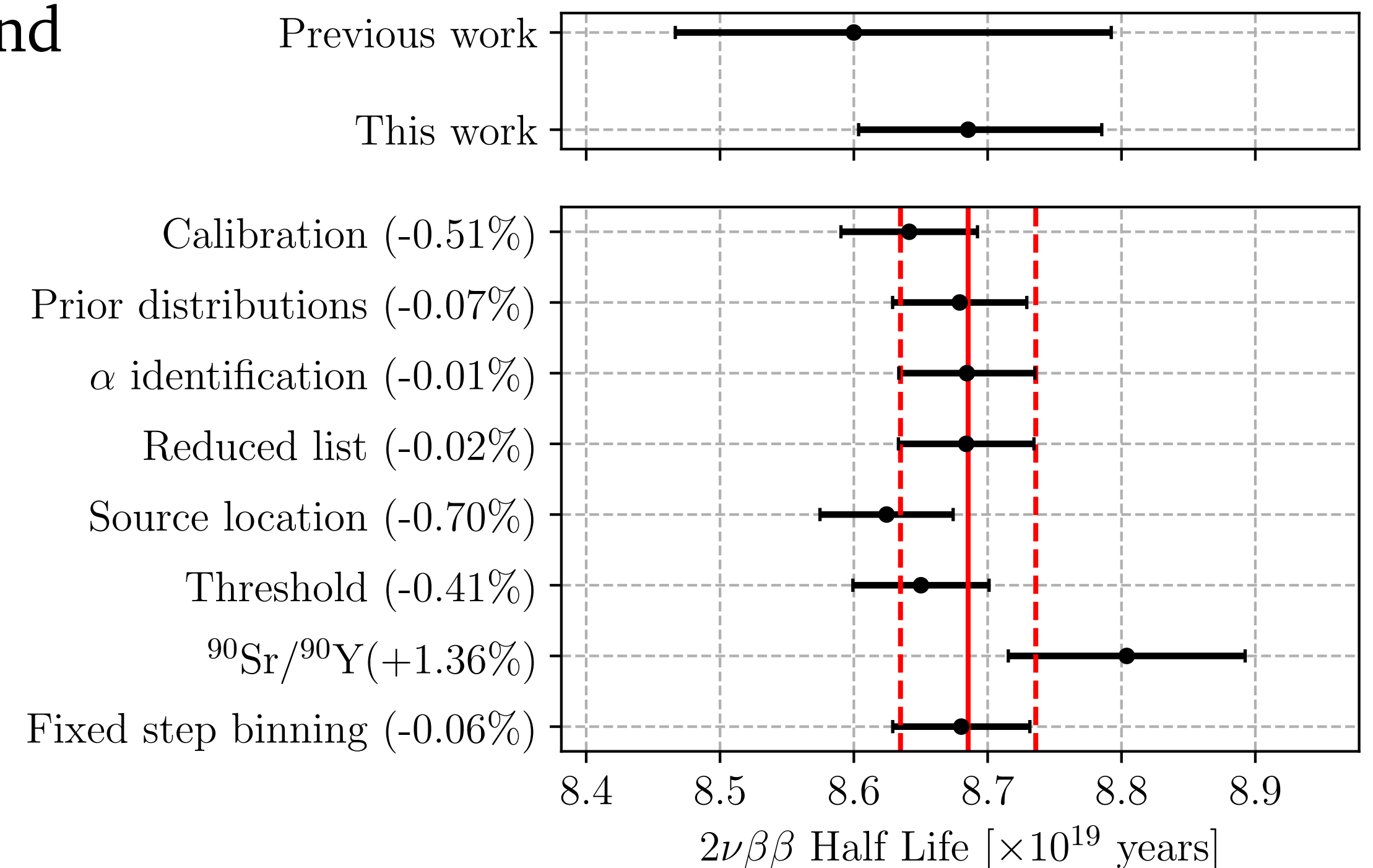
Final result:

$$T_{1/2}^{2\nu} = \left[8.69 \pm 0.05(\text{stat.})_{-0.09}^{+0.06}(\text{syst.}) \right] \times 10^{19} \text{yr}$$

In terms of NME:

$$\mathcal{M}_{2\nu}^{\text{eff}} = 0.0760 \begin{matrix} + 0.0006 \\ - 0.0007 \end{matrix}$$

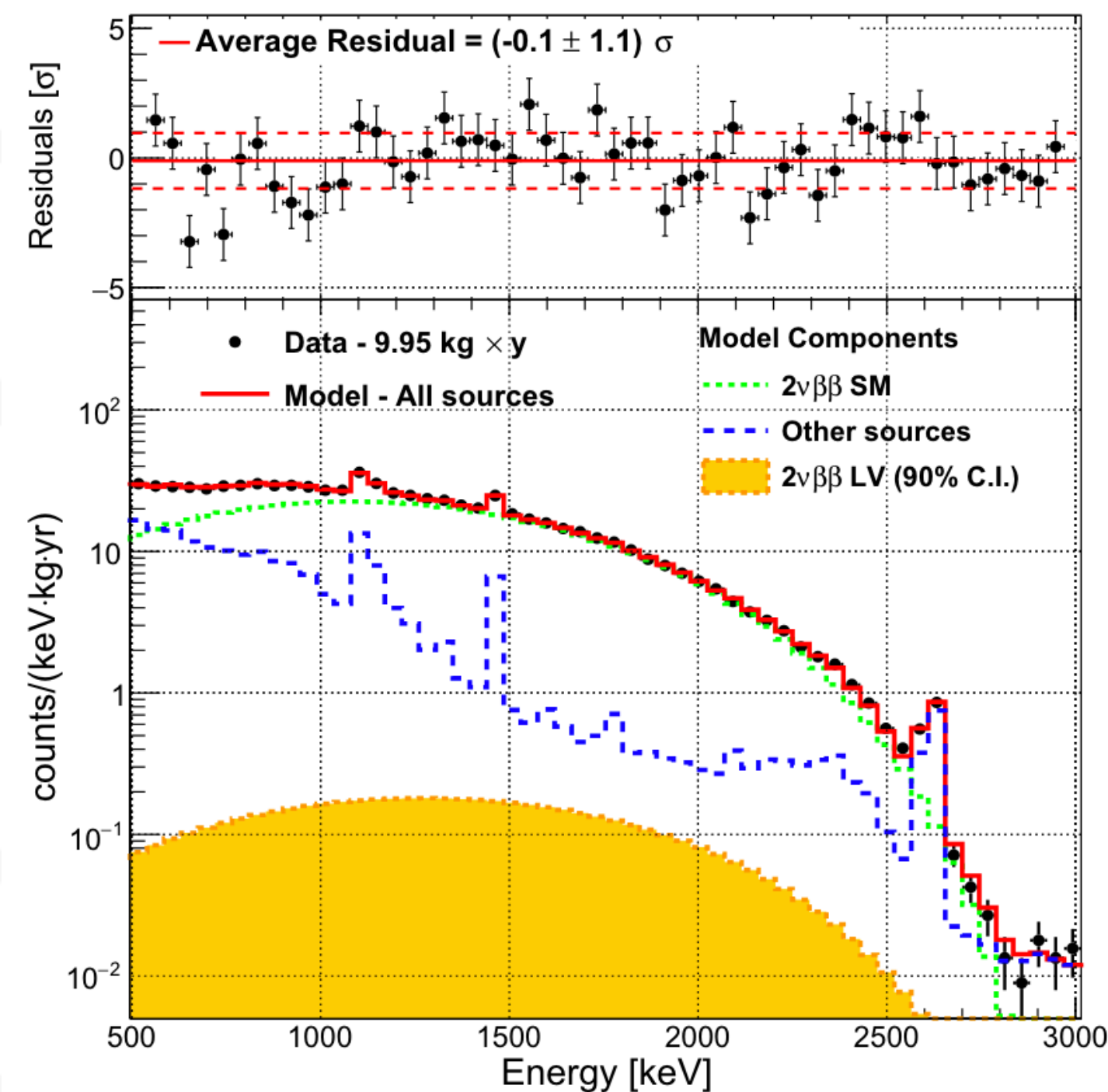
Published on PRL
Phys.Rev.Lett. 131 (2023) 22



From BM to BSM studies

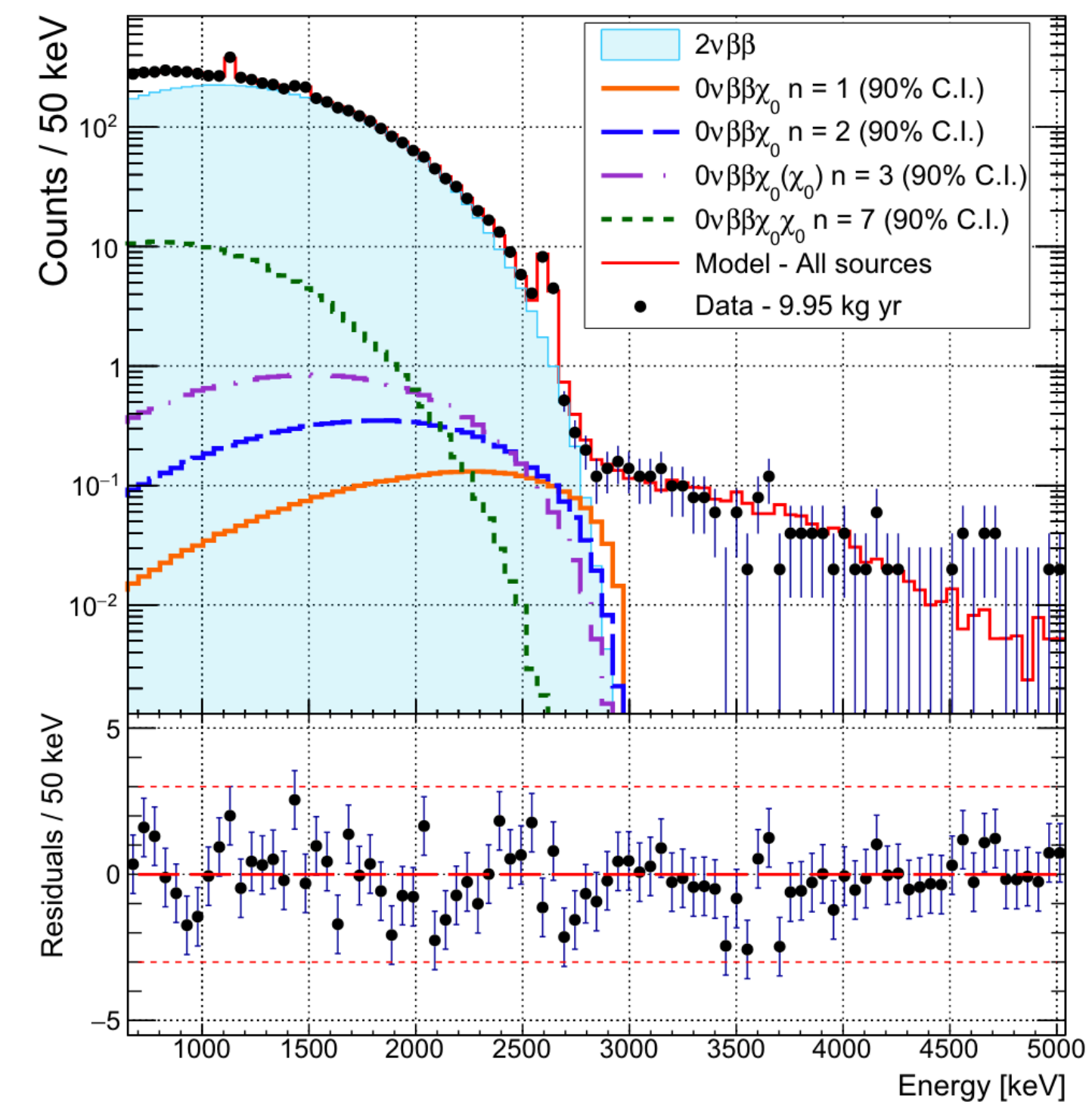
The background model serves as a starting point in the search for exotic double- β decays

LV $2\nu\beta\beta$ in CUPID-0 phase I



Phys. Rev. D **100**, 092002 (2019)

Majoron emitting modes in CUPID-0 phase I



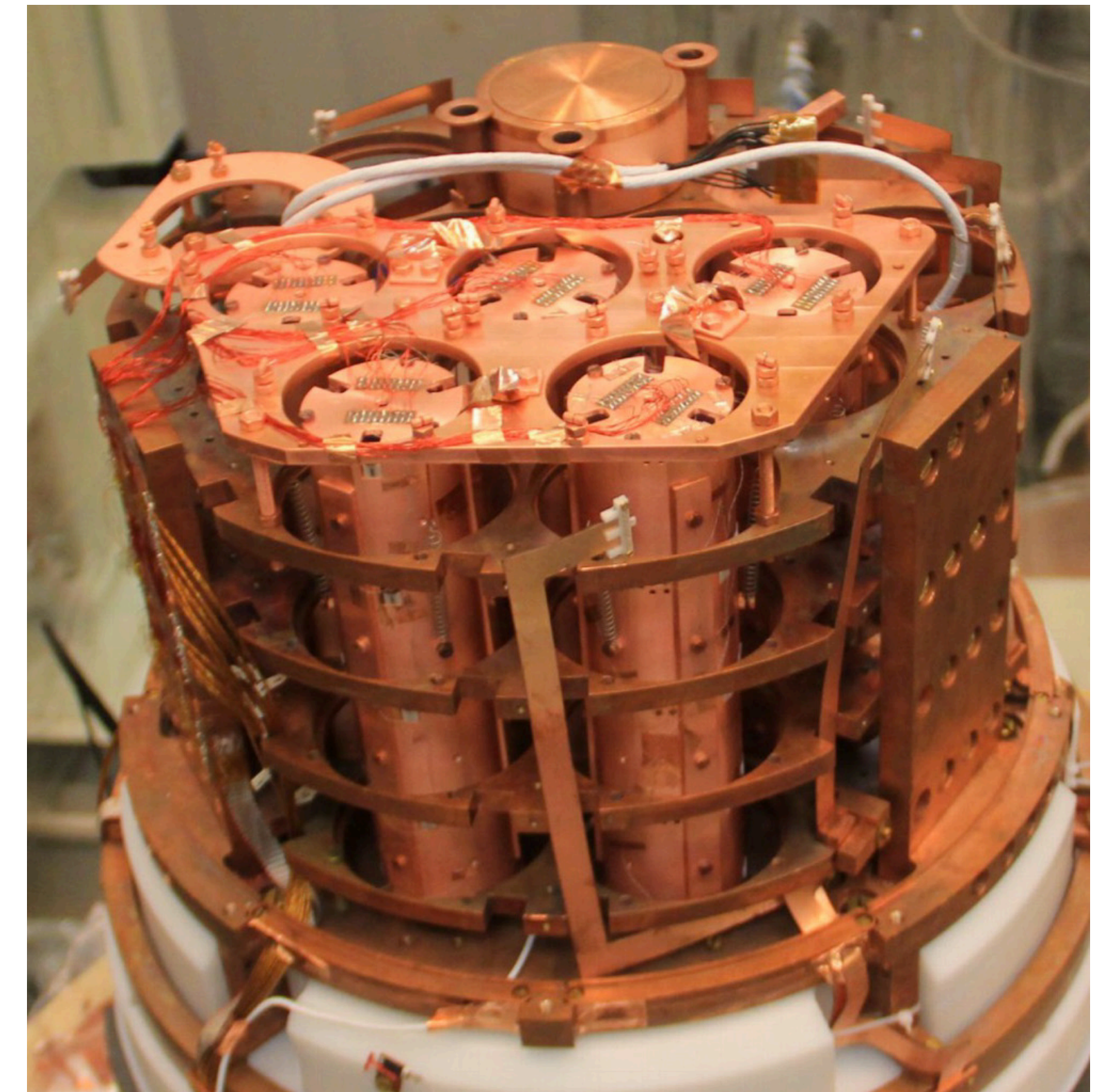
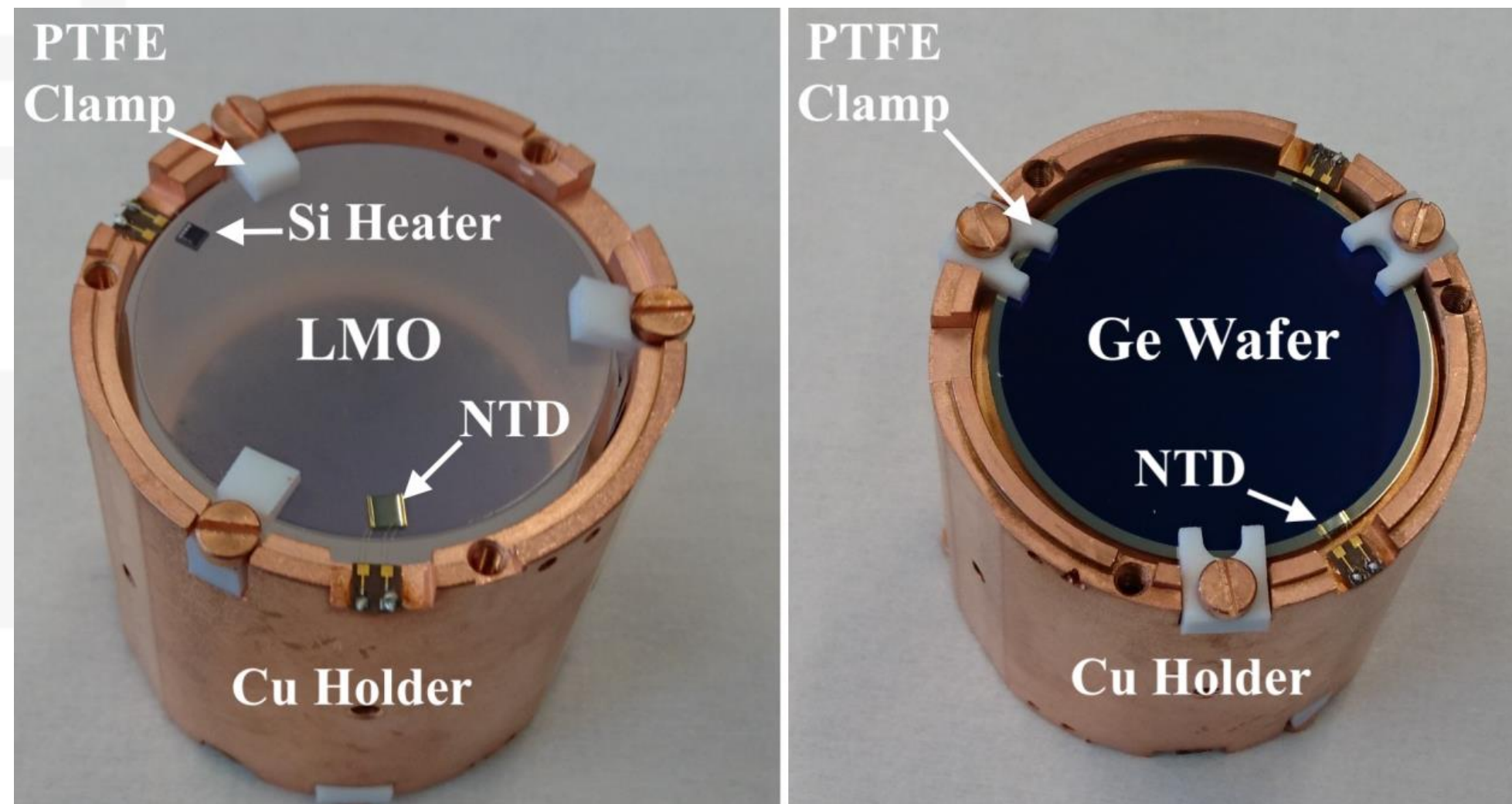
Phys. Rev. D **107**, 032006 (2023)

Outline

- 1 Double- β decays
- 2 Scintillating cryogenic calorimeters
- 3 CUPID-0 combined background model
- 4 CUPID-Mo BSM studies
- 5 CUPID sensitivity
- 6 Conclusion and outlook

The CUPID-Mo experiment

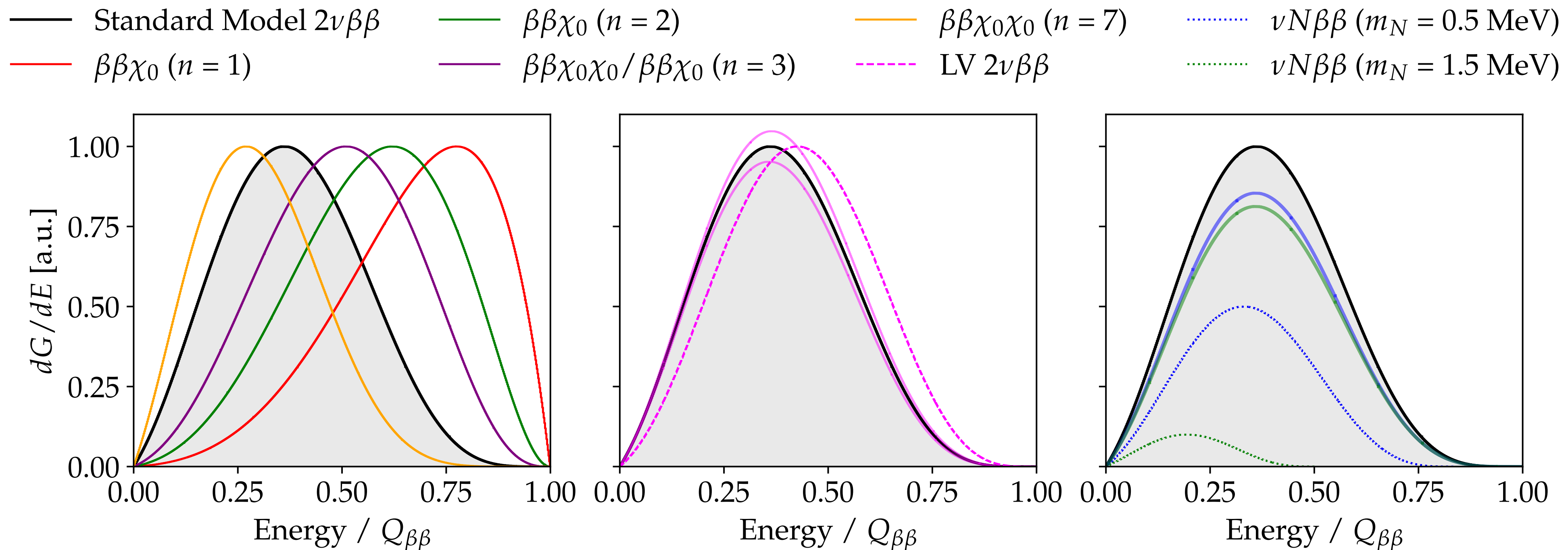
- ❖ 20 Li_2MoO_4 crystals enriched at $>95\%$ of ^{100}Mo + 20 Ge Light detectors
- ❖ Located at MODANE in EDELWEISS cryostat
- ❖ $Q_{\beta\beta}(^{100}\text{Mo}) \sim 3034 \text{ keV}$
- ❖ NTD-Ge thermistors as temperature sensors
- ❖ Total exposure: $2.71 \text{ kg} \times \text{yr}$



Spectral shape studies - introduction

Type I: e.g. **Majoron decays**, where the BSM decay is completely unrelated to the SM $2\nu\beta\beta \rightarrow$ **the lower the $2\nu\beta\beta$ decay rate, the higher the sensitivity (^{136}Xe)**

Type II: e.g. **Lorentz violation** and **Sterile neutrino emissions**, where the BSM process is in competition with the SM $2\nu\beta\beta$ and tends to decrease the decay rate \rightarrow **the higher the $2\nu\beta\beta$ decay rate, the higher the sensitivity (^{100}Mo)**



Spectral shape studies - analysis

1. Simulate the BSM spectra with GEANT4
2. Add the BSM spectrum into the background model fit
3. Extract from the fit the marginalised posterior p.d.f. over the parameter of interest for each BSM process and integrate it to get the limit
4. Systematics: Binning, source location, $2\nu\beta\beta$ bremsstrahlung ($\pm 10\%$), Energy scale (± 1 keV), Minimal model, $^{90}\text{Sr}/^{90}\text{Y}$

^{100}Mo $2\nu\beta\beta$ half-life

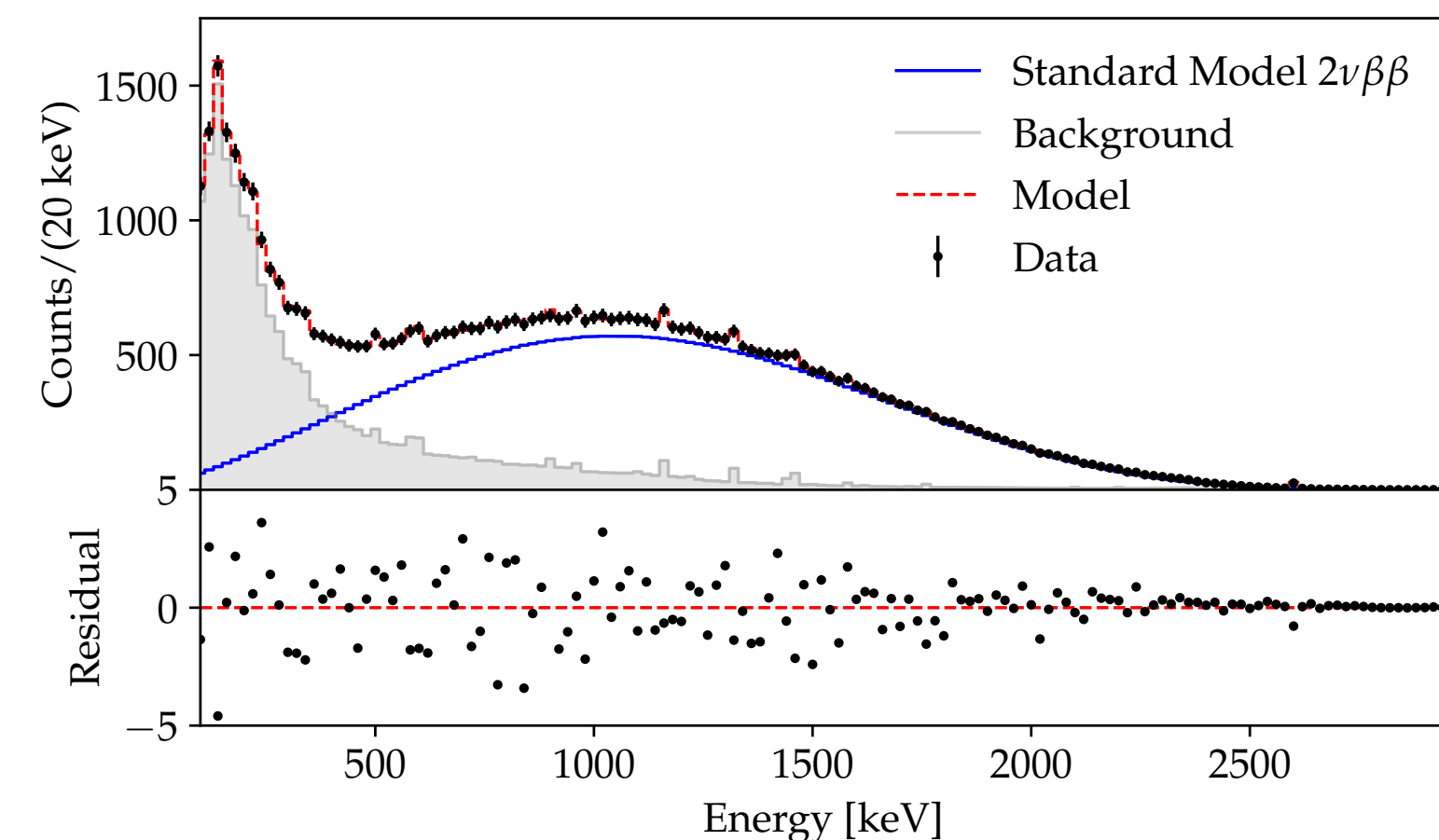
$$7.07 \pm 0.02(\text{stat.}) \pm 0.1(\text{syst.}) \times 10^{18}$$

Fixed $2\nu\beta\beta$ spectral shape under the SSD assumption

The result can be compared with the other experiments

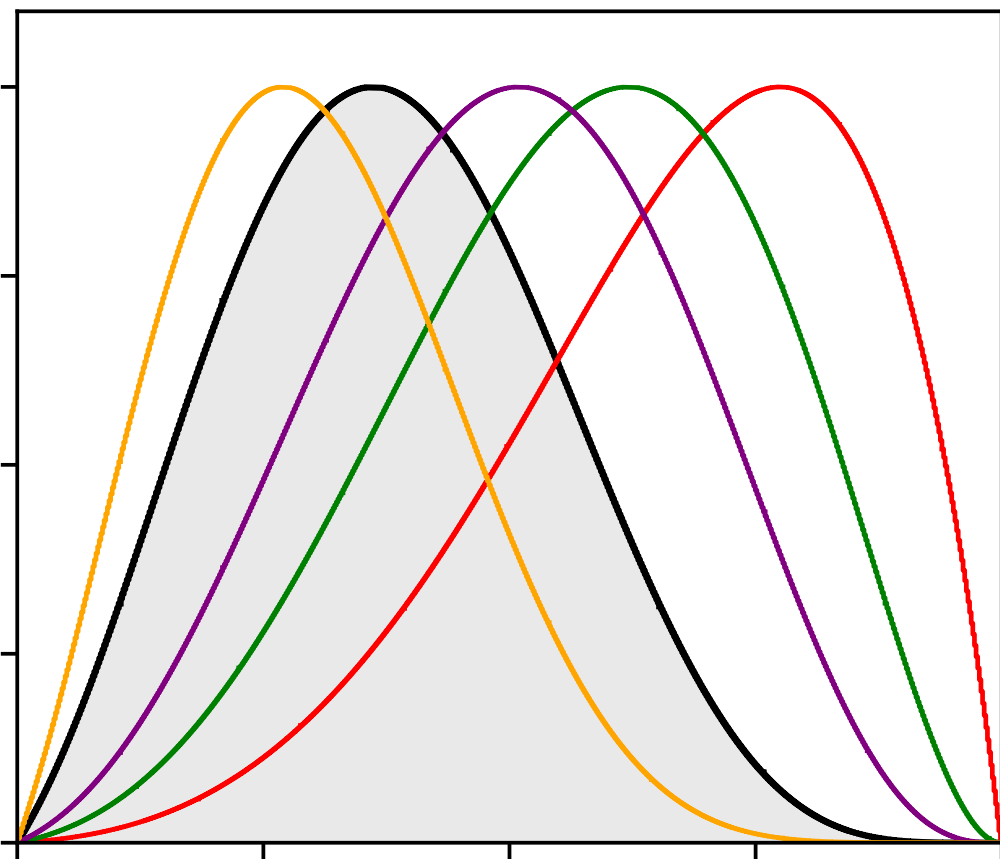
Fluctuating $2\nu\beta\beta$ spectral shape according to the improved description

Systematic effect never considered by any experiment before

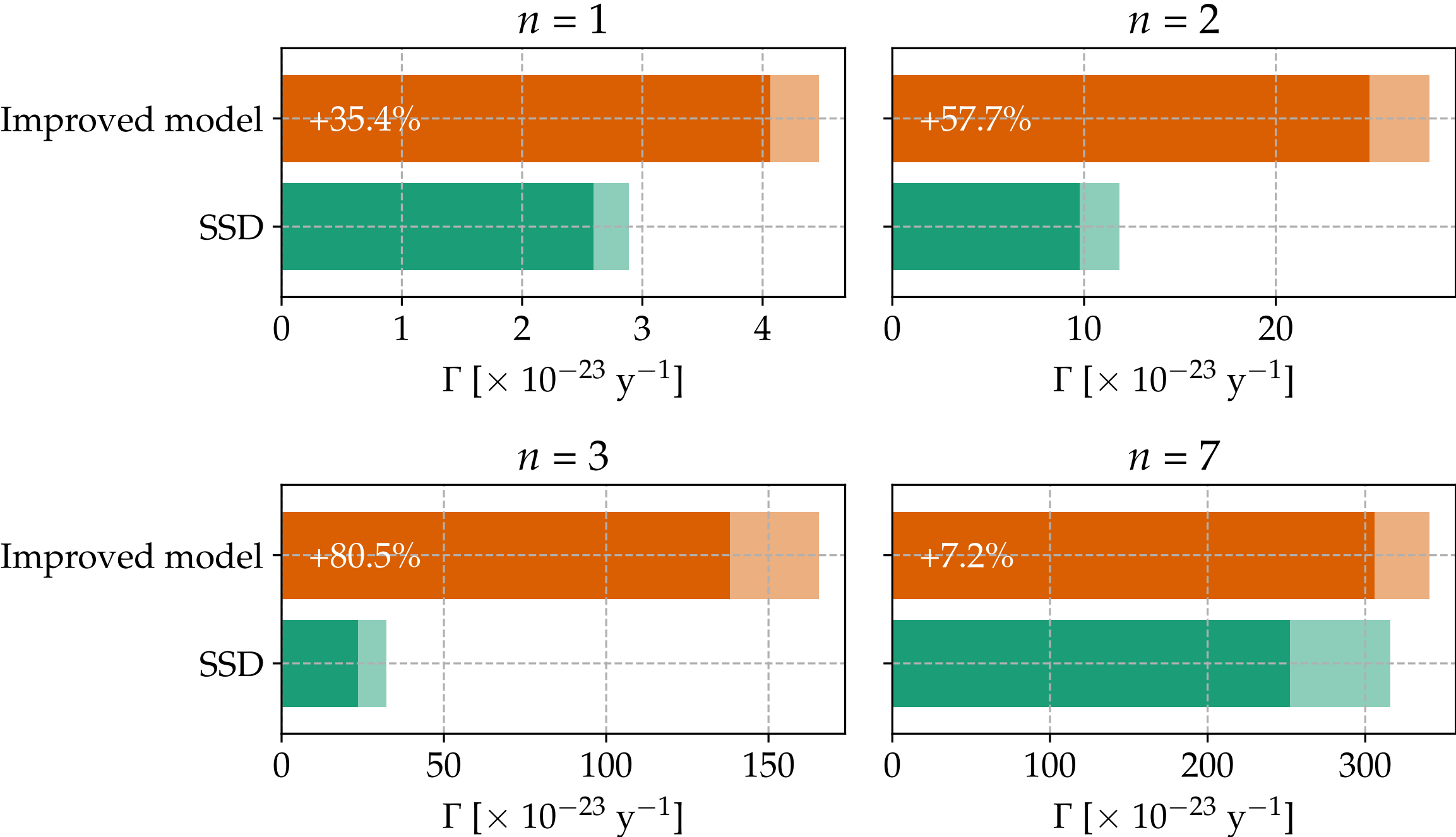


Phys.Rev.Lett. 131 (2023) 16, 162501

Results: Majoron emitting decays



- ❖ The improved model has a large impact on the final limit
- ❖ SSD limits are a factor 2 – 5 less stringent than NEMO-3, despite its exposure is 22 times higher than CUPID-Mo

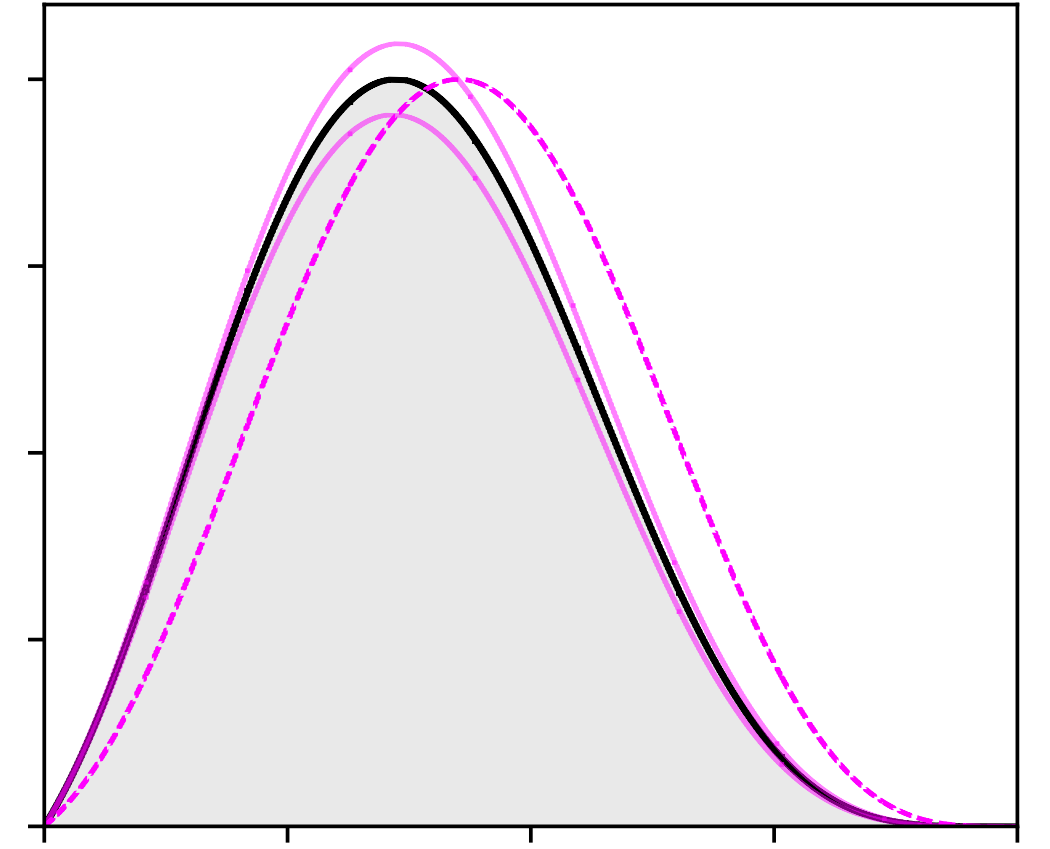


Decay mode	$T_{1/2}$		g_{ee}^M	
	limit SSD [y]	limit IM [y]	limit SSD	limit IM
	<i>this work</i>			
$\beta\beta\chi_0$ ($n = 1$)	2.4×10^{22}	1.6×10^{22}	$(4.0 - 6.9) \times 10^{-5}$	$(5.0 - 8.5) \times 10^{-5}$
$\beta\beta\chi_0$ ($n = 2$)	5.8×10^{21}	2.7×10^{21}	-	-
$\beta\beta\chi_0$ ($n = 3$)	2.2×10^{21}	0.5×10^{21}	0.053	0.112
$\beta\beta\chi_0\chi_0$ ($n = 3$)	2.2×10^{21}	0.5×10^{21}	2.1	3.1
$\beta\beta\chi_0\chi_0$ ($n = 7$)	2.2×10^{20}	2.0×10^{20}	2.2	2.3
	<i>NEMO-3 [57, 60]</i>			
$\beta\beta\chi_0$ ($n = 1$)	4.4×10^{22}		$(3.0 - 5.1) \times 10^{-5}$	
$\beta\beta\chi_0$ ($n = 2$)	9.9×10^{21}		-	
$\beta\beta\chi_0$ ($n = 3$)	4.4×10^{21}		0.023	
$\beta\beta\chi_0\chi_0$ ($n = 3$)	4.4×10^{21}		1.42	
$\beta\beta\chi_0\chi_0$ ($n = 7$)	1.2×10^{21}		1.15	

Results: Lorentz violating $2\nu\beta\beta$

- ❖ The countershaded operator can assume negative values \rightarrow negative fluctuations are allowed in the fit
- ❖ Strong anti correlation between the SM and LV components, it get worse with the improved model
- ❖ Double-sided limit at 90% C.I.

$$\dot{a}_{of}^{(3)} = 10 \cdot \frac{G_{SM}}{\delta G_{LV}} \cdot \frac{\Gamma_{LV}^m}{\Gamma_{SM}^m}$$



NEMO-3 limit

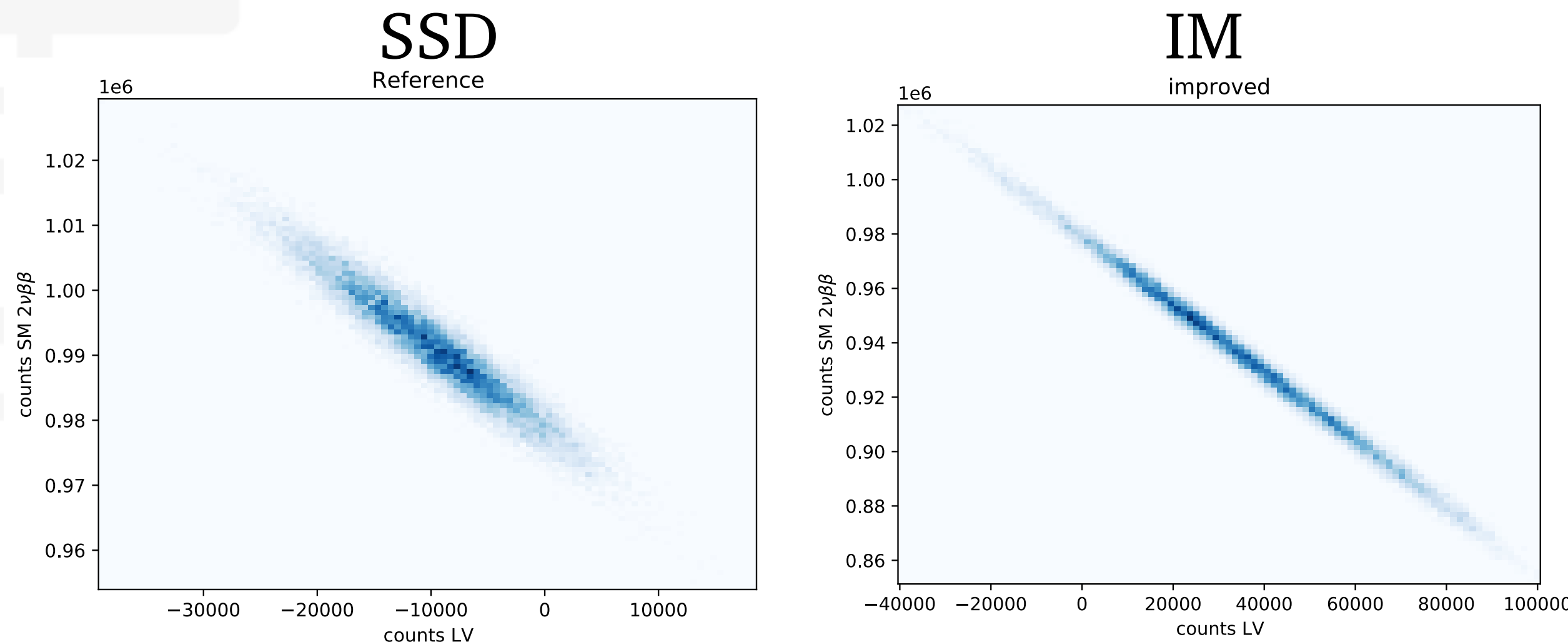
$$-4.2 \cdot 10^{-7} < \dot{a}_{of}^{(3)} < 3.5 \cdot 10^{-7}$$

CUPID-Mo SSD limit

$$-8.1 \cdot 10^{-6} < \dot{a}_{of}^{(3)} < 2.2 \cdot 10^{-6}$$

CUPID-Mo improved model limit

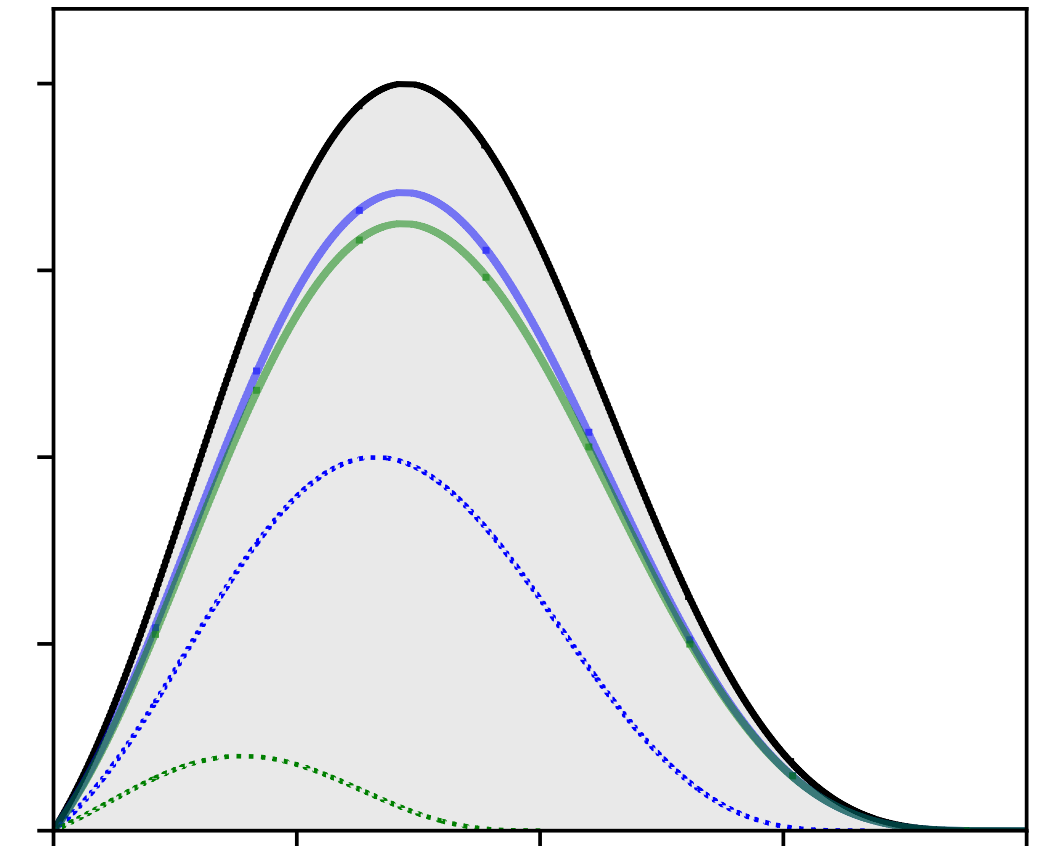
$$-6.5 \cdot 10^{-6} < \dot{a}_{of}^{(3)} < 2.5 \cdot 10^{-5}$$



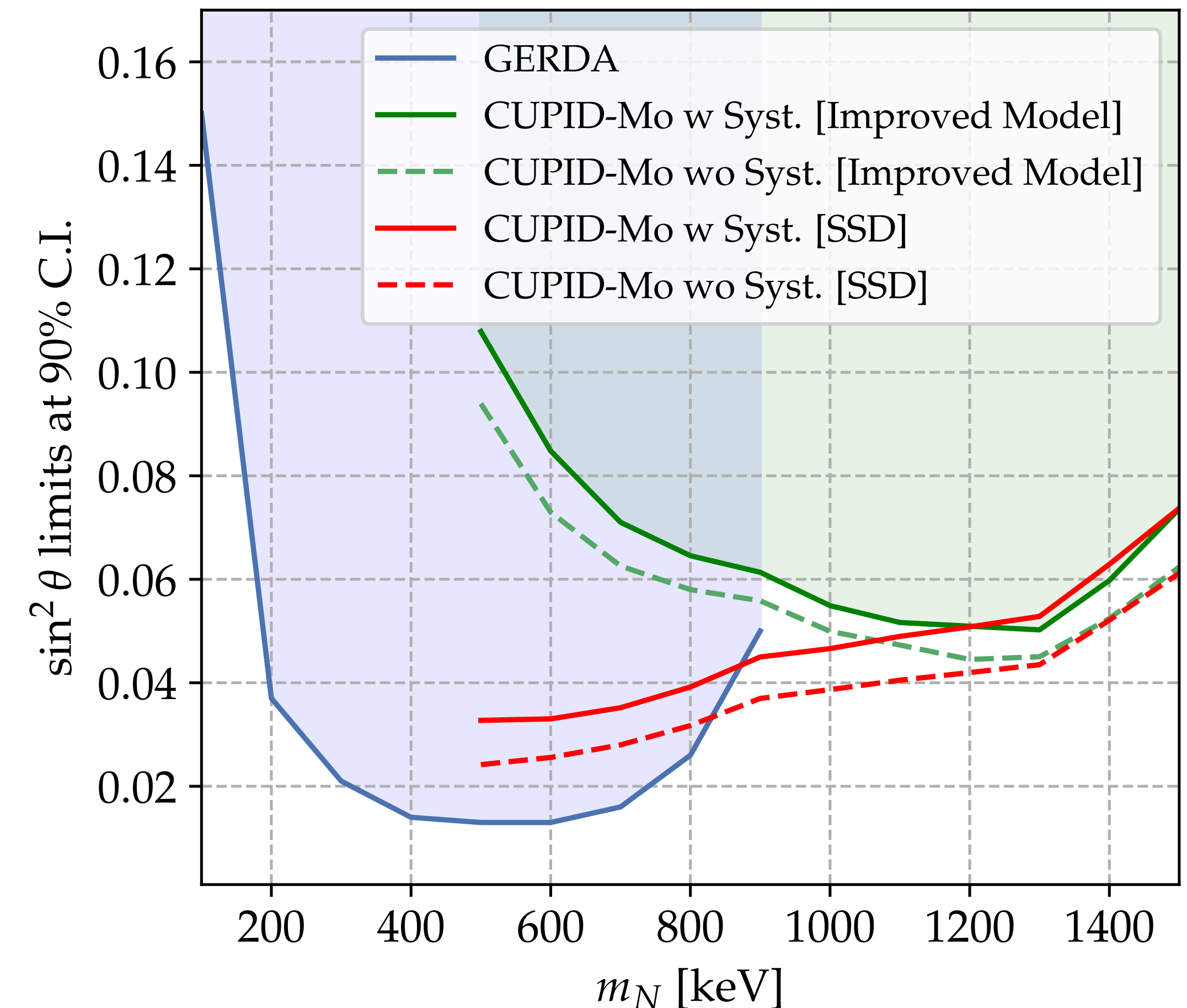
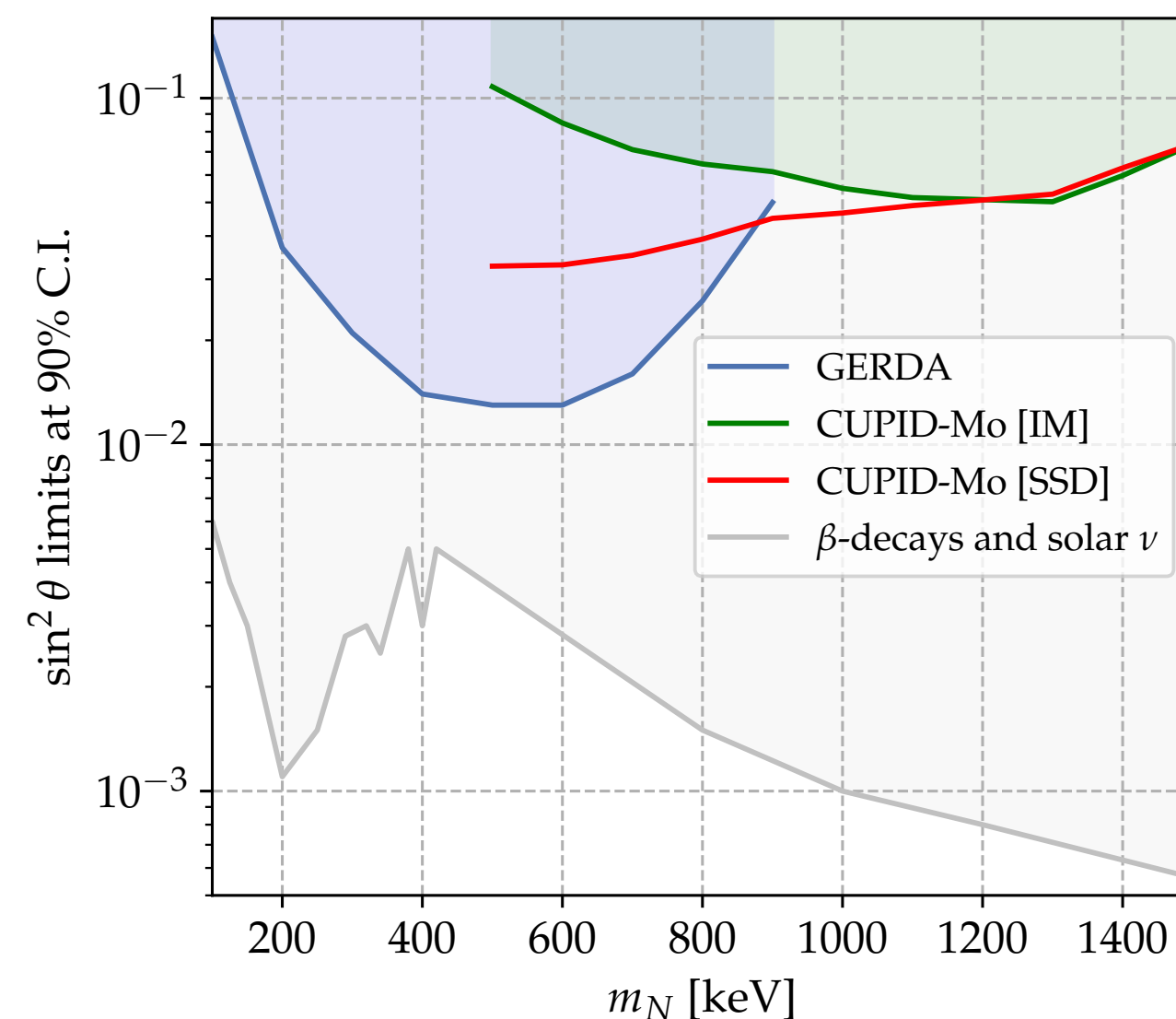
Results: Sterile neutrino emission

- ❖ First limit on sterile neutrino mixing angles from a bolometric experiment
- ❖ The large $Q_{\beta\beta}$ of ^{100}Mo allows to investigate a larger range
- ❖ The uncertainties on the $2\nu\beta\beta$ shape affects mostly the low values of m_N

$$\sin^2 \theta = \frac{G_{SM}}{2G_{\nu N}} \cdot \frac{\Gamma_{\nu N}^m}{\Gamma_{SM}^m}$$



Still far from exploring the not-excluded region



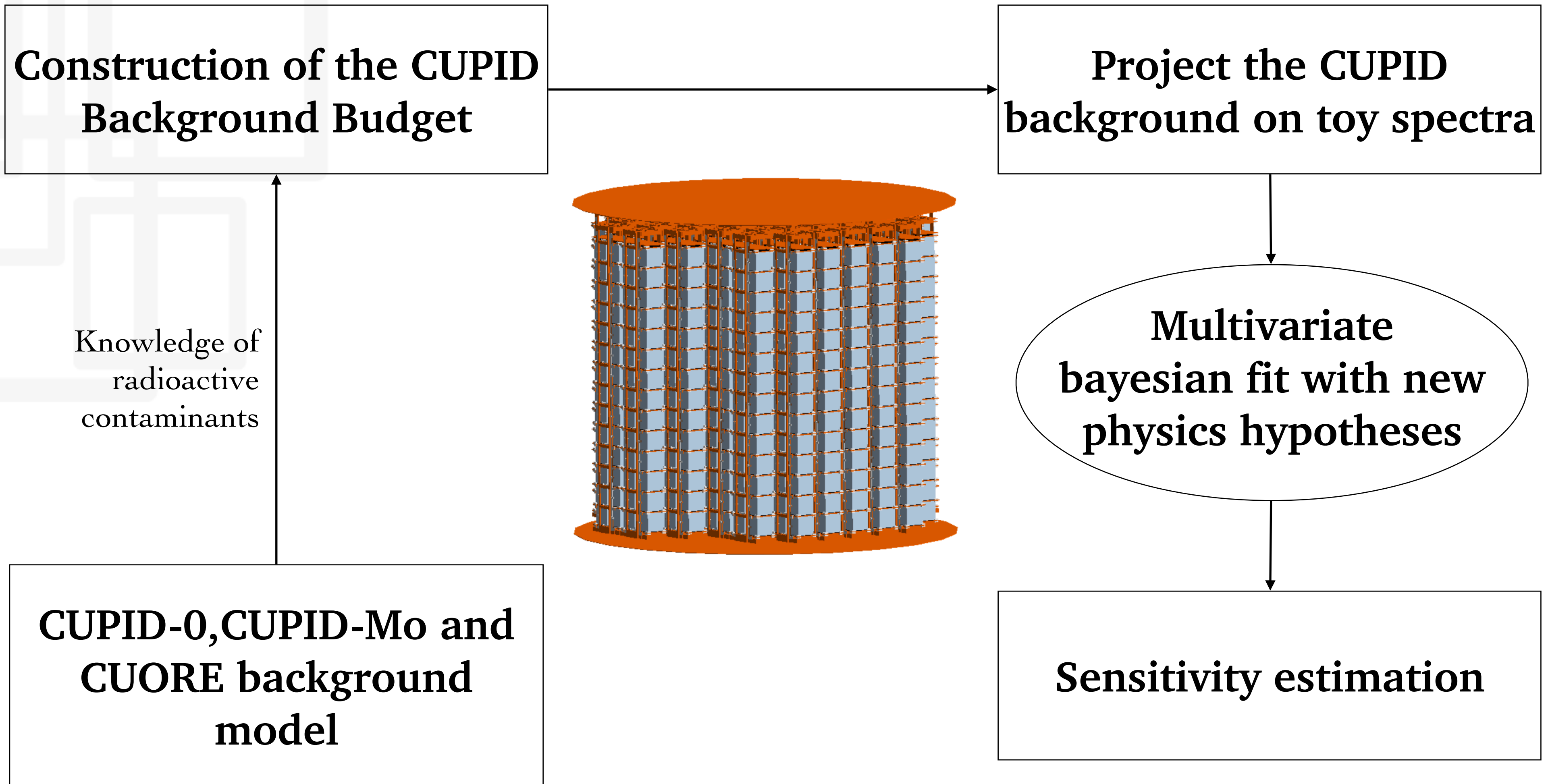
Outline

- 1 Double- β decays
- 2 Scintillating cryogenic calorimeters
- 3 CUPID-0 combined background model
- 4 CUPID-Mo BSM studies
- 5 CUPID sensitivity
- 6 Conclusion and outlook

CUPID will be the
experiment with the largest
amount of $2\nu\beta\beta$ events ever
collected



CUPID sensitivity studies



Preliminary background projection

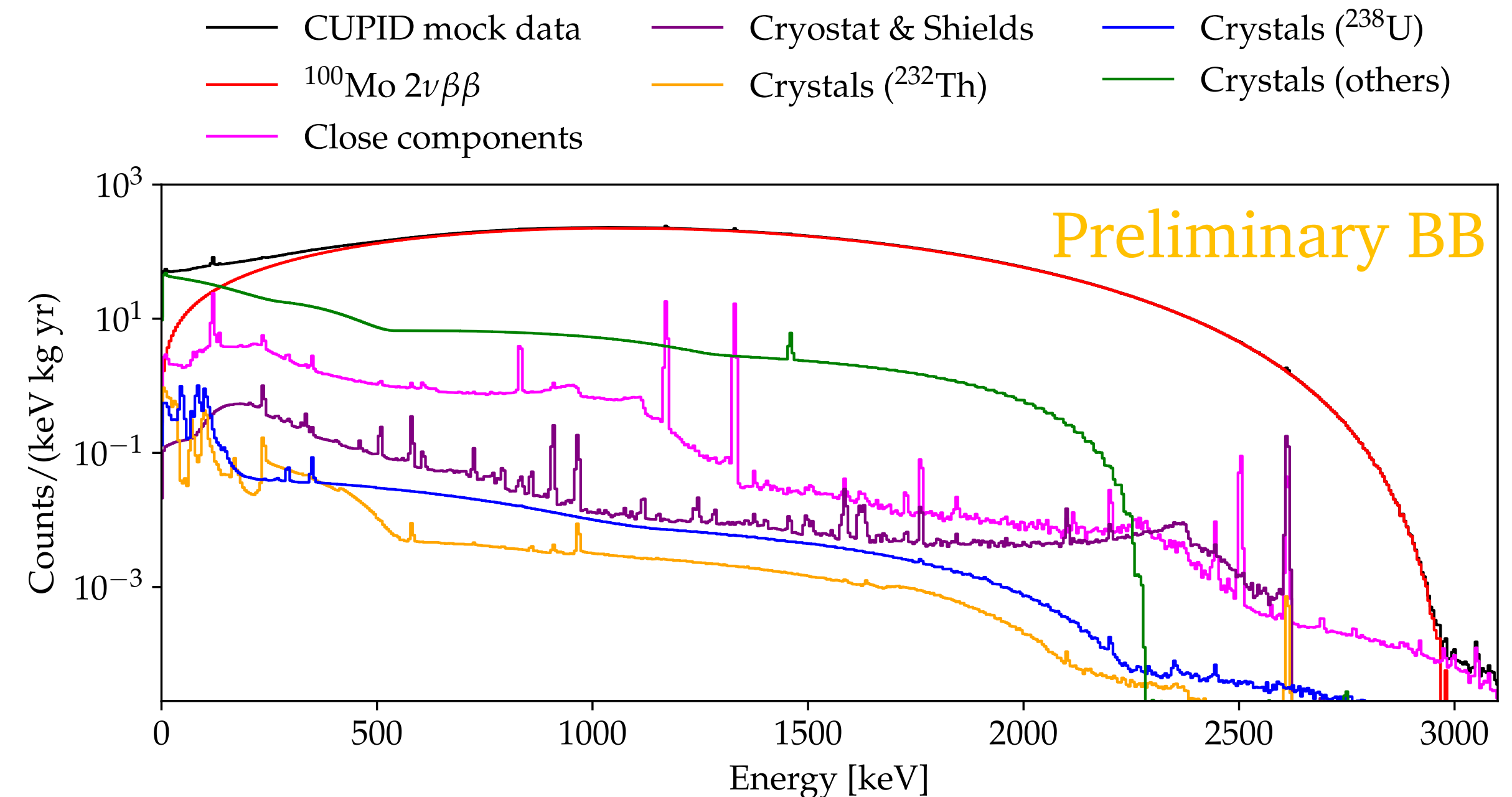
Most common radioactive sources:

- ❖ Long-living radioactive nuclei: ^{232}Th , ^{238}U and ^{40}K
- ❖ Anthropogenic radioactive isotopes such as ^{87}Rb and ^{90}Sr
- ❖ Cosmogenic activation products in holders and crystals

Only the SSD assumption for $2\nu\beta\beta$ was considered

Reference activities:

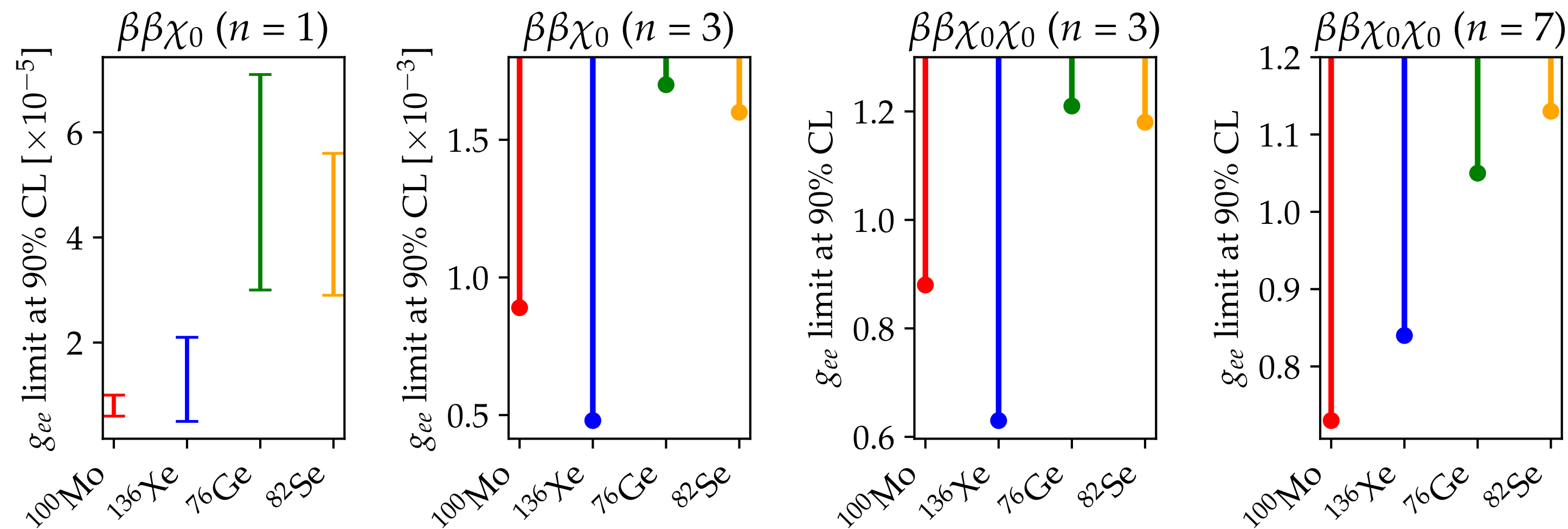
- ❖ Preliminary CUORE background model for cryostat and holders contaminants
- ❖ Preliminary CUPID-Mo background model for crystal contaminants
- ❖ ACTIVIA



Sensitivity: Majoron decays

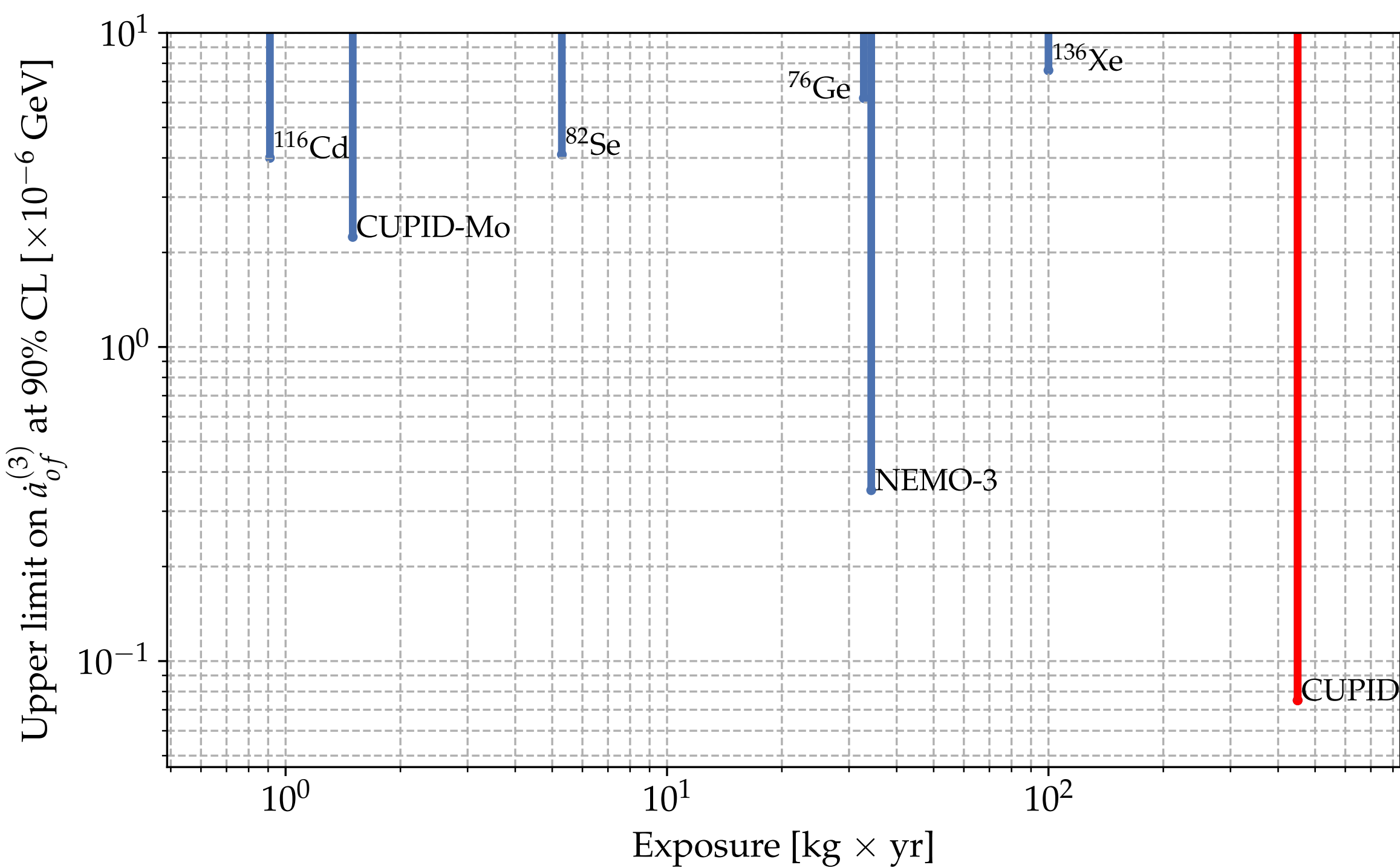
- ❖ 450 kg·yr of ^{100}Mo exposure (~ 2 years of CUPID data taking)
- ❖ With 450 kg·yr of ^{100}Mo the CUPID median exclusion sensitivity on the neutrino-Majoron coupling will be competitive with the limits set with ^{136}Xe

Decay mode	CUPID exclusion sensitivity		NEMO-3 [46, 135]	
	$T_{1/2}$ [yr]	g_{ee}^M	$T_{1/2}$ [yr]	g_{ee}^M
$\beta\beta\chi_0$ ($n = 1$)	1.2×10^{24}	$(0.6 - 1.0) \times 10^{-5}$	4.4×10^{22}	$(3.0 - 5.1) \times 10^{-5}$
$\beta\beta\chi_0$ ($n = 2$)	2.0×10^{23}	-	9.9×10^{21}	-
$\beta\beta\chi_0$ ($n = 3$)	7.5×10^{22}	0.0089	4.4×10^{21}	0.023
$\beta\beta\chi_0\chi_0$ ($n = 3$)	7.5×10^{22}	0.88	4.4×10^{21}	1.42
$\beta\beta\chi_0\chi_0$ ($n = 7$)	1.9×10^{22}	0.73	1.2×10^{21}	1.15



Sensitivity: Lorentz violating $2\nu\beta\beta$

With 450 kg·yr of ^{100}Mo we expect to reach the most stringent limit on the *countershaded* operator among $0\nu\beta\beta$ experiments



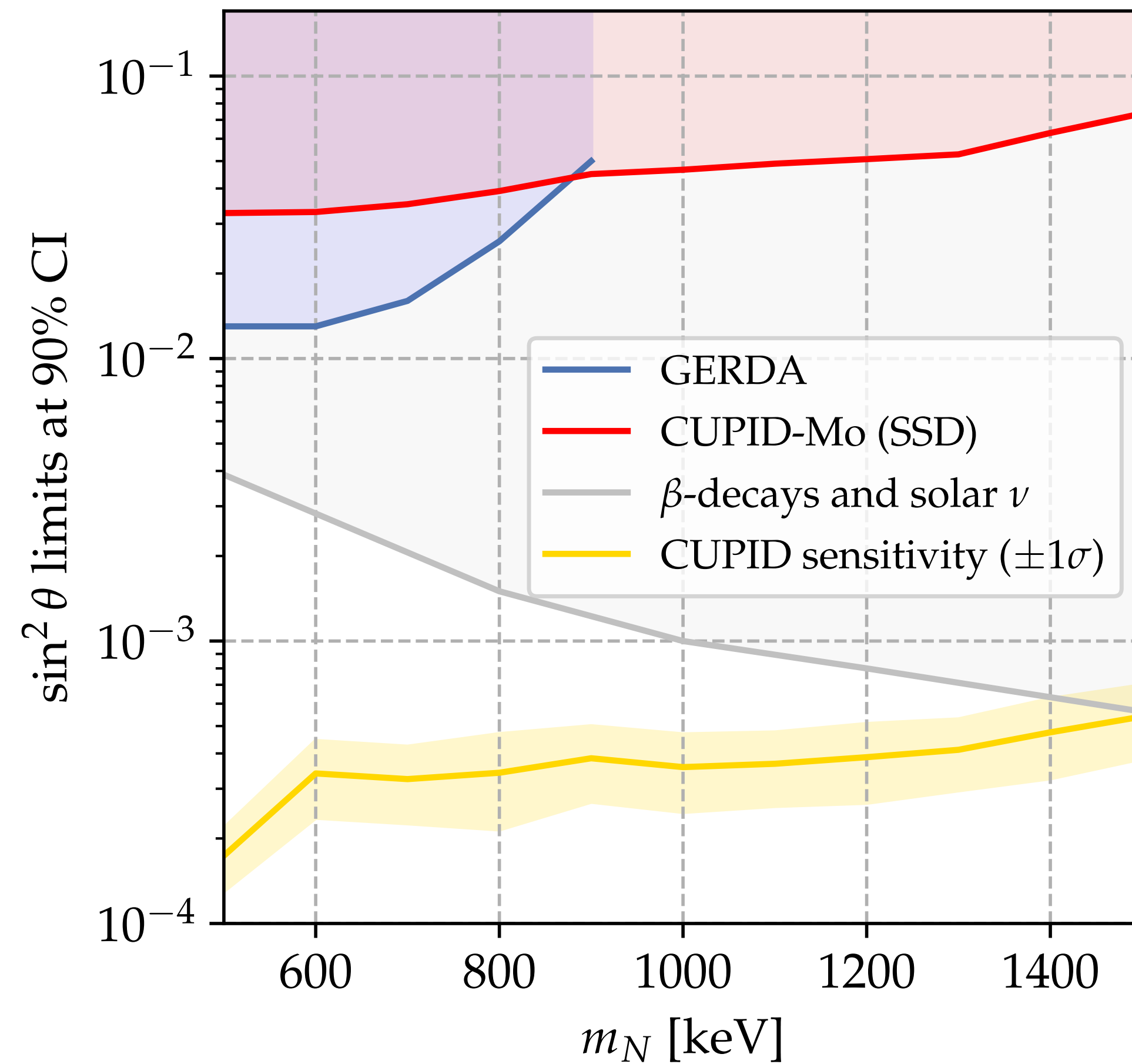
CUPID

$$-2.2 \cdot 10^{-7} < \dot{a}_{of}^{(3)} < 7.5 \cdot 10^{-8}$$

Isotope	Limit on $\dot{a}_{of}^{(3)}$ [GeV]
^{76}Ge	$(-2.7 < \dot{a}_{of}^{(3)} < 6.2) \cdot 10^{-6}$
^{82}Se	$\dot{a}_{of}^{(3)} < 4.1 \cdot 10^{-6}$
^{136}Xe	$-2.65 \cdot 10^{-5} < \dot{a}_{of}^{(3)} < 7.6 \cdot 10^{-6}$
^{116}Cd	$\dot{a}_{of}^{(3)} < 4.0 \cdot 10^{-6}$
^{100}Mo	$(-4.2 < \dot{a}_{of}^{(3)} < 3.5) \cdot 10^{-7}$
^3H	$ \dot{a}_{of}^{(3)} < 3.0 \cdot 10^{-8}$

Sensitivity: Sterile neutrino emission

CUPID median exclusion sensitivity with 450 kg·yr of ^{100}Mo



Outline

- 1 Double- β decays
- 2 Scintillating cryogenic calorimeters
- 3 CUPID-0 combined background model
- 4 CUPID-Mo BSM studies
- 5 CUPID sensitivity
- 6 Conclusion and outlook

Conclusions

- ❖ The increasing interest in the search for $0\nu\beta\beta$ leads experiments to reach higher and higher exposures
- ❖ The large statistic of $2\nu\beta\beta$ events collected by these experiments can be used to study the nuclear properties of $2\nu\beta\beta$ and to search for exotic double- β decays
- ❖ On this purpose, scintillating cryogenic calorimeters is a promising technology due to its excellent resolution, high detection efficiency and particle identification that allow the accurate background reconstruction
- ❖ In CUPID-0 we measured the unprecedented sensitivity the half-life of ^{82}Se $2\nu\beta\beta$ thanks to the excellent data reconstruction provided by the combined background model
- ❖ In CUPID-Mo we demonstrated the potential of Li_2MoO_4 based detectors in the search for exotic double- β decays, considering a systematic effect never considered before and paving the way for the future experiments
- ❖ The CUPID exclusion sensitivity demonstrates that we expect to set competitive limits on the exotic double- β decays parameters



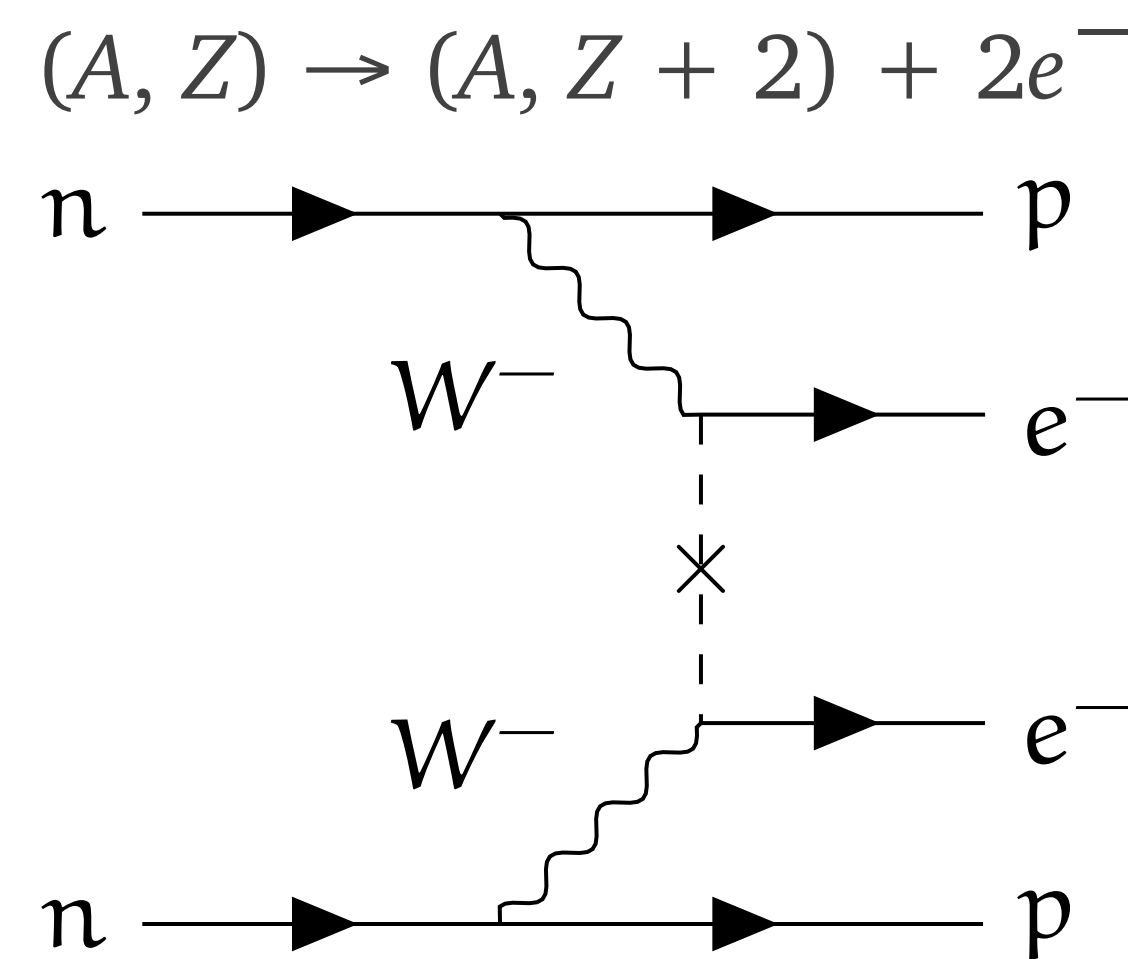
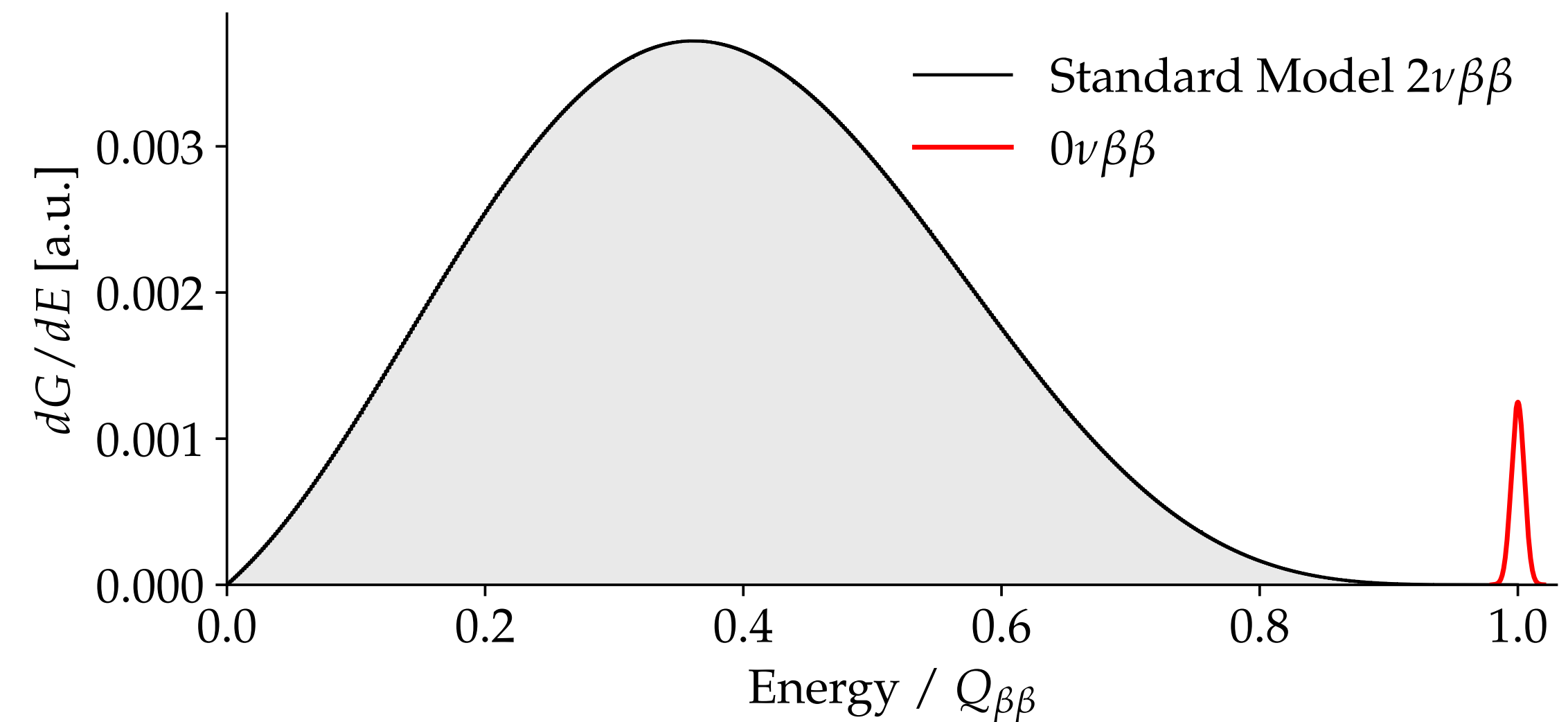
Thanks for the attention

Backup slides

Neutrinoless double- β decay ($0\nu\beta\beta$)

$0\nu\beta\beta$ is a nuclear process implying the decay of two neutrons into protons and electrons without the emission of antineutrinos.

- ❖ It would establish a total lepton number violation ($\Delta L = 2$) not conserving the B-L symmetry of the SM
- ❖ Only practical way to probe that neutrinos are Majorana particles, validating the so called “see-saw” mechanism
- ❖ Its signature is a sharp peak at the Q-value of the decay

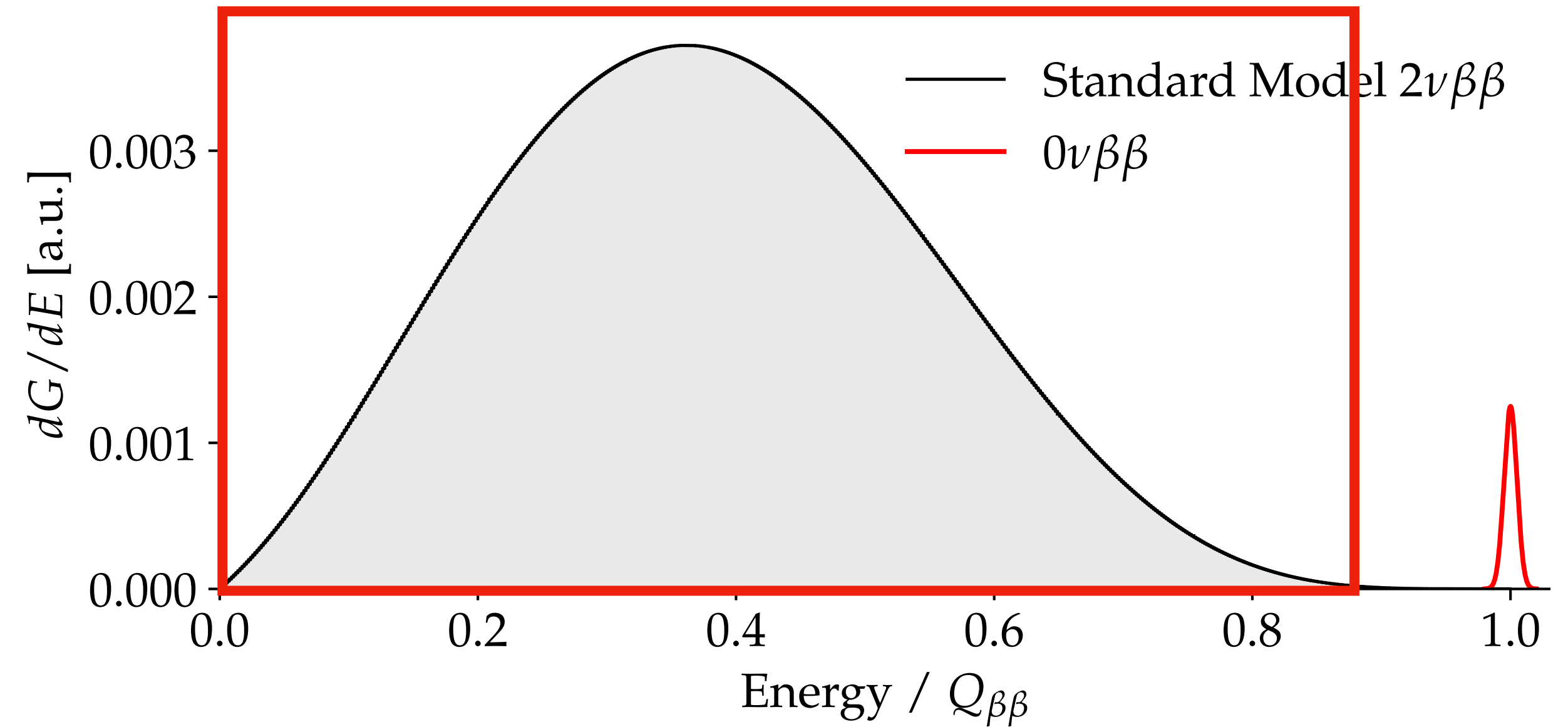
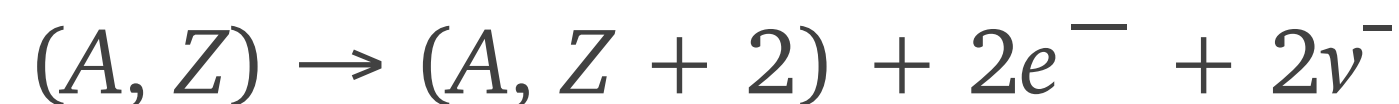
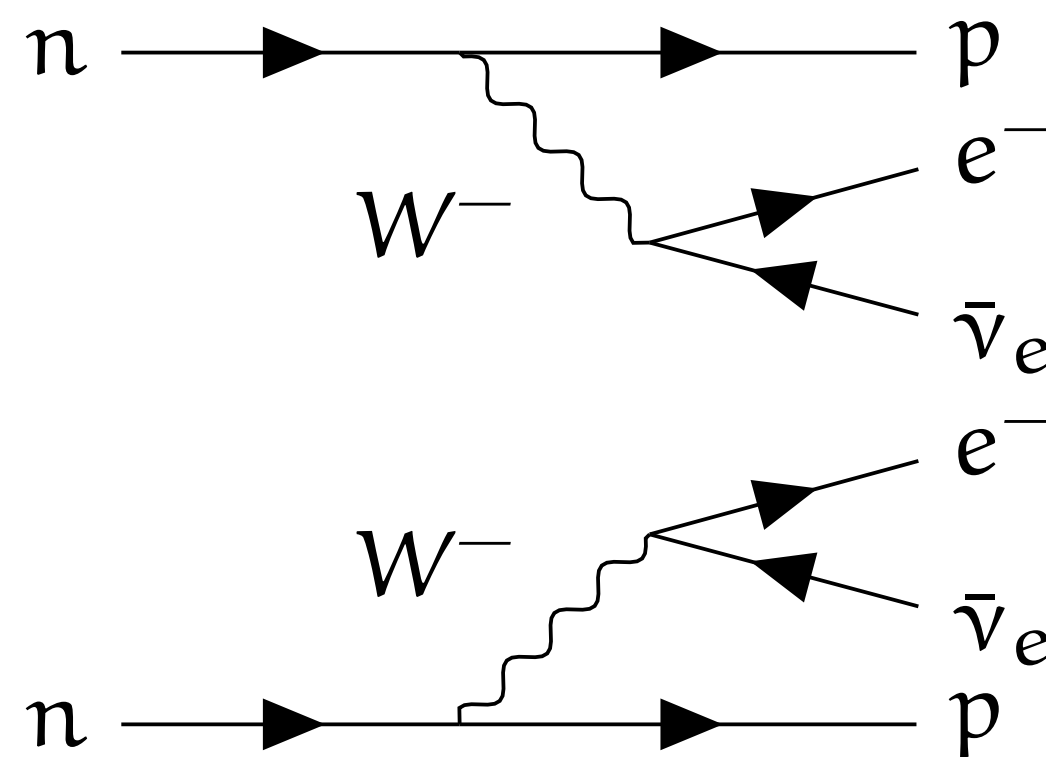


Isotope	$T_{1/2}^{0\nu}$ [y]
^{76}Ge	$> 1.8 \times 10^{26}$
^{82}Se	$> 4.6 \times 10^{24}$
^{100}Mo	$> 1.8 \times 10^{24}$
^{116}Cd	$> 2.2 \times 10^{23}$
^{130}Te	$> 2.2 \times 10^{25}$
^{136}Xe	$> 2.3 \times 10^{26}$

Two-neutrinos double- β decay ($2\nu\beta\beta$)

$0\nu\beta\beta$ is a nuclear process implying the decay of two neutrons into protons, electrons and antineutrinos.

- ❖ SM allowed second order weak process which half-life spans the range 10^{18} - 10^{21} years
- ❖ It has been observed for several nuclei

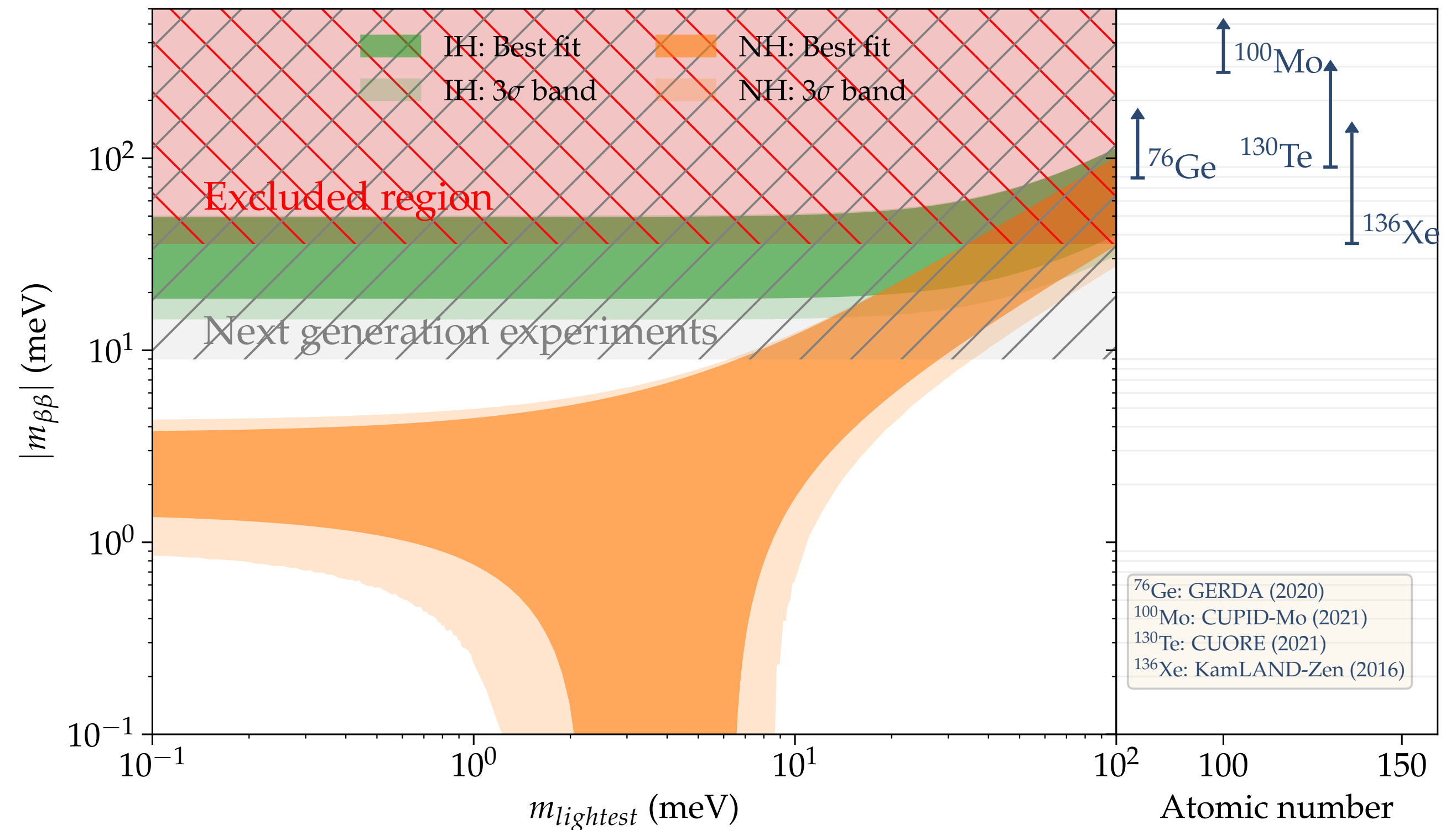


Isotope	$Q_{\beta\beta}$ [MeV]	$T_{1/2}^{2\nu}$ [yr]
^{48}Ca	4.263	$6.4^{+0.7}_{-0.6} \text{ (stat.) } ^{+1.2}_{-0.9} \text{ (syst.) } \times 10^{19}$
^{76}Ge	2.039	$2.022 \pm 0.018 \text{ (stat.) } \pm 0.038 \text{ (syst.) } \times 10^{21}$
^{82}Se	2.998	$8.69 \pm 0.05 \text{ (stat.) } ^{+0.09}_{-0.06} \text{ (syst.) } \times 10^{19}$
^{96}Zr	3.348	$2.35 \pm 0.14 \text{ (stat.) } \pm 0.16 \text{ (syst.) } \times 10^{19}$
^{100}Mo	3.035	$7.07 \pm 0.02 \text{ (stat.) } \pm 0.11 \text{ (syst.) } \times 10^{18}$
^{116}Cd	2.813	$2.63 \pm 0.01 \text{ (stat.) } ^{+0.11}_{-0.13} \text{ (syst.) } \times 10^{19}$
^{130}Te	2.527	$8.76^{+0.09}_{-0.07} \text{ (stat.) } ^{+0.14}_{-0.17} \text{ (syst.) } \times 10^{20}$
^{136}Xe	2.459	$2.165 \pm 0.016 \text{ (stat.) } \pm 0.059 \text{ (syst.) } \times 10^{21}$
^{150}Nd	3.371	$9.34 \pm 0.22 \text{ (stat.) } ^{+0.62}_{-0.60} \text{ (syst.) } \times 10^{18}$

$0\nu\beta\beta$ experimental limits

- ❖ The uncertainties on the nuclear matrix elements affects the limits on the effective Majorana mass
- ❖ The lobster plot shows which regions are favoured assuming Inverted Hierarchy and Normal Hierarchy

Isotope	$T_{1/2}^{0\nu}$ [y]	$m_{\beta\beta}$ [eV]
^{76}Ge	$> 1.8 \times 10^{26}$	$< (0.079 - 0.180)$
^{82}Se	$> 4.6 \times 10^{24}$	$< (0.263 - 0.545)$
^{100}Mo	$> 1.8 \times 10^{24}$	$< (0.280 - 0.490)$
^{116}Cd	$> 2.2 \times 10^{23}$	$< (1.0 - 1.7)$
^{130}Te	$> 2.2 \times 10^{25}$	$< (0.090 - 0.305)$
^{136}Xe	$> 2.3 \times 10^{26}$	$< (0.036 - 0.156)$



$$m_{\beta\beta} = \left| \sum_{j=1}^3 U_{ej}^2 m_j \right| = \left| U_{e1}^2 m_1 + U_{e2}^2 e^{i\beta_1} m_2 + U_{e3}^2 e^{i\beta_2} m_3 \right|$$

Experimental sensitivity

We are looking for an extremely rare decay whose signature is a sharp peak, the sensitivity is half-life corresponding to the maximum signal that can be hidden by a background fluctuation:

$$T_{1/2}^{0\nu}(n_\sigma) = \frac{\ln 2}{n_\sigma} \frac{N_A i \epsilon}{A} \sqrt{\frac{Mt}{(BI)\Delta E}}$$

Where it assumes Poissonian background fluctuations in the region of interest (ROI). The dependence of the square root of the exposure (Mt) is the main limiting factor.

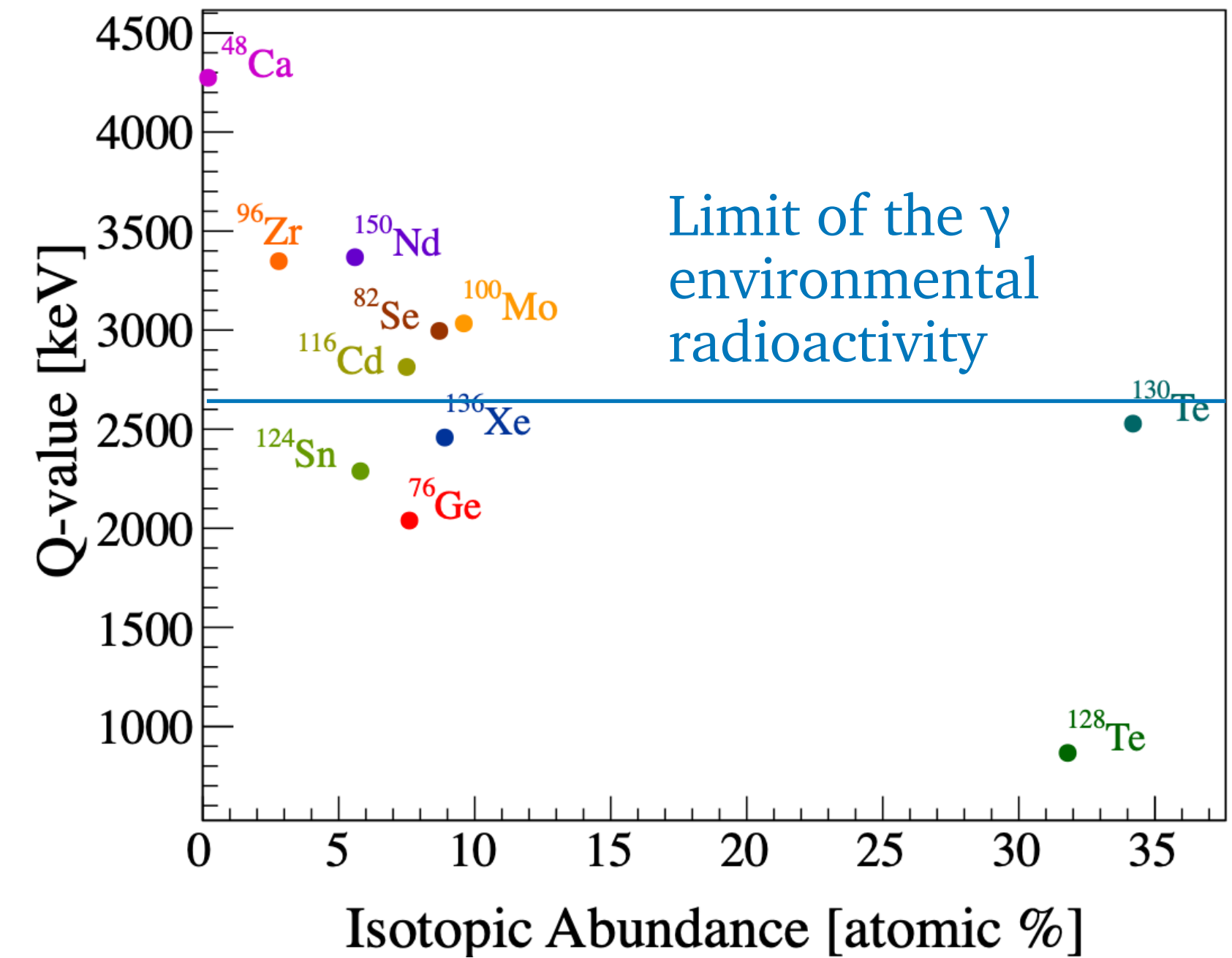
Nevertheless, if we assume zero-background in the ROI:

$$T_{0\nu} > \ln 2 \frac{x \eta \epsilon N_A}{A} \frac{Mt}{n_L}$$

Zero background is the key ingredient to boost the sensitivity!

Experimental sensitivity

- ❖ **Large exposure** (Mt) necessary to reach high sensitivities (enrichment required for most of the candidate isotopes)
- ❖ **High Q-value**, for larger PSF and reject most of the environmental radioactivity
- ❖ **High detection efficiency** (ϵ)
- ❖ **High energy resolution** (ΔE)



- ❖ (BI) = background index

Formula with background:

$$T_{1/2}^{0\nu}(n_\sigma) = \frac{\ln 2}{n_\sigma} \frac{N_A i \epsilon}{A} \sqrt{\frac{Mt}{(BI) \Delta E}}$$

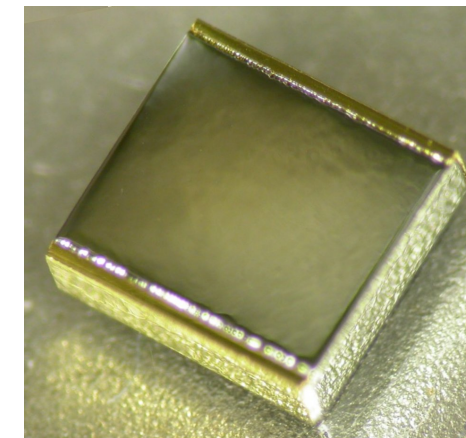
Formula without background:

$$T_{0\nu} > \ln 2 \frac{x \eta \epsilon N_A}{A} \frac{Mt}{n_L}$$

NTD-Ge thermistors

- ▶ For macro-calorimeters the best temperature sensor is the Neutrons Transmutation Doped Ge thermistor, Small Ge crystals with a extremely high and uniform distribution of impurities, obtained exposing the the Ge-wafer to a neutron beam

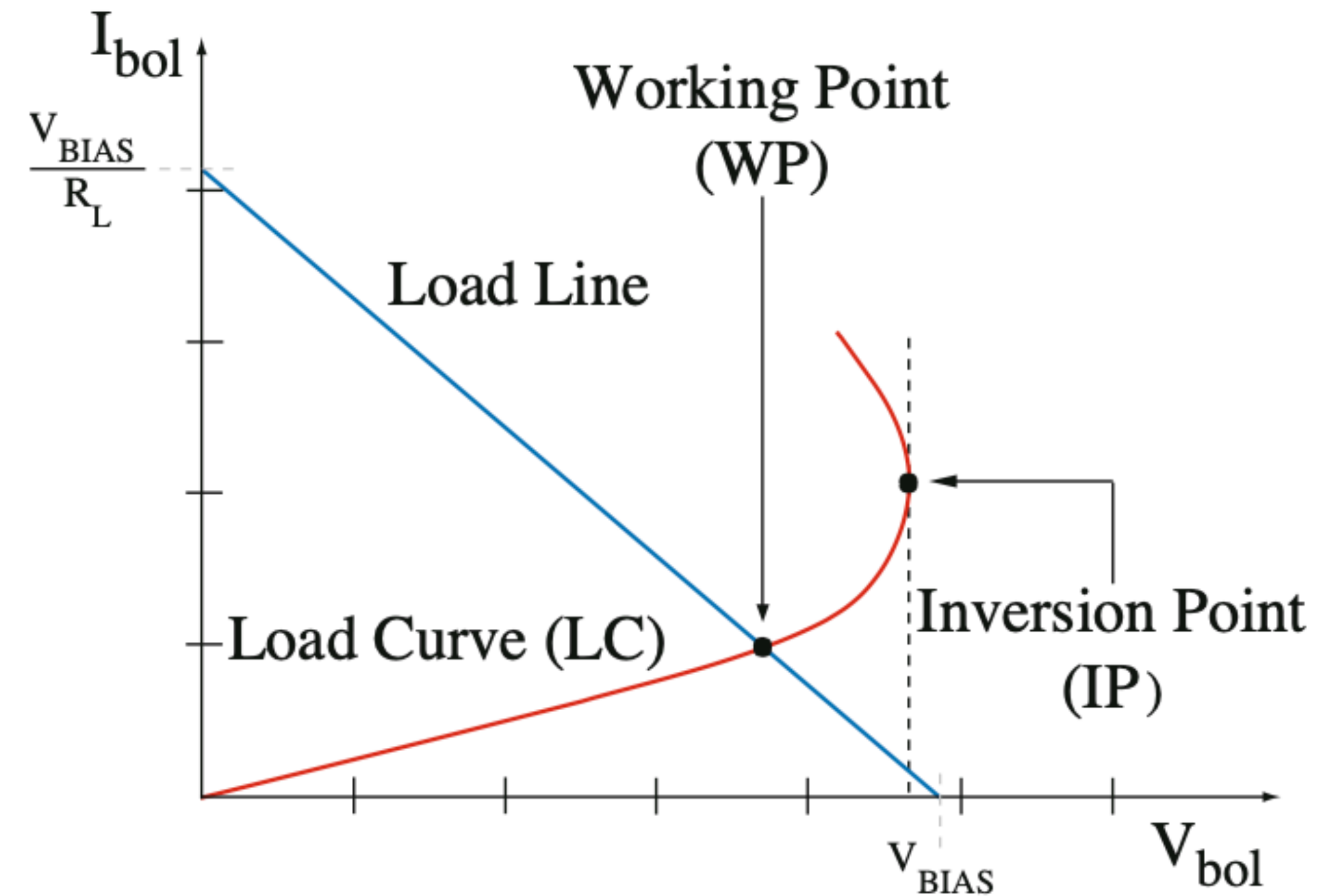
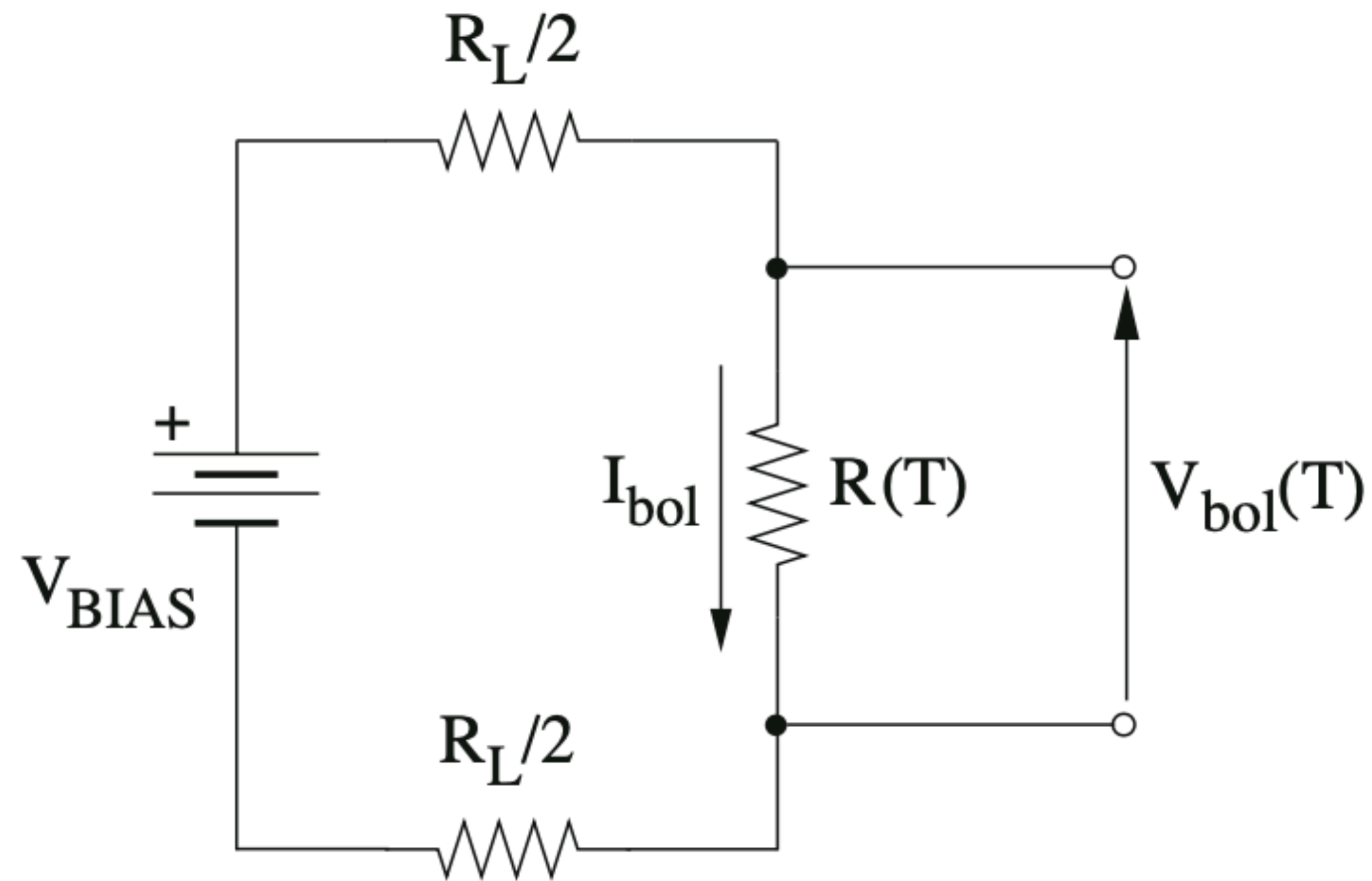
$$R(T) = R_0 \exp (T_0/T)^\gamma$$



- ▶ Each crystal is equipped with one NTD and one heater, used to inject artificial pulses to characterize the sensor performances and stabilize drifts in temperature
- ▶ Thermal and electric contact made with 50 μm gold wires thermally coupled to the thermal bath

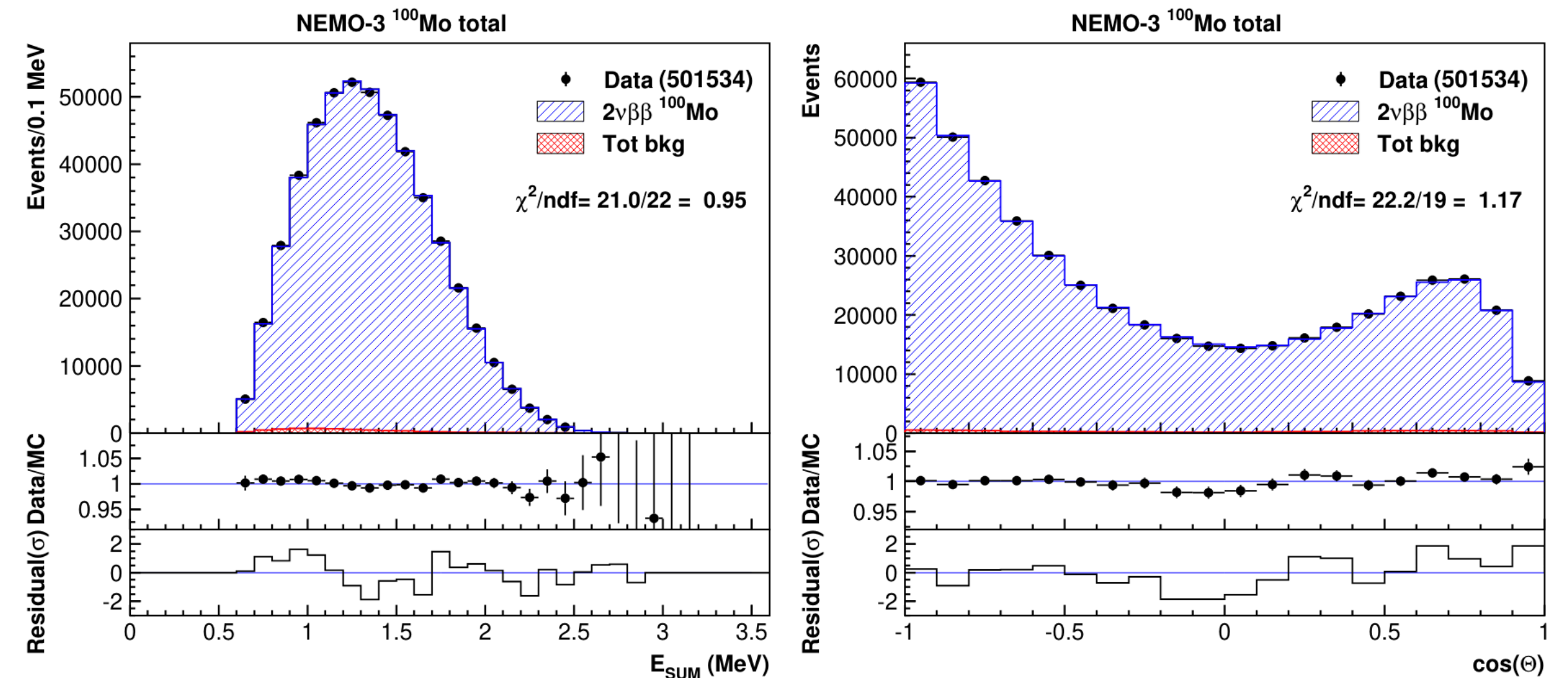
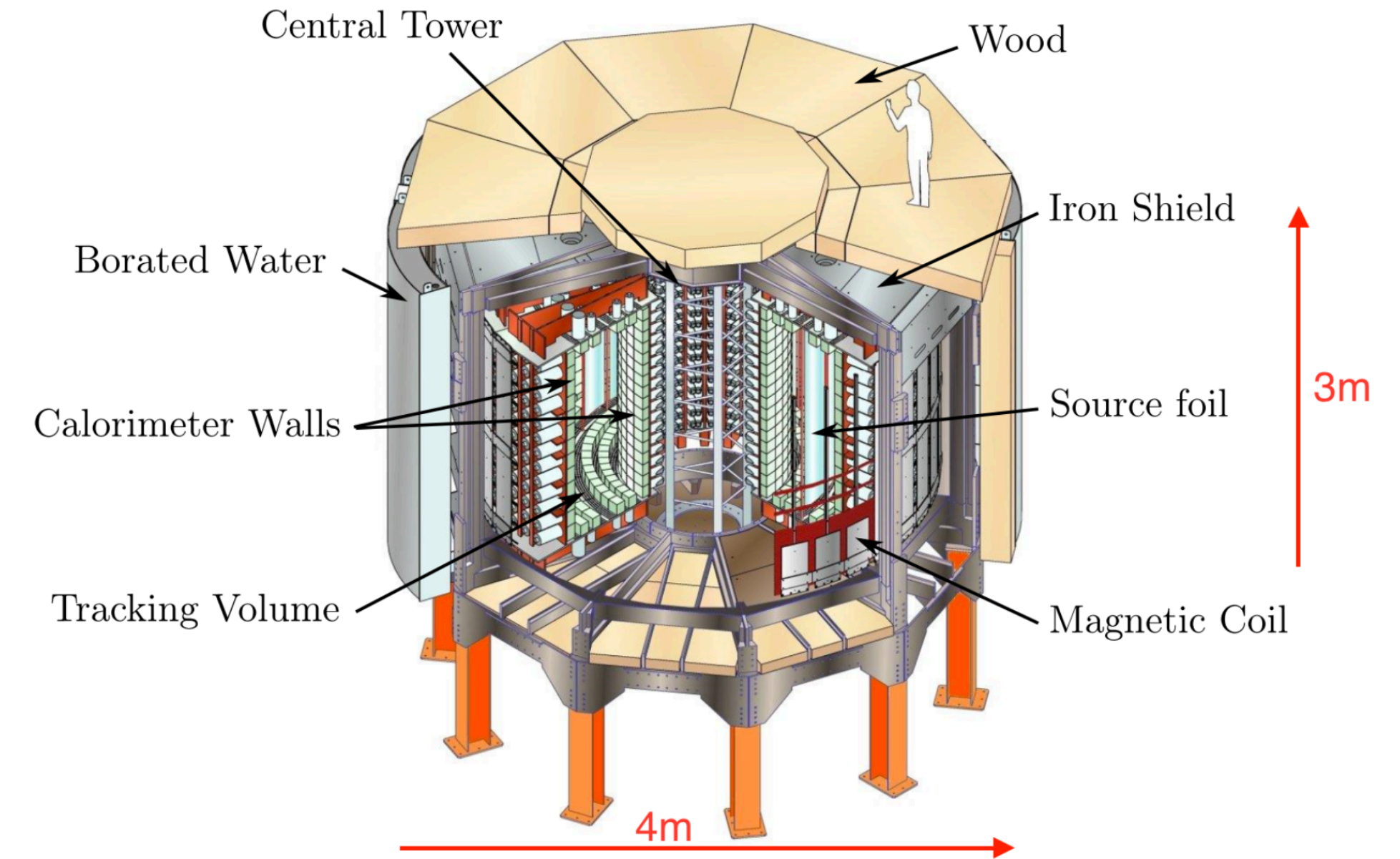
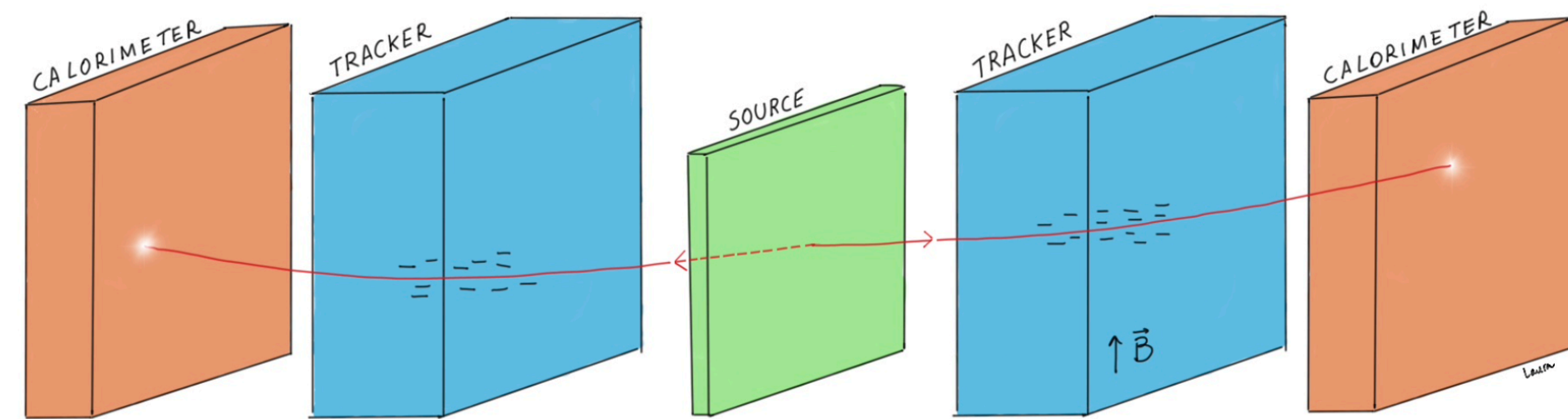


NTD-Ge thermistors: read-out



NEMO-3 experiment

- ❖ Tracking calorimeters
- ❖ Detection of both electrons emitted separately → possibility to measure the angle between the two electrons emitted
- ❖ energy resolution of a single calorimeter $\sigma \sim 100$ keV
- ❖ Detector acceptance and selection efficiency $\varepsilon = (2.356 \pm 0.002)\%$



Majoron emitting modes

One ($\beta\beta\chi_0$) or two ($\beta\beta\chi_0\chi_0$) Majorons can be emitted according to the different models

The parameter of interest is the neutrino-Majoron coupling:

$$[T_{0\nu M}^{1/2}]^{-1} = G_{0\nu M} \left| \langle g_{ee}^M \rangle \right|^{2m} \left| M_{0\nu M} \right|^2$$

model	spectral index	Decay mode	NG boson	ΔL	Ref.
IB	1	$\beta\beta\chi_0$	No	0	[121]
IC			Yes	0	
IIB			No	-2	
“bulk”	2	$\beta\beta\chi_0$	bulk field	0	[123]
IIF	3	$\beta\beta\chi_0$	Gauge boson	-2	[122]
IIC			Yes	-2	[121]
ID	3	$\beta\beta\chi_0\chi_0$	No	0	[121]
IE			Yes	0	
IID			No	-1	
IIE	7	$\beta\beta\chi_0\chi_0$	Yes	-2	[124]

decay mode	$T_{1/2}$ [yr]	$G [\times 10^{-18} \text{yr}^{-1}]$	NME	g_{ee} lower limit
⁷⁶ Ge [133]				
$\beta\beta\chi_0 (n=1)$	$> 6.4 \times 10^{23}$	44.2	(2.66 - 6.34)	$(3.0 - 7.1) \times 10^{-5}$
$\beta\beta\chi_0 (n=2)$	$> 2.9 \times 10^{23}$	-	-	-
$\beta\beta\chi_0 (n=3)$	$> 1.2 \times 10^{23}$	0.073	0.381	1.7×10^{-2}
$\beta\beta\chi_0\chi_0 (n=3)$	$> 1.2 \times 10^{23}$	0.22	0.0026	1.21
$\beta\beta\chi_0\chi_0 (n=7)$	$> 1.1 \times 10^{23}$	0.420	0.0026	1.05
⁸² Se [134]				
$\beta\beta\chi_0 (n=1)$	$> 1.2 \times 10^{23}$	361	(2.72 - 5.30)	$(2.9 - 5.6) \times 10^{-5}$
$\beta\beta\chi_0 (n=2)$	$> 3.8 \times 10^{22}$	-	-	-
$\beta\beta\chi_0 (n=3)$	$> 1.4 \times 10^{22}$	1.22	0.305	1.6×10^{-2}
$\beta\beta\chi_0\chi_0 (n=3)$	$> 1.4 \times 10^{22}$	3.54	0.002	1.18
$\beta\beta\chi_0\chi_0 (n=7)$	$> 2.2 \times 10^{21}$	26.9	0.002	1.13
¹⁰⁰ Mo [46, 135]				
$\beta\beta\chi_0 (n=1)$	$> 4.4 \times 10^{22}$	598	(3.84 - 6.59)	$(3.0 - 5.1) \times 10^{-5}$
$\beta\beta\chi_0 (n=2)$	$> 9.9 \times 10^{21}$	-	-	-
$\beta\beta\chi_0 (n=3)$	$> 4.4 \times 10^{21}$	2.42	0.263	2.3×10^{-2}
$\beta\beta\chi_0\chi_0 (n=3)$	$> 4.4 \times 10^{21}$	6.15	0.0019	1.42
$\beta\beta\chi_0\chi_0 (n=7)$	$> 1.2 \times 10^{21}$	50.8	0.0019	1.15
¹¹⁶ Cd [57]				
$\beta\beta\chi_0 (n=1)$	$> 8.2 \times 10^{21}$	569	(3.105 - 5.43)	$(8.5 - 15) \times 10^{-5}$
$\beta\beta\chi_0 (n=2)$	$> 4.1 \times 10^{21}$	-	-	-
$\beta\beta\chi_0 (n=3)$	$> 2.6 \times 10^{21}$	2.28	0.144	5.6×10^{-2}
$\beta\beta\chi_0\chi_0 (n=3)$	$> 2.6 \times 10^{21}$	5.23	0.0009	2.37
$\beta\beta\chi_0\chi_0 (n=7)$	$> 8.9 \times 10^{20}$	33.9	0.0009	1.94
¹³⁶ Xe [131, 132]				
$\beta\beta\chi_0 (n=1)$	$> 2.6 \times 10^{24}$ $> 4.3 \times 10^{24}$	409	(1.11 - 4.77)	$(0.6 - 2.8) \times 10^{-5}$ $(0.5 - 2.1) \times 10^{-5}$
$\beta\beta\chi_0 (n=2)$	$> 1.0 \times 10^{24}$ $> 9.8 \times 10^{23}$	-	-	- -
$\beta\beta\chi_0 (n=3)$	$> 4.5 \times 10^{23}$ $> 6.3 \times 10^{23}$	1.47	0.160	4.8×10^{-3} 4.0×10^{-3}
$\beta\beta\chi_0\chi_0 (n=3)$	$> 4.5 \times 10^{23}$ $> 6.3 \times 10^{23}$	3.05	0.0011	0.69 0.63
$\beta\beta\chi_0\chi_0 (n=7)$	$> 1.1 \times 10^{22}$ $> 5.1 \times 10^{22}$	12.5	0.0011	1.23 0.84

Lorentz violating $2\nu\beta\beta$

SM is an effective quantum field theory that includes all possible operators that can be constructed with the SM fields and that introduce Lorentz violation but preserve the SM gauge invariance. Experimental searches for Lorentz violation are done in different sectors of physics, including **matter, photon, neutrino, and gravity**. Four operators, called *countershaded*, equally change all neutrino energies and have no impact on oscillations, therefore they are labeled as “oscillation free” (of) and can be studied only through weak decays.

$$p = (E, \mathbf{p}) \longrightarrow p = (E, \mathbf{p} + \mathbf{a}_{of}^{(3)} - \dot{a}_{of}^{(3)} \hat{\mathbf{p}})$$

Lorentz violation does not affect the NME but appears as a kinematic effect modifying the phase space factor, thus the summed electron energy distribution:

$$\frac{d\Gamma_{SME}^{2\nu}}{dK} = |\mathcal{M}_{2\nu}|^2 \left(\frac{d\mathcal{G}_{SM}}{dK} + \frac{d(\delta\mathcal{G}_{LV})}{dK} \right)$$

Isotope	Limit on $\dot{a}_{of}^{(3)}$ [GeV]
^{76}Ge	$(-2.7 < \dot{a}_{of}^{(3)} < 6.2) \cdot 10^{-6}$
^{82}Se	$\dot{a}_{of}^{(3)} < 4.1 \cdot 10^{-6}$
^{136}Xe	$-2.65 \cdot 10^{-5} < \dot{a}_{of}^{(3)} < 7.6 \cdot 10^{-6}$
^{116}Cd	$\dot{a}_{of}^{(3)} < 4.0 \cdot 10^{-6}$
^{100}Mo	$(-4.2 < \dot{a}_{of}^{(3)} < 3.5) \cdot 10^{-7}$
^3H	$ \dot{a}_{of}^{(3)} < 3.0 \cdot 10^{-8}$

Sterile neutrino emissions

If the sterile neutrino N has a mass $m_N < Q_{\beta\beta}$, it can be emitted instead of an antineutrinos in the $2\nu\beta\beta$ ($\nu N\beta\beta$):

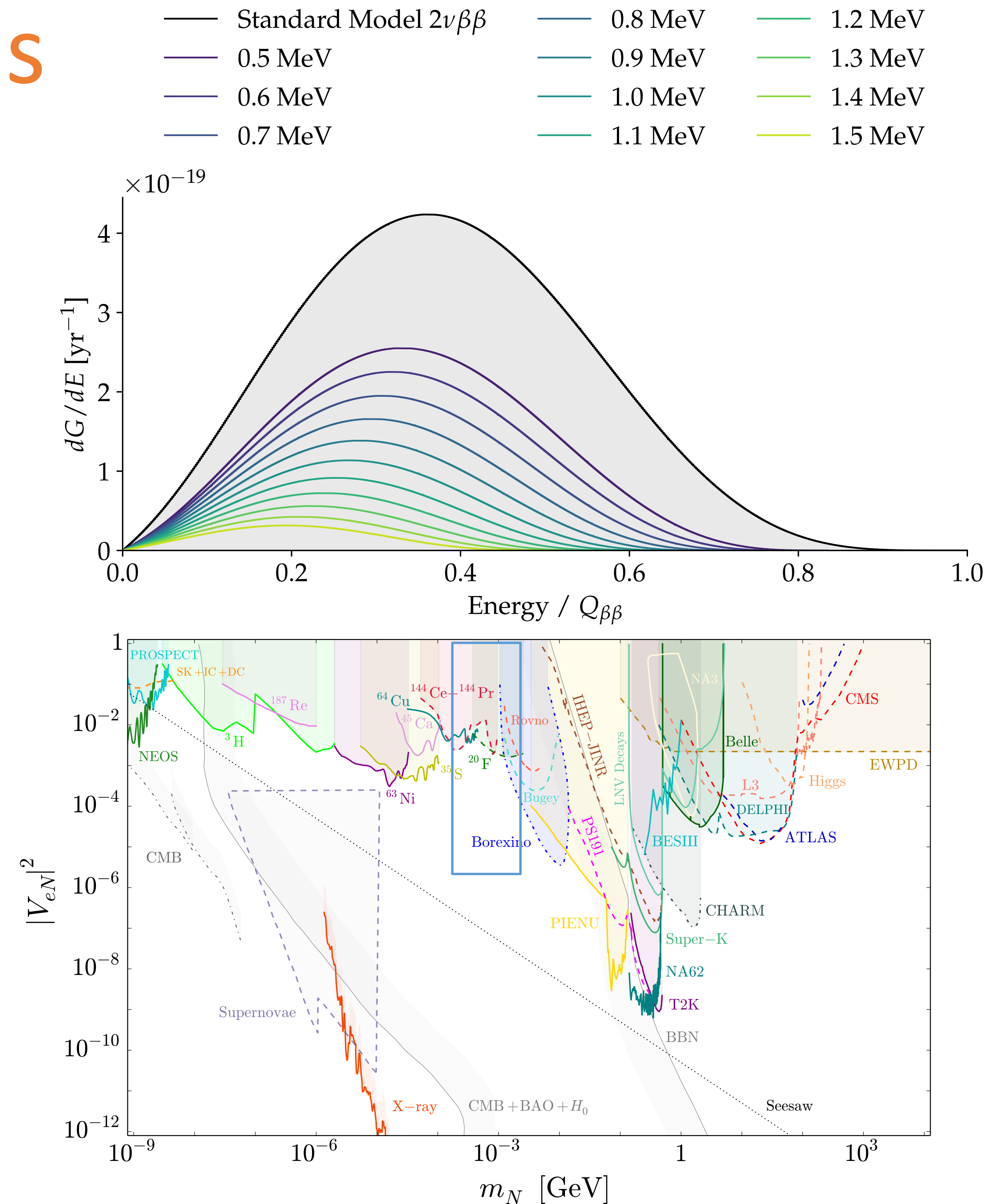
$$(A, Z) \rightarrow (A, Z + 2) + 2e^{-} + \bar{\nu} + N$$

The effect on the total decay rate is:

$$\Gamma = \cos^4 \theta \Gamma_{SM} + 2 \cos^2 \theta \sin^2 \theta \Gamma_{\nu N}$$

Where $\sin^2 \theta$ is called active-sterile mixing strength

We can set limits where the actual boundaries are relatively weak

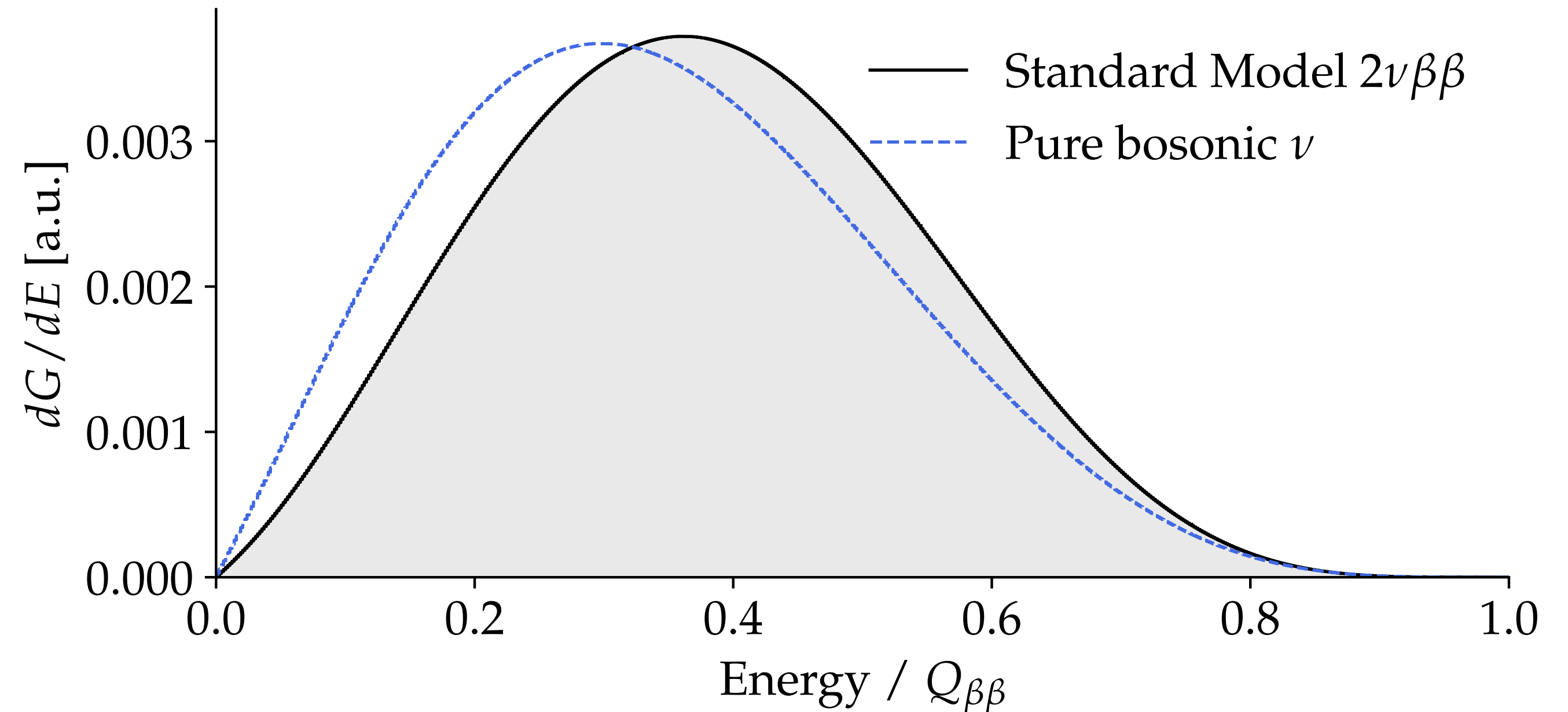


Bosonic neutrinos

In the hypothesis in which neutrinos partly obey to the Bose-Einstein statistic, the emission of two identical neutrinos in $2\nu\beta\beta$ offers the opportunity to investigate the Pauli's exclusion principle.

$$\Gamma_{2\nu\beta\beta} = \cos^4 \chi \Gamma_f + \sin^4 \chi \Gamma_b$$

Where $\sin^4 \chi$ represents the bosonic fraction of the neutrino wave function, while Γ_f and Γ_b are the decay rates for the pure fermionic and pure bosonic neutrinos.



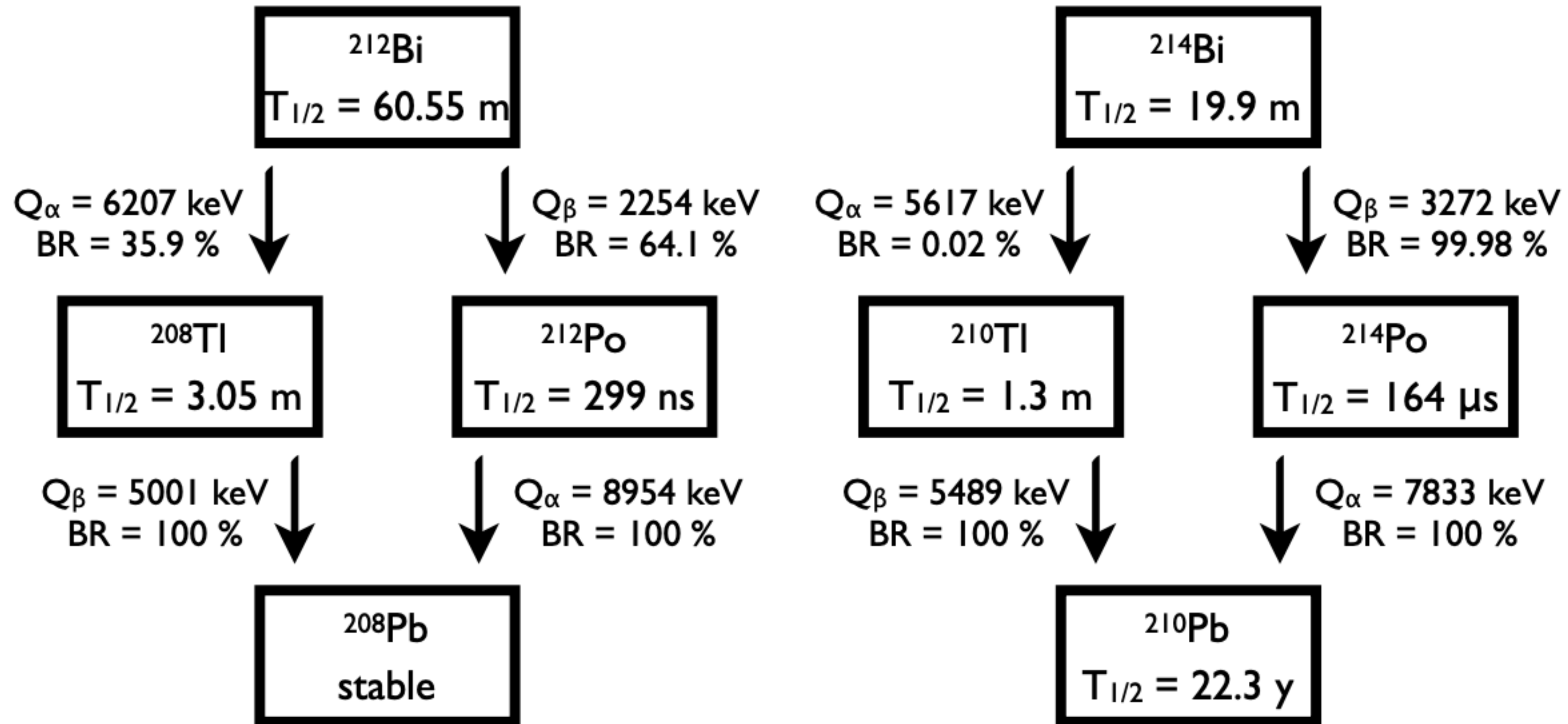
$$r_0 = \Gamma_b / \Gamma_f \longrightarrow$$

$$r_0(^{100}\text{Mo}) = 0.076$$

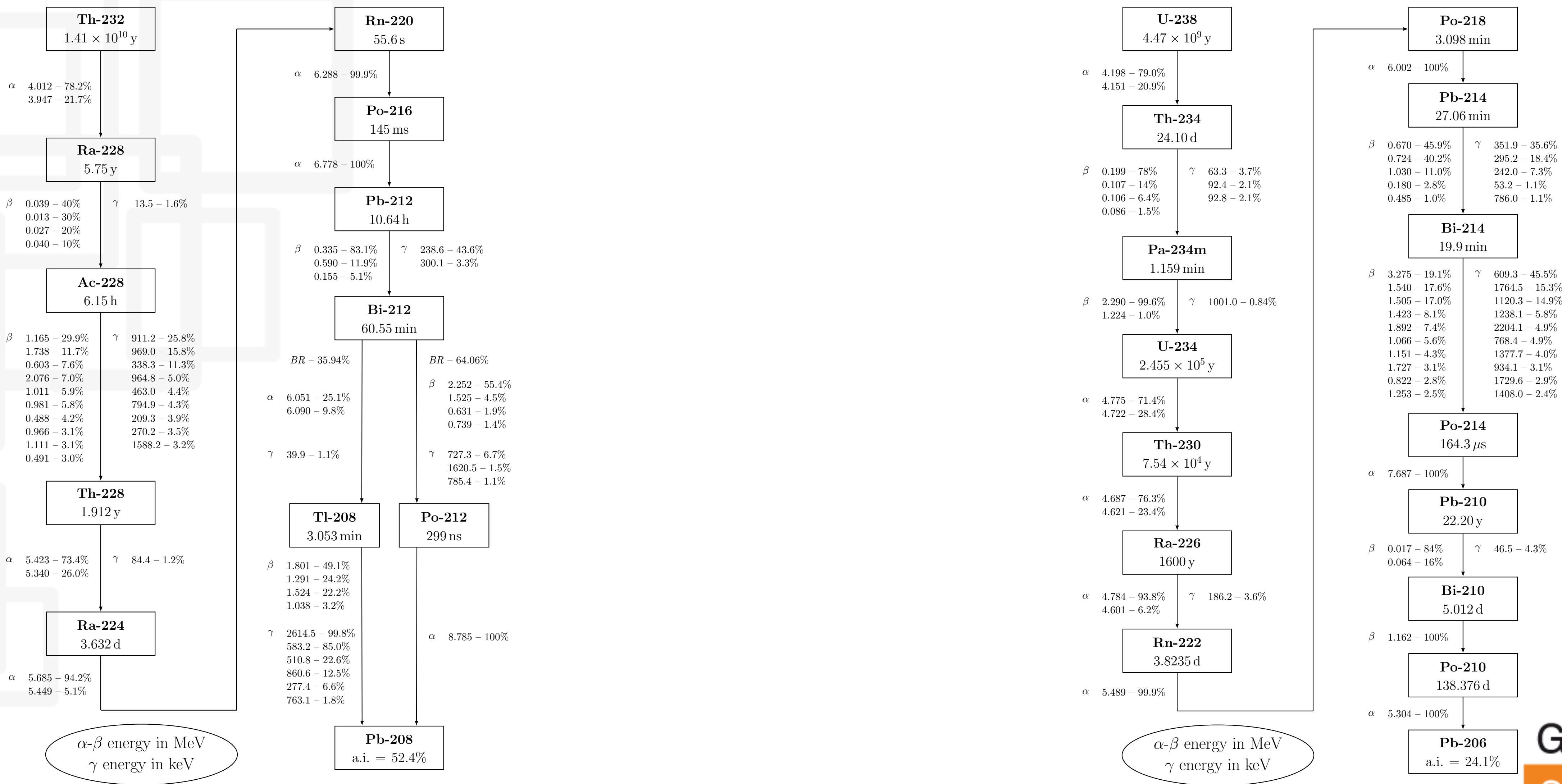
$$r_0(^{76}\text{Ge}) = 0.0014$$

Has to be calculated from the theory and it depends on the nuclear model adopted

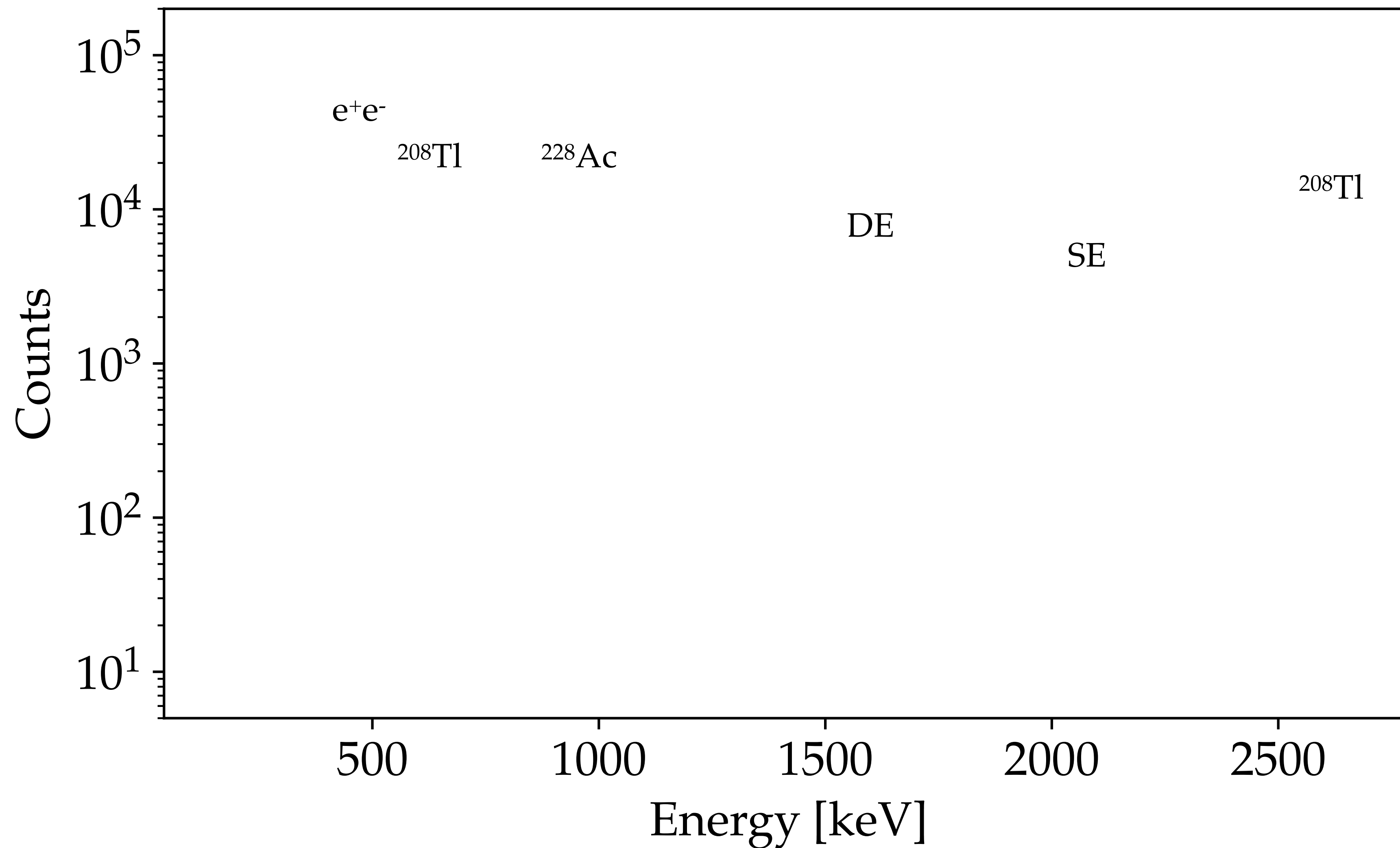
Background in the ROI



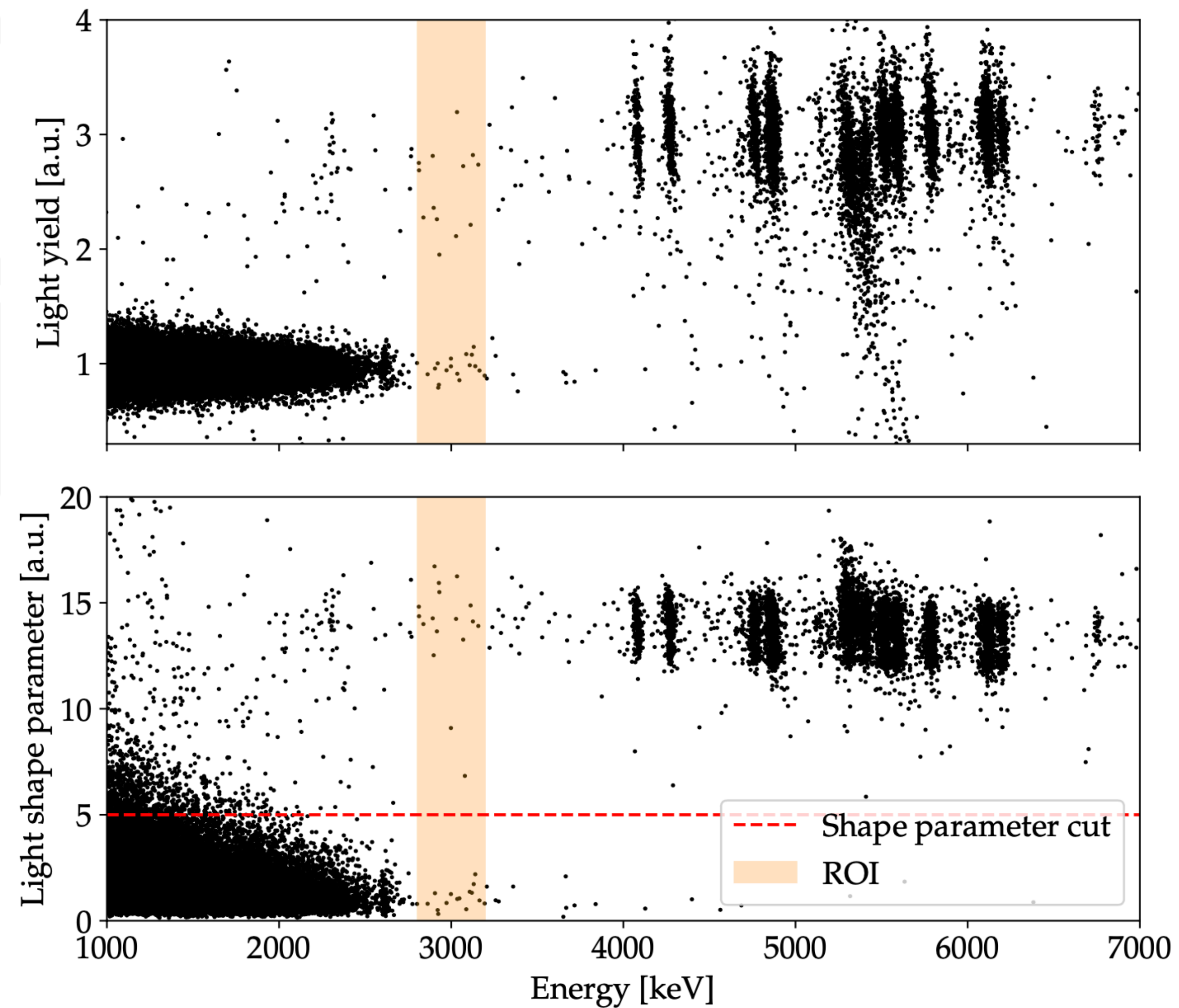
Radioactive chains



CUPID-0 calibration spectrum

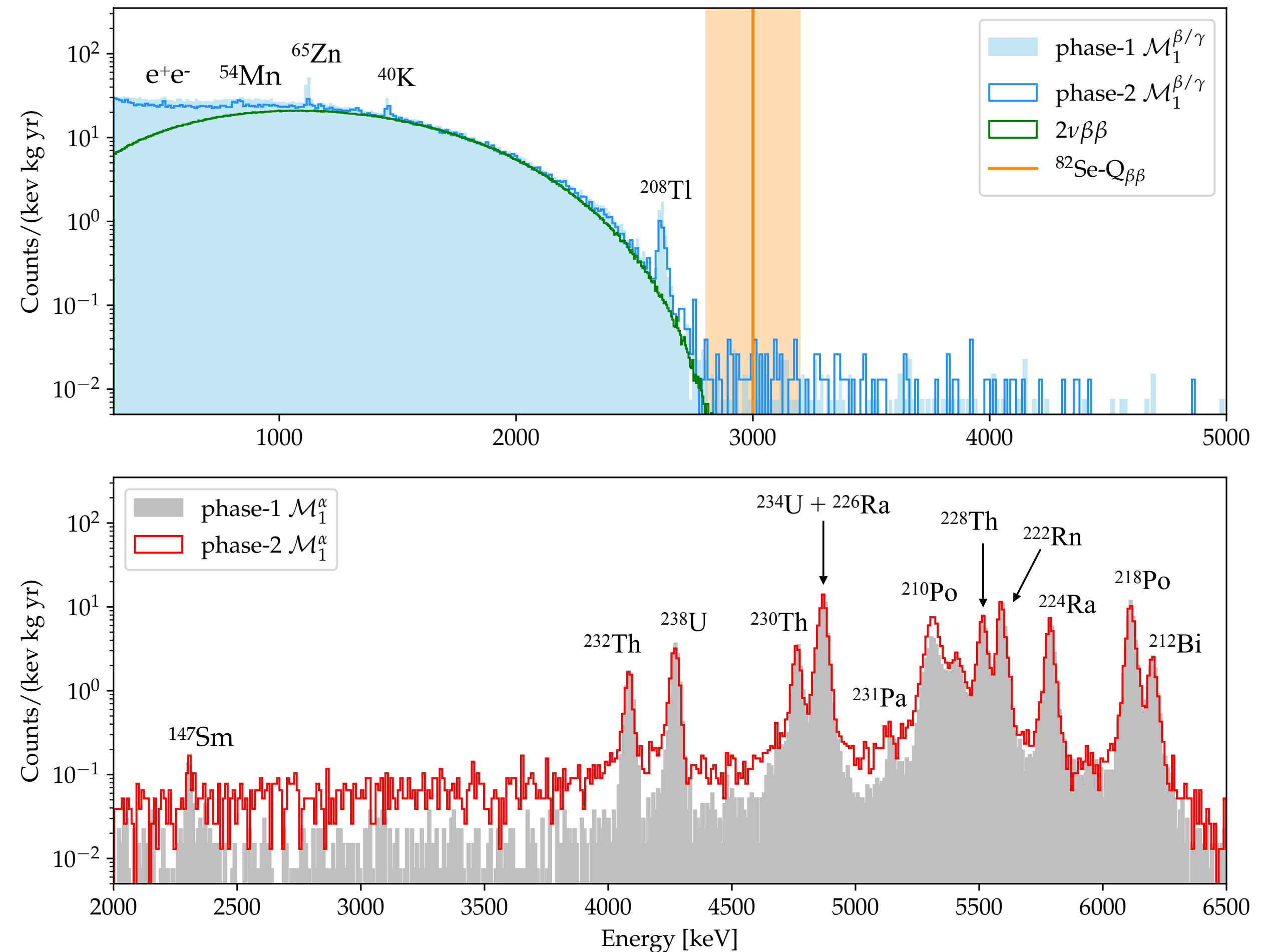
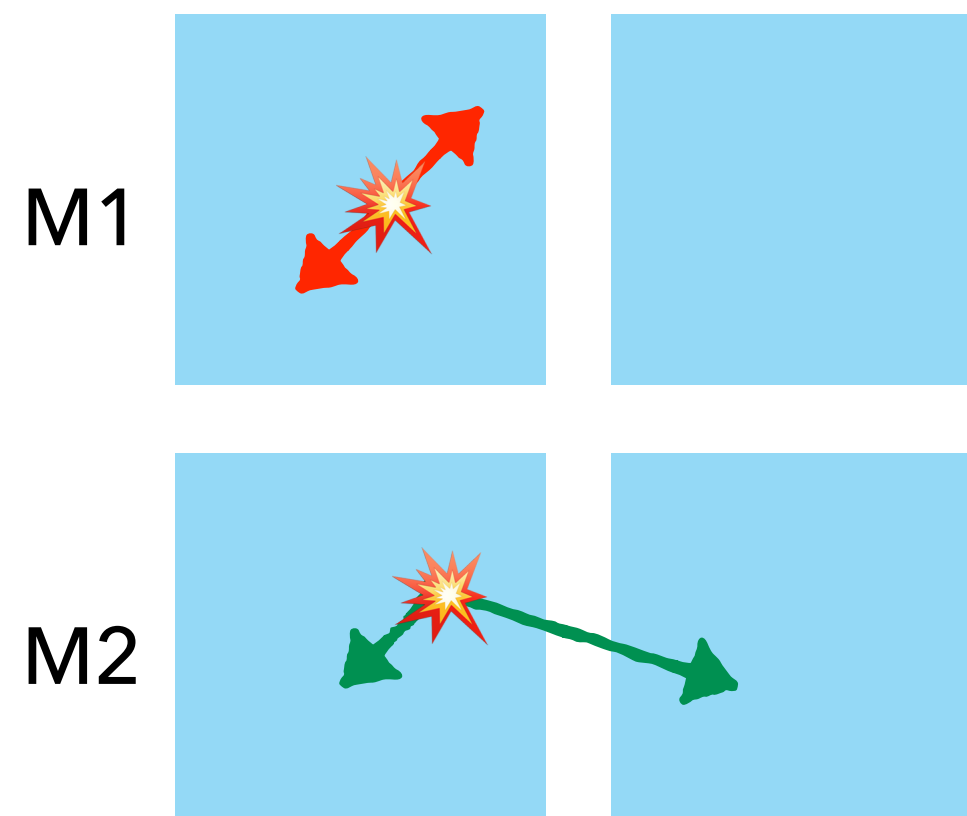


CUPID-0 particle identification



From phase-I to phase-II - M1

- ❖ Almost all the α -peaks have the same intensity in phase-I and phase-II
- ❖ ^{65}Zn decayed in phase-II, while other peaks appeared (from cosmogenic activation of copper)
- ❖ Higher α continuum from close component contaminations (10 mK)
- ❖ $2\nu\beta\beta$ is dominant up to 3 MeV

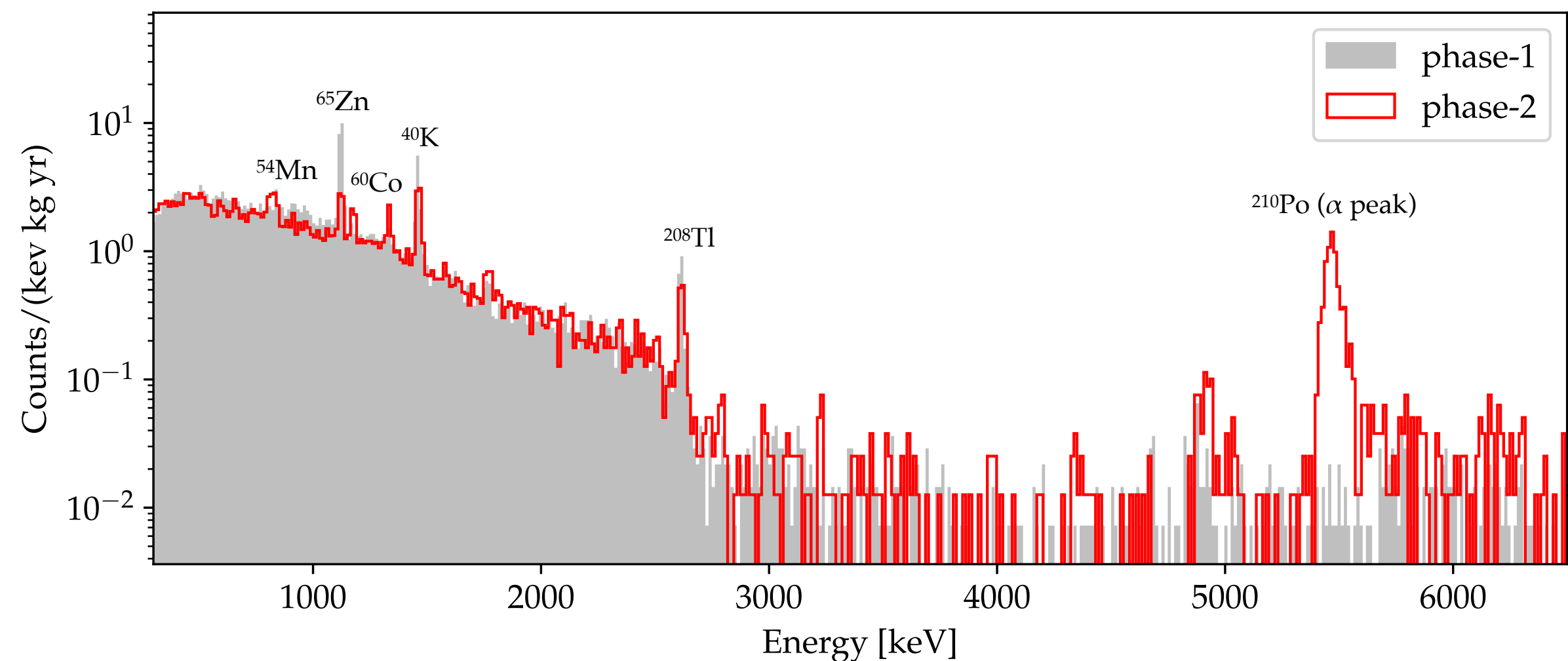
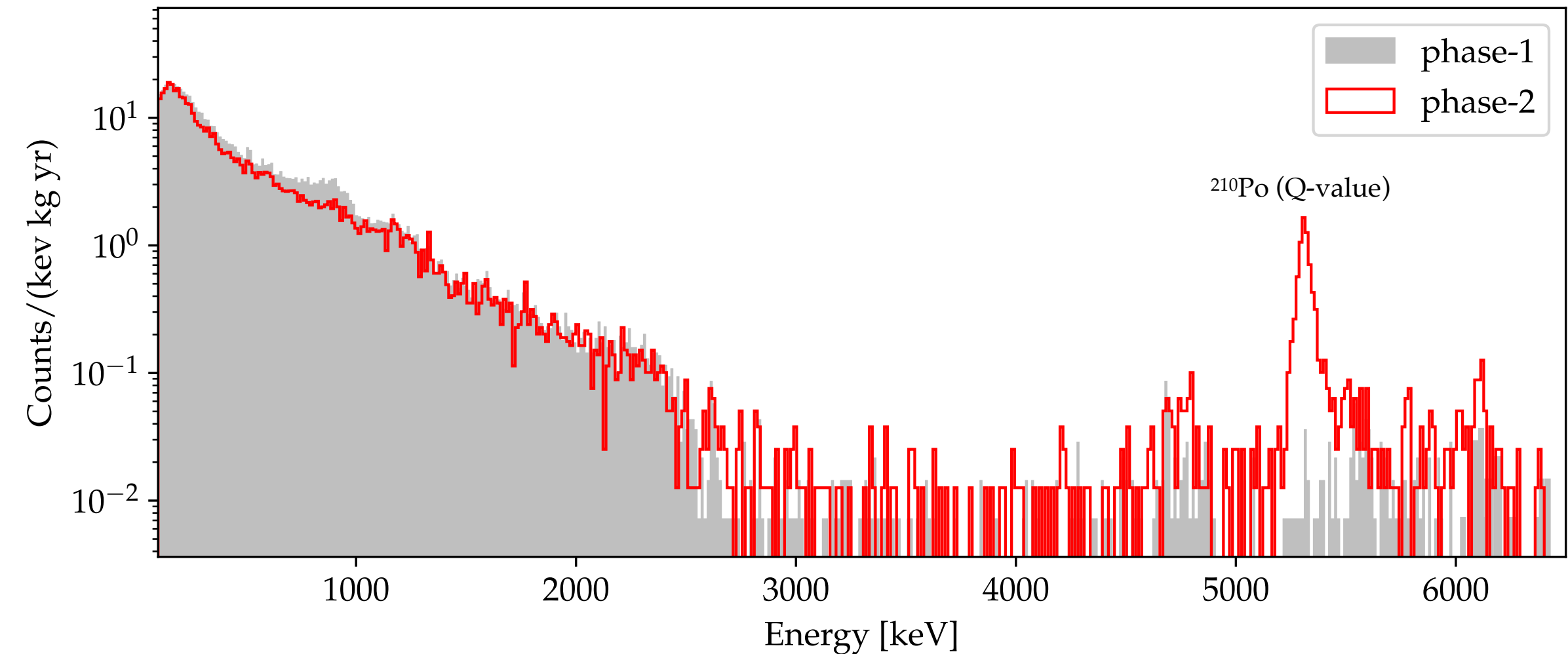
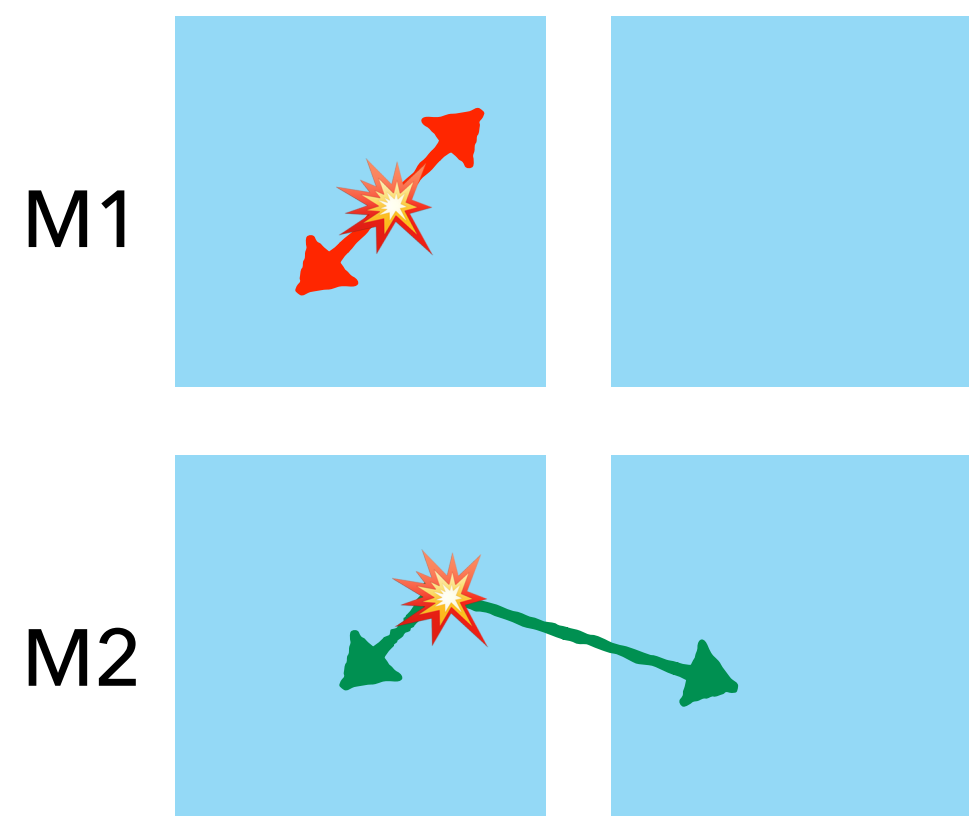


From phase-I to phase-II - M2 and M2sum

Multiplicity = 2 \rightarrow events hitting two crystals simultaneously

\mathcal{M}_2 = single energy deposition in both the crystals

Σ_2 = sum of the two energies deposited (peak structures)



Background model - Fit

Binned simultaneous Maximum Likelihood fit using a Bayesian framework with a Markov Chain Monte Carlo (MCMC) approach.

Expectation value of the counts in the i -th bin $\langle C_{i,\delta}^{\text{exp}} \rangle = \sum_{j=1}^m N_j \cdot \langle C_{ij,\delta}^{\text{MC}} \rangle$

From the Bayes theorem the *joint posterior pdf* is defined as

$$\begin{aligned} \text{Posterior} \left(N_j, \langle C_{ij,\delta}^{\text{MC}} \rangle \mid C_{i,\delta}^{\text{exp}}, C_{ij,\delta}^{\text{MC}} \right) &= \prod_{i,\delta} \text{Pois} \left(C_{i,\delta}^{\text{exp}} \mid \langle C_{i,\delta}^{\text{exp}} \rangle \right) \times \prod_j \text{Prior} \left(N_j \right) \\ &\quad \times \prod_{ij,\delta} \text{Pois} \left(C_{ij,\delta}^{\text{MC}} \mid \langle C_{ij,\delta}^{\text{MC}} \rangle \right) \times \text{Prior} \left(\langle C_{ij,\delta}^{\text{MC}} \rangle \right) \end{aligned}$$

$$\text{Activity} \left[\frac{\text{Bq}}{\text{kg}} \right] = \frac{N_j^{\text{Fit}} \cdot N^{\text{MC}}}{\text{Mass}[\text{kg}] \times \text{lifetime}[\text{s}]}$$

$2\nu\beta\beta$ half-life measurement

Final result

$$T_{1/2}^{2\nu} = \left[8.69 \pm 0.05(\text{stat.})_{-0.09}^{+0.06}(\text{syst.}) \right] \times 10^{19} \text{yr}$$

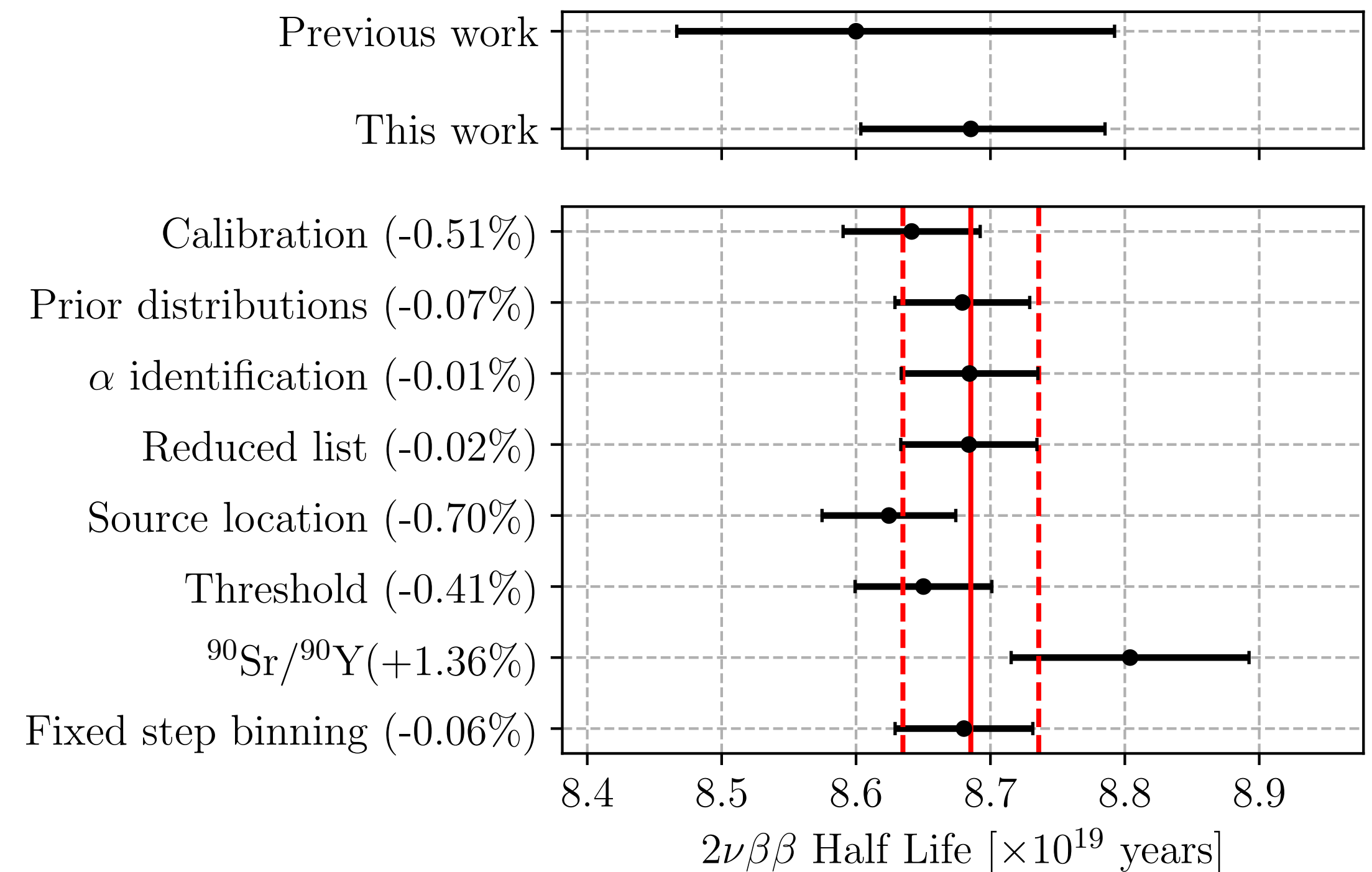
Using as Phase Space Factor the value

$$G^{2\nu} = (1.996 \pm 0.028) \times 10^{-18}$$

The final result on the nuclear matrix element is:

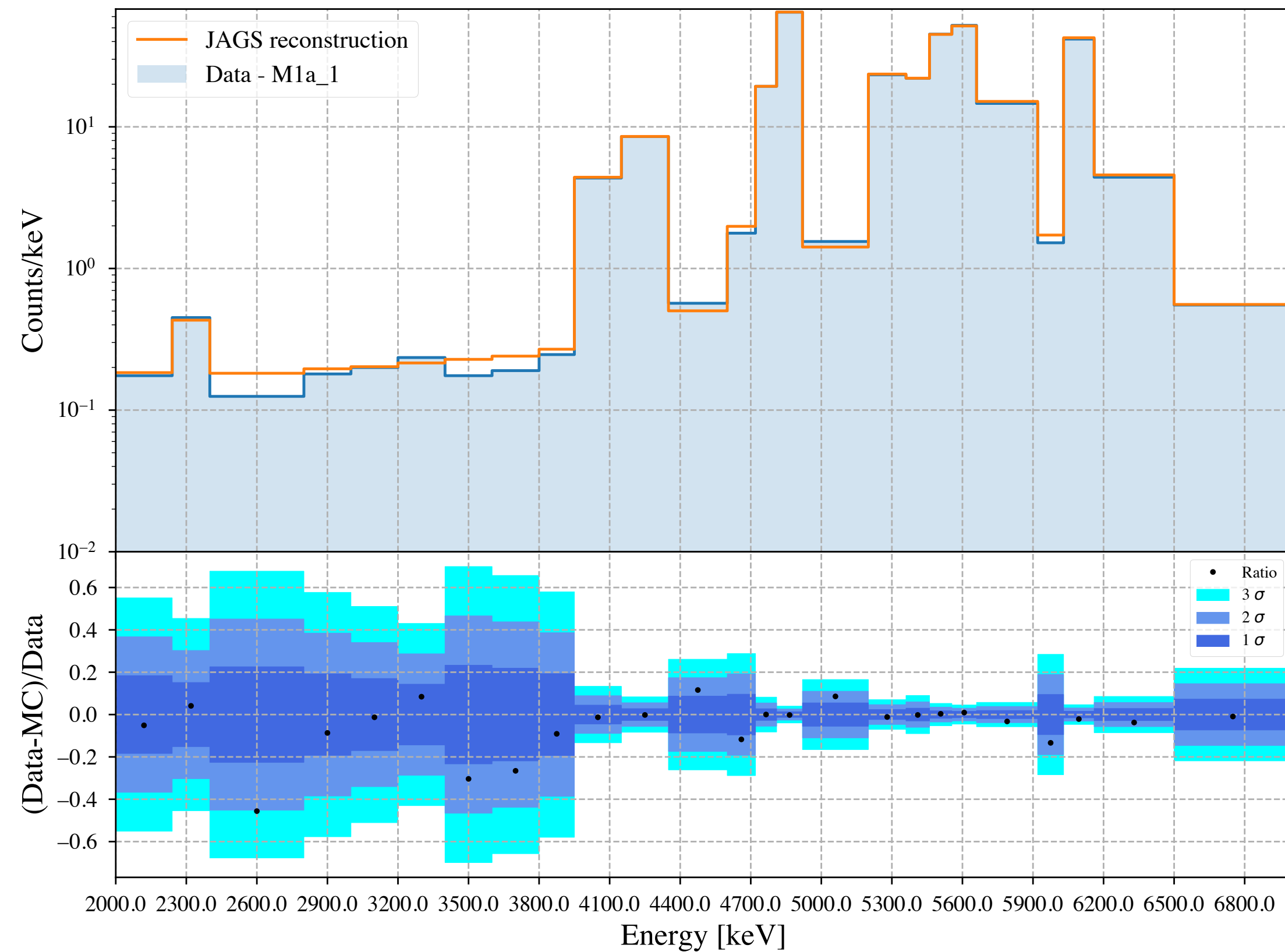
$$\mathcal{M}_{2\nu}^{\text{eff}} = 0.0760 \begin{array}{l} + 0.0006 \\ - 0.0007 \end{array}$$

Published on PRL
Phys.Rev.Lett. 131 (2023) 22

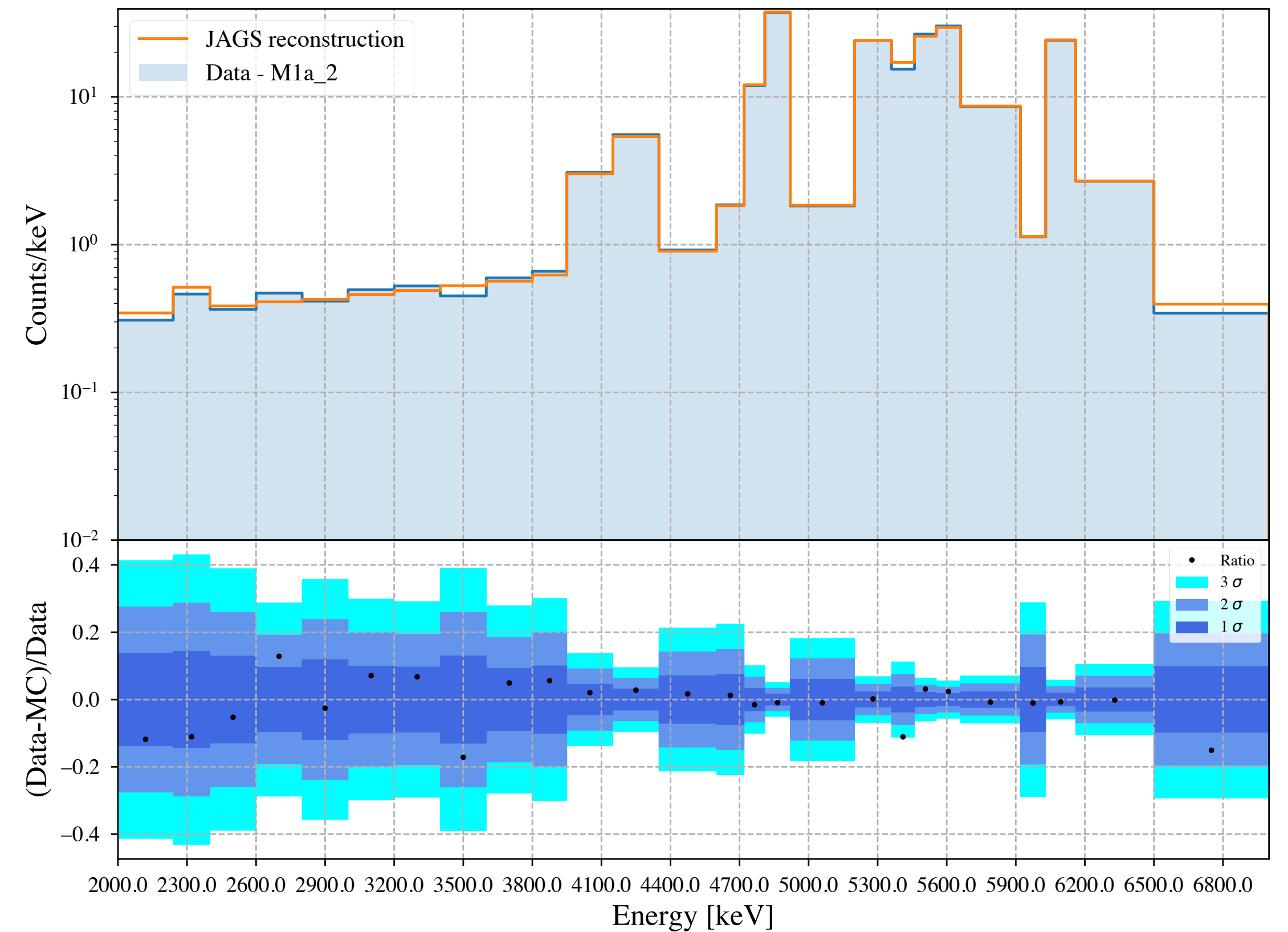


CUPID-0 Fit reconstruction M1a

PhaseI

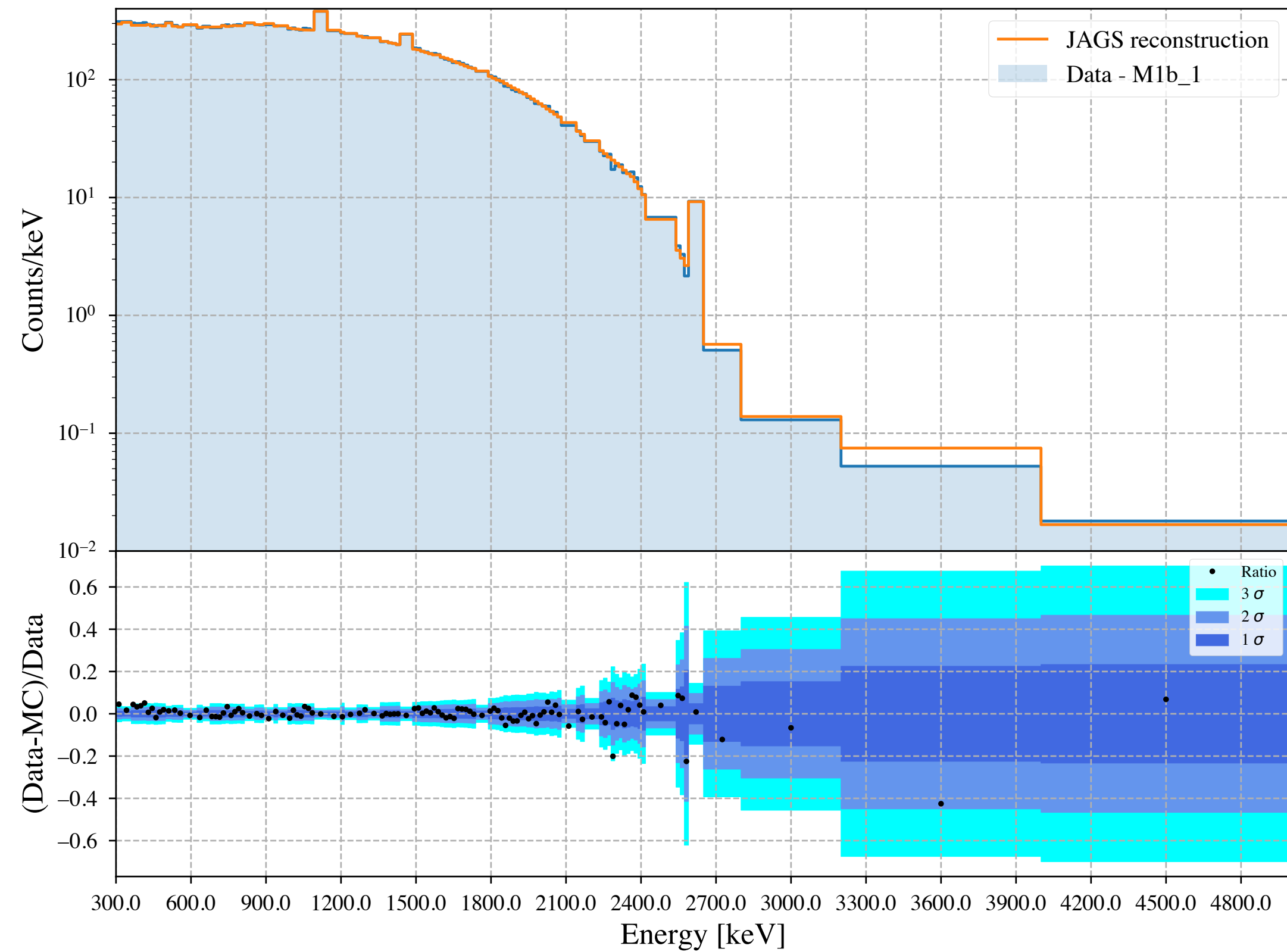


PhaseII

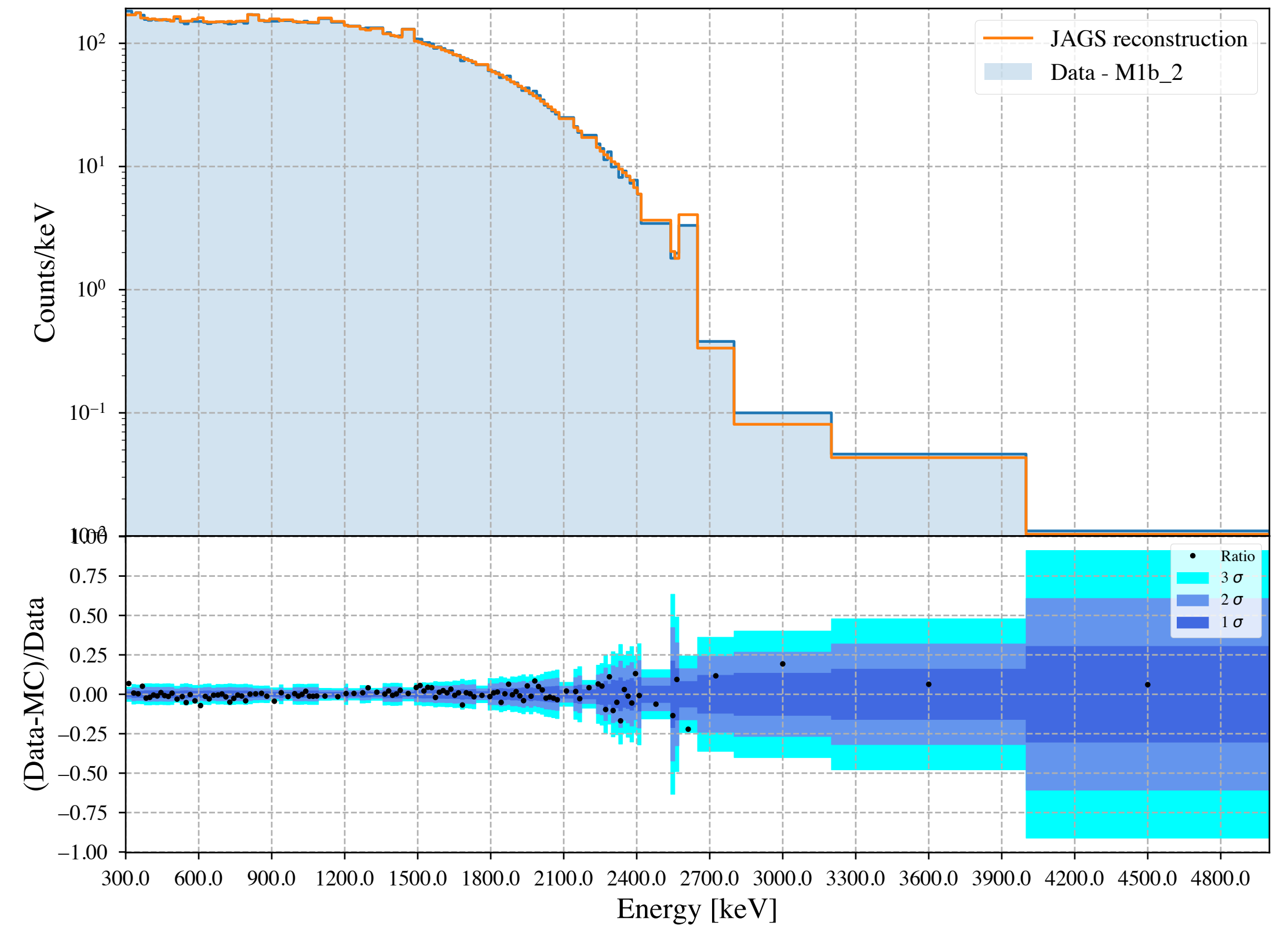


CUPID-0 Fit reconstruction M1b

PhaseI

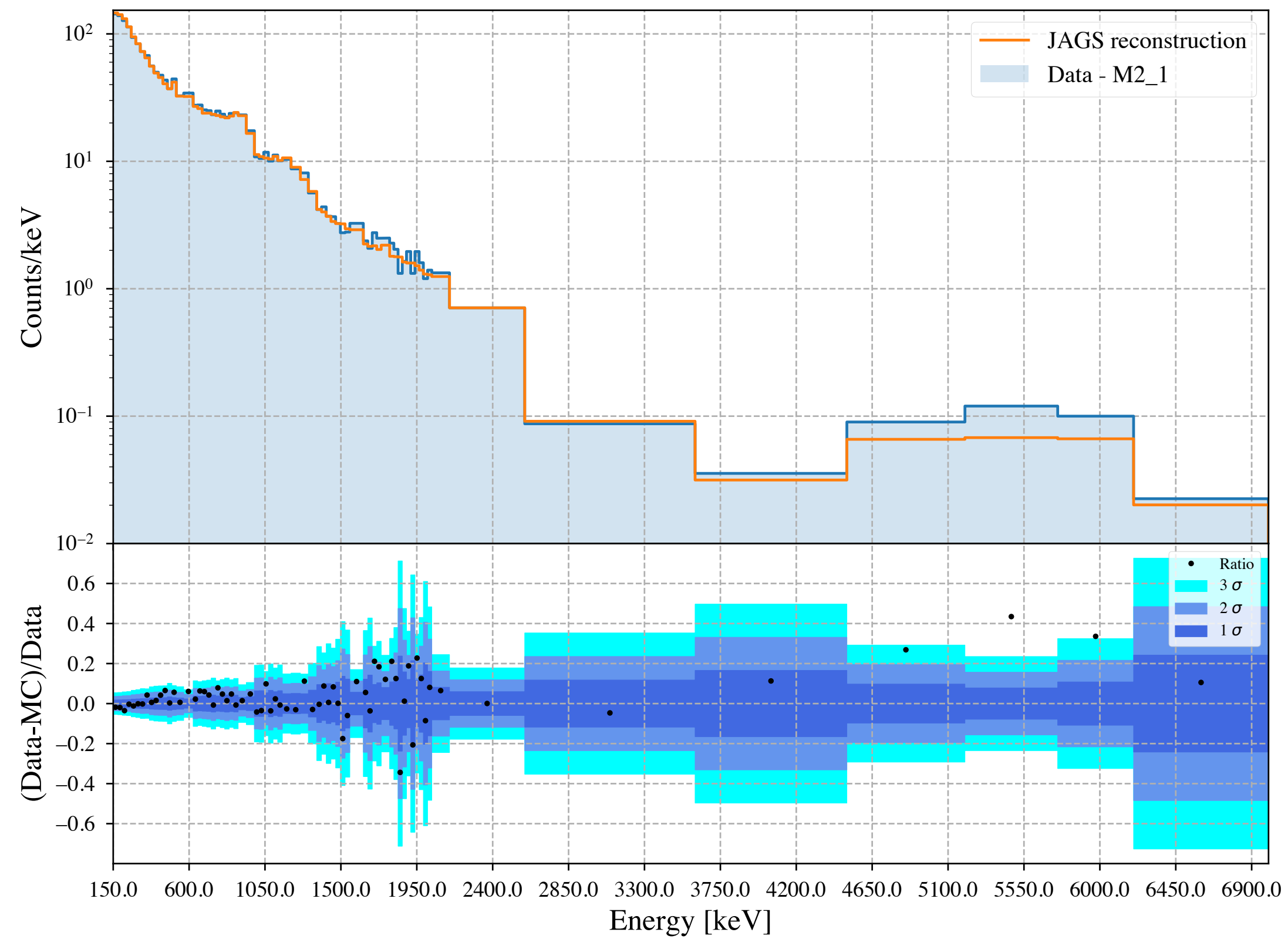


PhaseII

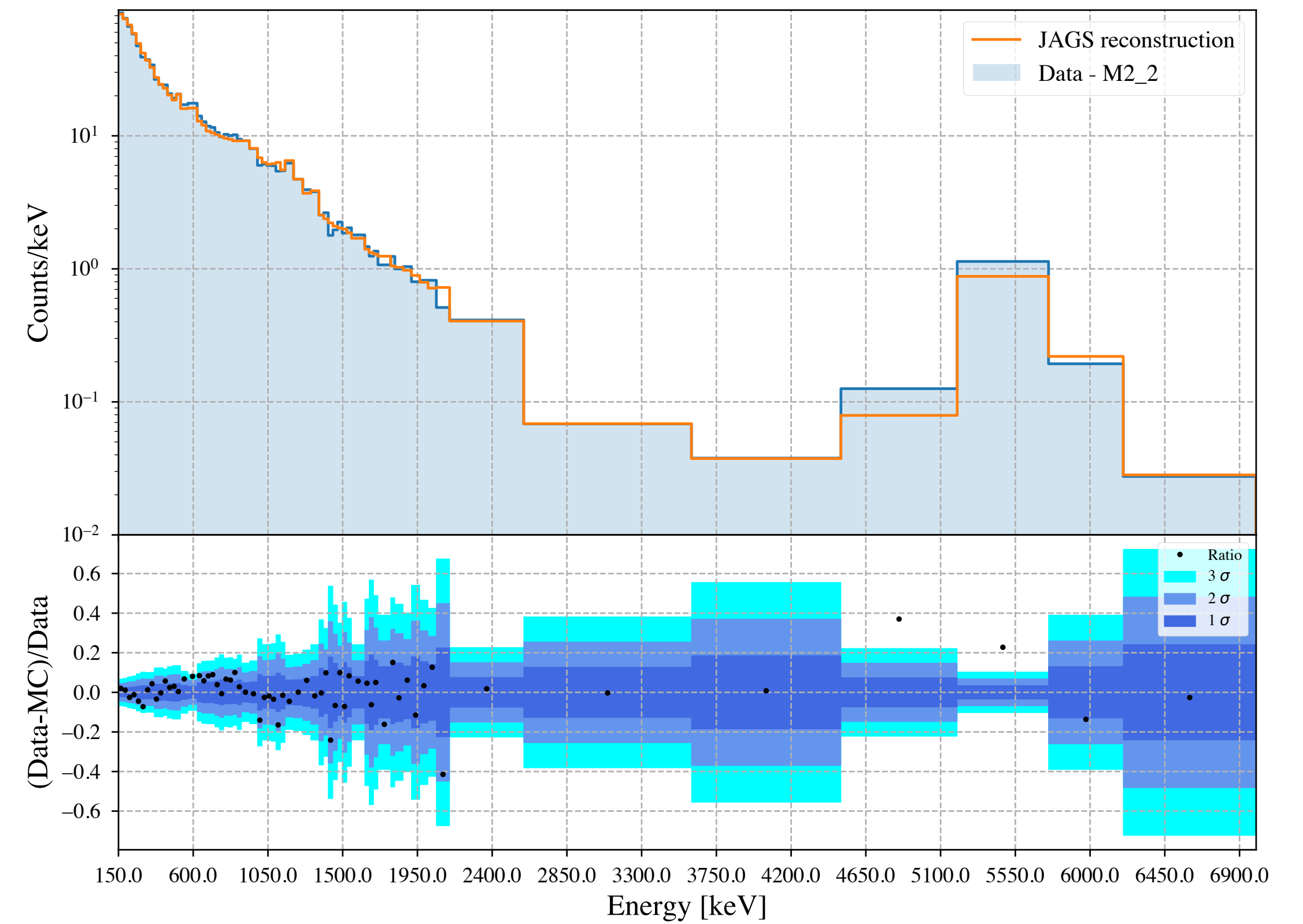


CUPID-0 Fit reconstruction M2

Phasel

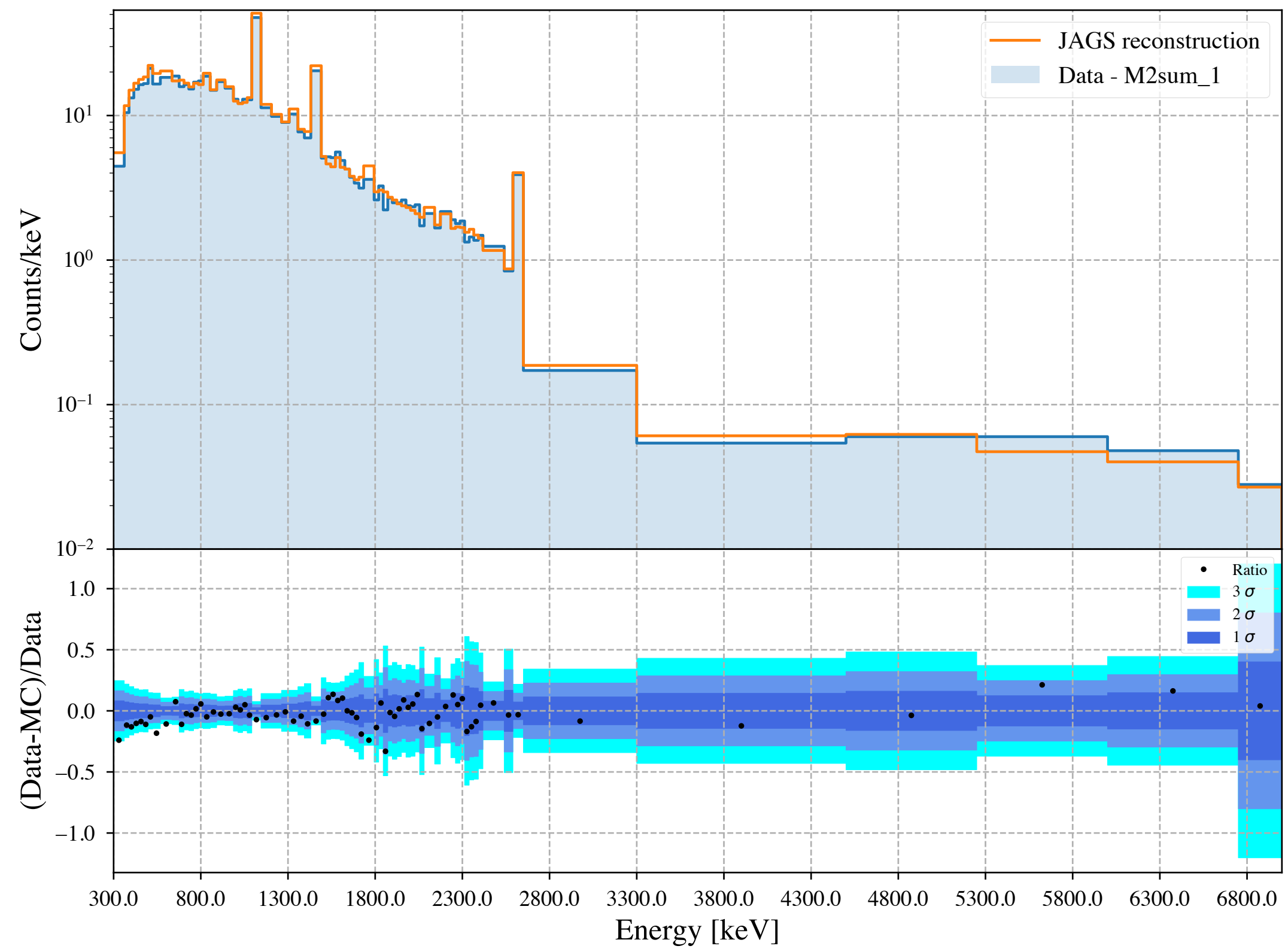


Phasel1

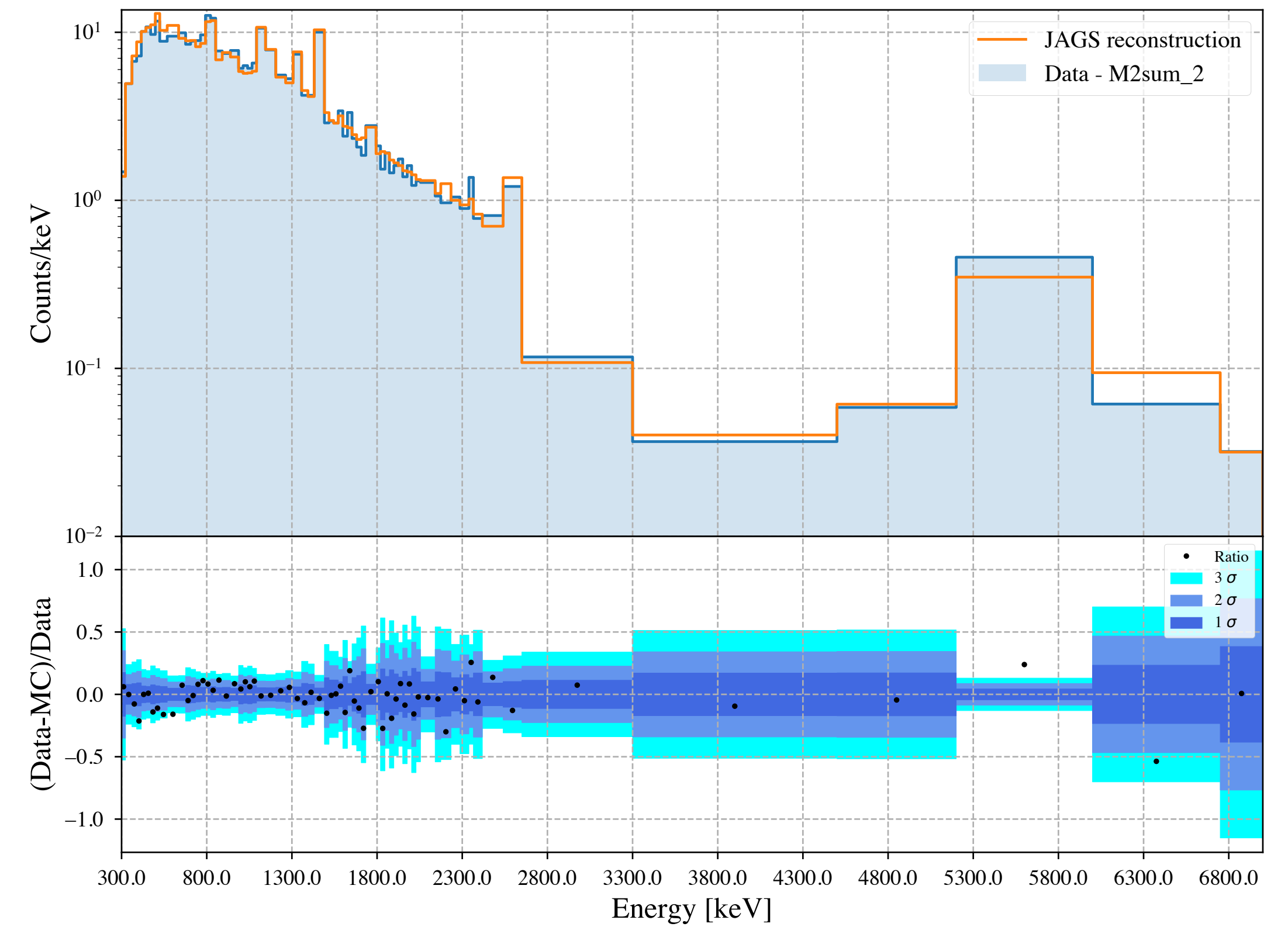


CUPID-0 Fit reconstruction M2sum

PhaseI



PhaseII



CUPID-0 crystal contaminations

Bulk Source	Specific Activity [Bq/kg]		Constrained	Prior [Bq/kg]
	phase-I	phase-II		
$^{82}\text{Se } 2\nu\beta\beta$	$(9.87 \pm 0.02) \times 10^{-4}$		yes	Uniform
^{65}Zn	$(3.63 \pm 0.06) \times 10^{-4}$	$(0.71 \pm 0.06) \times 10^{-4}$	no	Uniform
^{40}K	$(6.0 \pm 0.3) \times 10^{-5}$		yes	Uniform
^{60}Co	$(1.3 \pm 0.3) \times 10^{-5}$	$(1.3 \pm 0.4) \times 10^{-5}$	no	Uniform
^{147}Sm	$(1.3 \pm 0.3) \times 10^{-7}$		yes	Uniform
$^{238}\text{U to } ^{226}\text{Ra}$	$(5.48 \pm 0.08) \times 10^{-6}$		yes	Uniform
$^{226}\text{Ra to } ^{210}\text{Pb}$	$(1.47 \pm 0.02) \times 10^{-5}$		yes	Uniform
^{210}Pb	$< 1.4 \times 10^{-7}$		yes	Uniform
$^{232}\text{Th to } ^{228}\text{Ra}$	$(2.74 \pm 0.08) \times 10^{-6}$		yes	Uniform
^{228}Ra	$(1.26 \pm 0.03) \times 10^{-5}$		yes	Uniform
$^{235}\text{U to } ^{231}\text{Pa}$	$(6.2 \pm 0.7) \times 10^{-7}$		yes	Uniform
Surface Source	Specific Activity [Bq/cm ²]		Constrained	Prior [Bq/cm ²]
	phase-I	phase-II		
$^{226}\text{Ra to } ^{210}\text{Pb (10nm)}$	$(2.8 \pm 0.2) \times 10^{-8}$		yes	$\mathcal{G}(1.49, 0.01) \cdot \text{Bulk}$
$^{228}\text{Ra (10nm)}$	$(6.8 \pm 1.1) \times 10^{-9}$		yes	$\mathcal{G}(4.190, 0.008) \cdot \text{Bulk}$
$^{226}\text{Ra to } ^{210}\text{Pb (10}\mu\text{m)}$	$< 2.0 \times 10^{-9}$		yes	Uniform
$^{228}\text{Ra (10}\mu\text{m)}$	$(2.8 \pm 1.5) \times 10^{-9}$		yes	Uniform
$^{210}\text{Pb (1nm)}$	$(3.39 \pm 0.08) \times 10^{-8}$	$(1.39 \pm 0.03) \times 10^{-7}$	no	Uniform

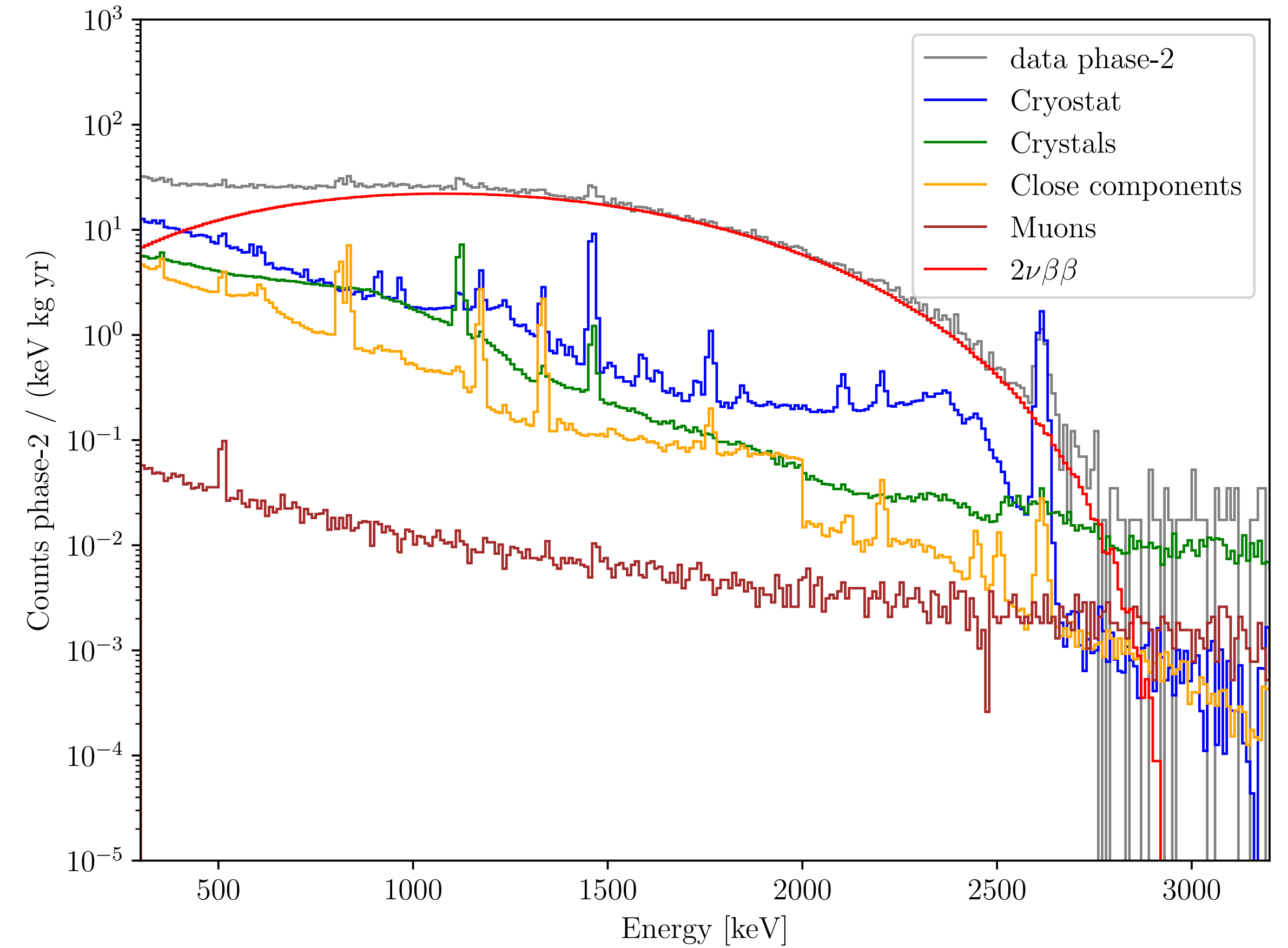
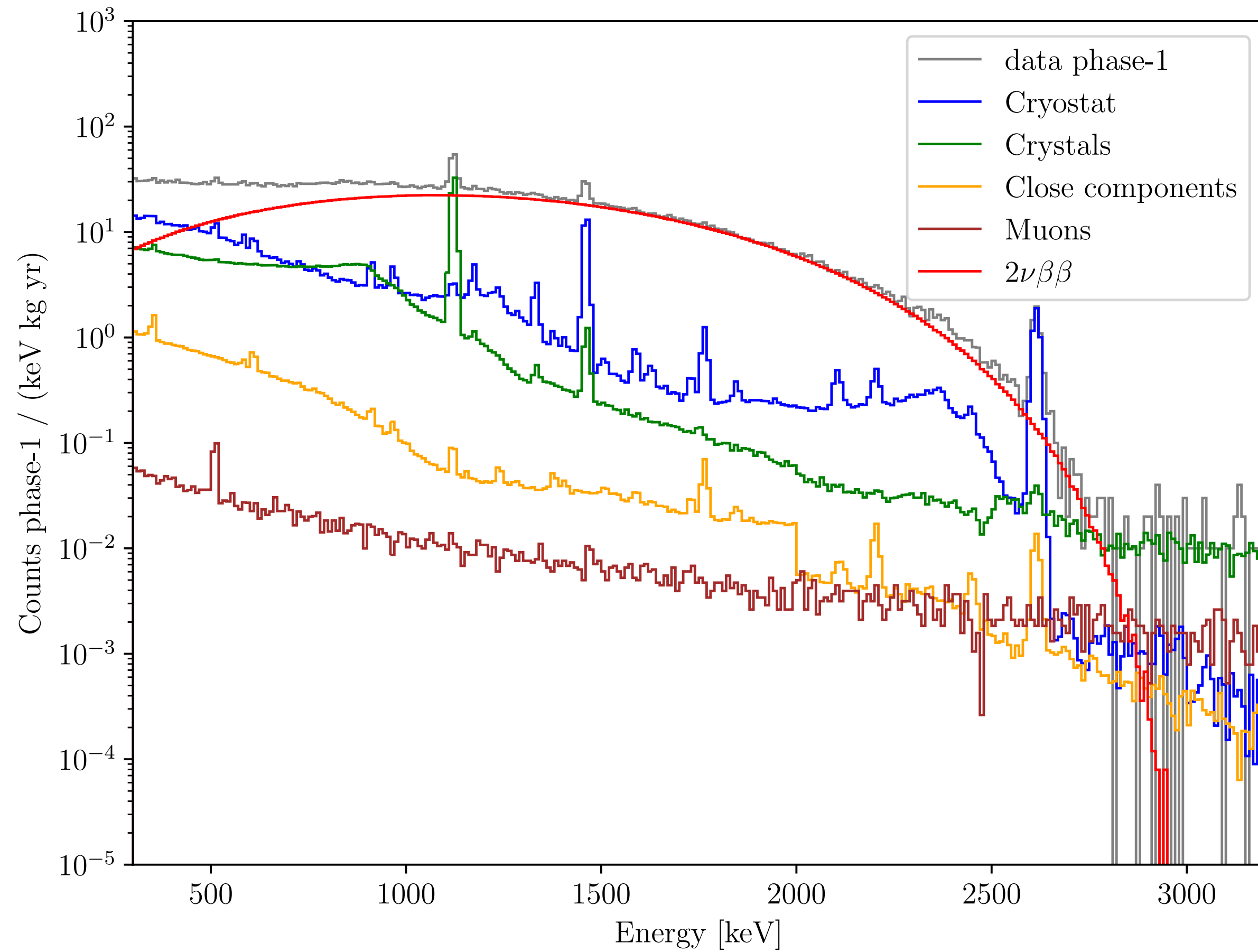
CUPID-0 close components contaminations

Bulk source	Volume	Specific Activity [Bq/kg]		Constrained	Prior [Bq/kg]
		phase-I	phase-II		
^{54}Mn	<i>Holders</i>	$(3.7 \pm 0.5) \times 10^{-4}$	-	-	Uniform
^{54}Mn	<i>10mK</i>	-	$(6.3 \pm 0.6) \times 10^{-5}$	-	Uniform
^{58}Co	<i>10mK</i>	-	$(5.7 \pm 0.6) \times 10^{-5}$	-	Uniform
^{60}Co	<i>10mK</i>	-	$(4.5 \pm 2.4) \times 10^{-5}$	-	Uniform
Surface source	Volume	Specific Activity [Bq/cm ²]		Constrained	Prior [Bq/cm ²]
		phase-I	phase-II		
$^{232}\text{Th}(10\mu\text{m})$	<i>Holders</i>	$(5.2 \pm 0.2) \times 10^{-9}$		yes	$\mathcal{G}(5.0, 0.2) \times 10^{-9}$
$^{238}\text{U}(10\mu\text{m})$	<i>Holders</i>	$(1.3 \pm 0.2) \times 10^{-8}$		yes	$\mathcal{G}(1.4, 0.2) \times 10^{-8}$
$^{232}\text{Th}(10\mu\text{m})$	<i>Reflectors</i>	$< 7.7 \times 10^{-10}$	-	-	Uniform
$^{238}\text{U}(10\mu\text{m})$	<i>Reflectors</i>	$< 2.7 \times 10^{-9}$	-	-	Uniform
$^{210}\text{Pb}(10\mu\text{m})$	<i>Reflectors</i>	$(1.9 \pm 0.5) \times 10^{-8}$	-	-	Uniform
$^{210}\text{Pb}(10\text{nm})$	<i>Reflectors</i>	$(8.1 \pm 0.3) \times 10^{-8}$	-	-	Uniform
$^{232}\text{Th}(10\mu\text{m})$	<i>10mK</i>	-	$< 2.2 \times 10^{-8}$	-	Uniform
$^{238}\text{U}(10\mu\text{m})$	<i>10mK</i>	-	$(6.1 \pm 1.8) \times 10^{-8}$	-	Uniform
$^{210}\text{Pb}(10\mu\text{m})$	<i>10mK</i>	-	$(2.1 \pm 1.2) \times 10^{-7}$	-	Uniform
$^{210}\text{Pb}(10\text{nm})$	<i>10mK</i>	-	$(5.5 \pm 0.2) \times 10^{-7}$	-	Uniform
$^{210}\text{Pb}(1\mu\text{m})$	<i>10mK</i>	-	$(1.7 \pm 0.2) \times 10^{-7}$	-	Uniform

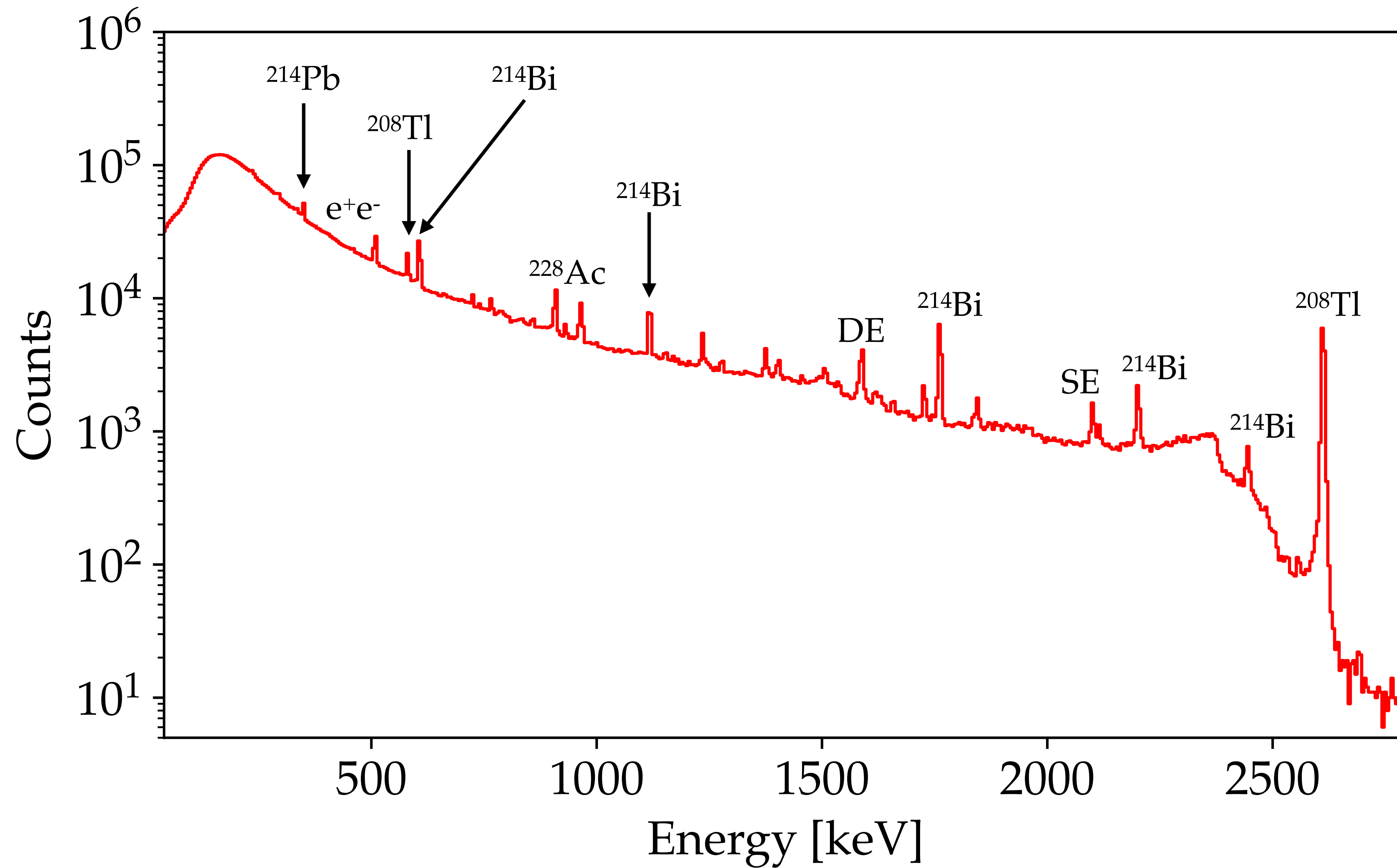
CUPID-0 cryostat contaminations

Bulk source	Volume	Specific Activity [Bq/kg]		Constrained	Prior [Bq/kg]
		phase-I	phase-II		
^{232}Th	<i>CryoInt</i>	$(4.5 \pm 2.6) \times 10^{-4}$		yes	Uniform
^{238}U	<i>CryoInt</i>	$(4.4 \pm 2.1) \times 10^{-4}$		yes	Uniform
^{40}K	<i>CryoInt</i>	$(2.7 \pm 0.7) \times 10^{-3}$	$(4.1 \pm 0.5) \times 10^{-3}$	no	Uniform
^{60}Co	<i>CryoInt</i>	$(7.4 \pm 1.4) \times 10^{-5}$	$(8.9 \pm 5.6) \times 10^{-5}$	no	Uniform
^{232}Th	<i>CryoExt+ExtPb</i>	$(3.8 \pm 0.6) \times 10^{-4}$		yes	Uniform
^{238}U	<i>CryoExt+ExtPb</i>	$(4.6 \pm 0.9) \times 10^{-4}$		yes	Uniform
^{40}K	<i>CryoExt+ExtPb</i>	$(3.8 \pm 0.8) \times 10^{-3}$	$< 1.3 \times 10^{-3}$	no	Uniform
^{210}Pb	<i>ExtPb</i>	(8.0 ± 0.3)		yes	Uniform
^{60}Co	<i>CryoExt</i>	$(3.0 \pm 0.8) \times 10^{-5}$	$< 6.5 \times 10^{-5}$	no	$\mathcal{G}(2.5, 0.9) \times 10^{-5}$
^{232}Th	<i>IntPb</i>	$(3.2 \pm 2.2) \times 10^{-5}$		yes	Uniform
^{238}U	<i>IntPb</i>	$< 3.7 \times 10^{-5}$		yes	Uniform

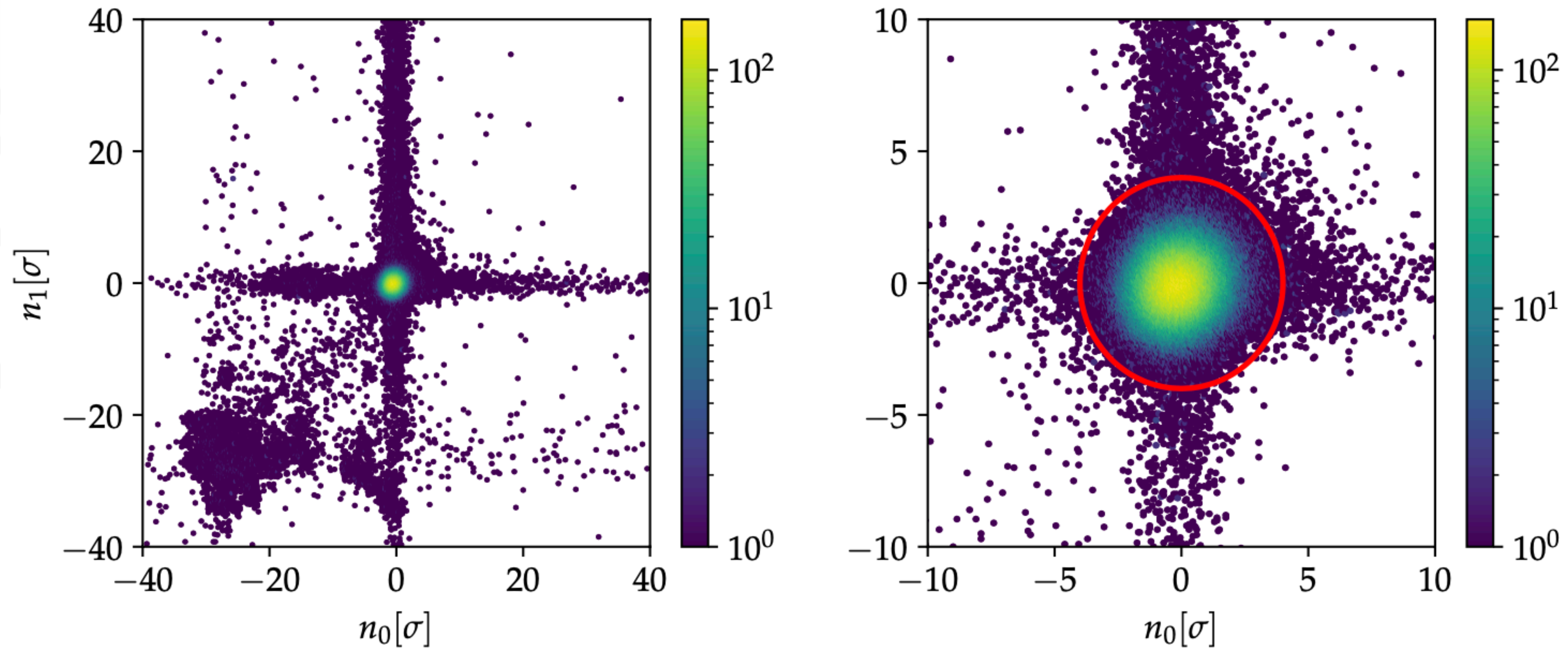
Background model - reconstruction



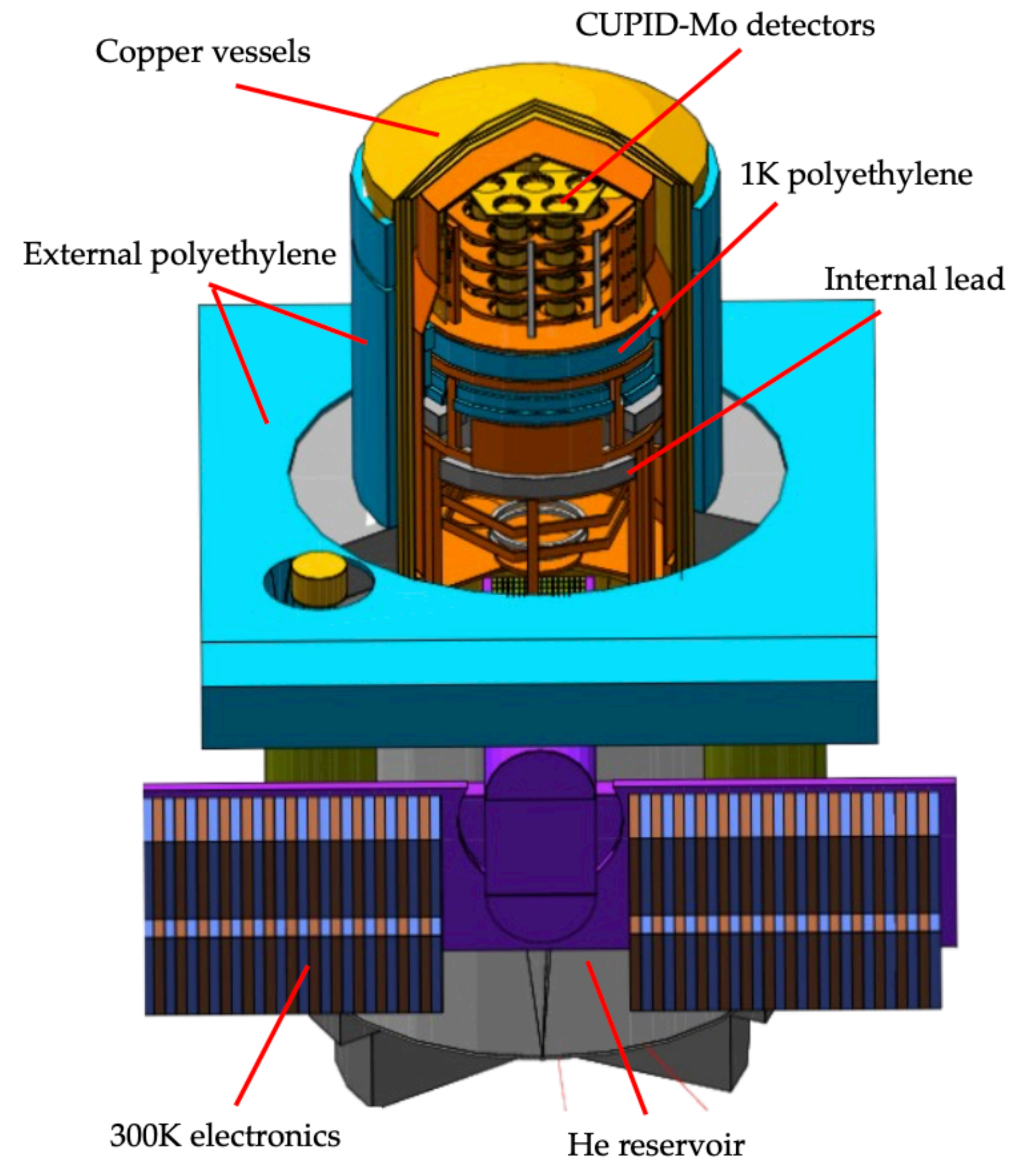
CUPID-Mo calibration spectrum



CUPID-Mo particle identification



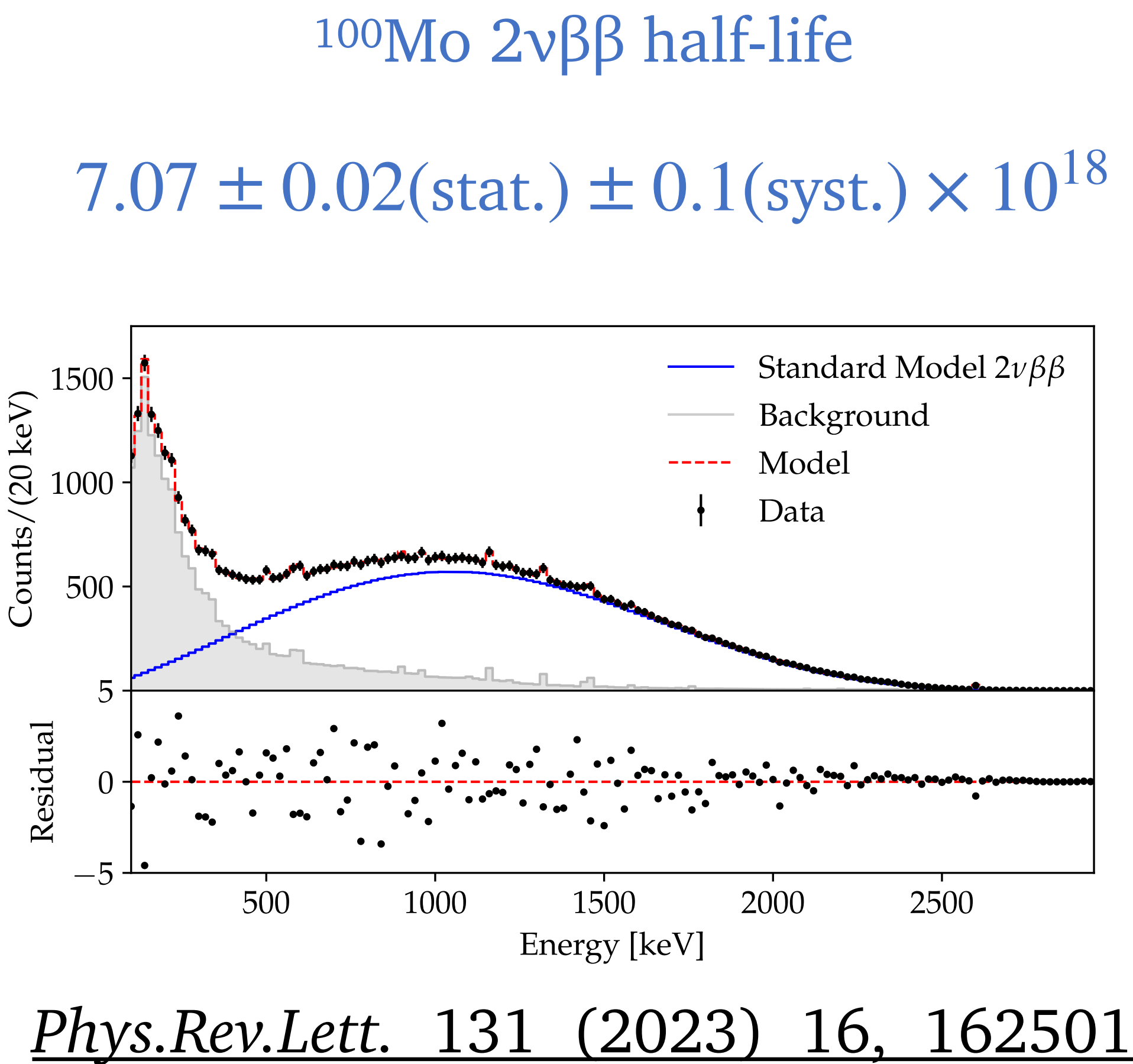
CUPID-Mo simulations



Measurement of ^{100}Mo $2\nu\beta\beta$ spectral shape

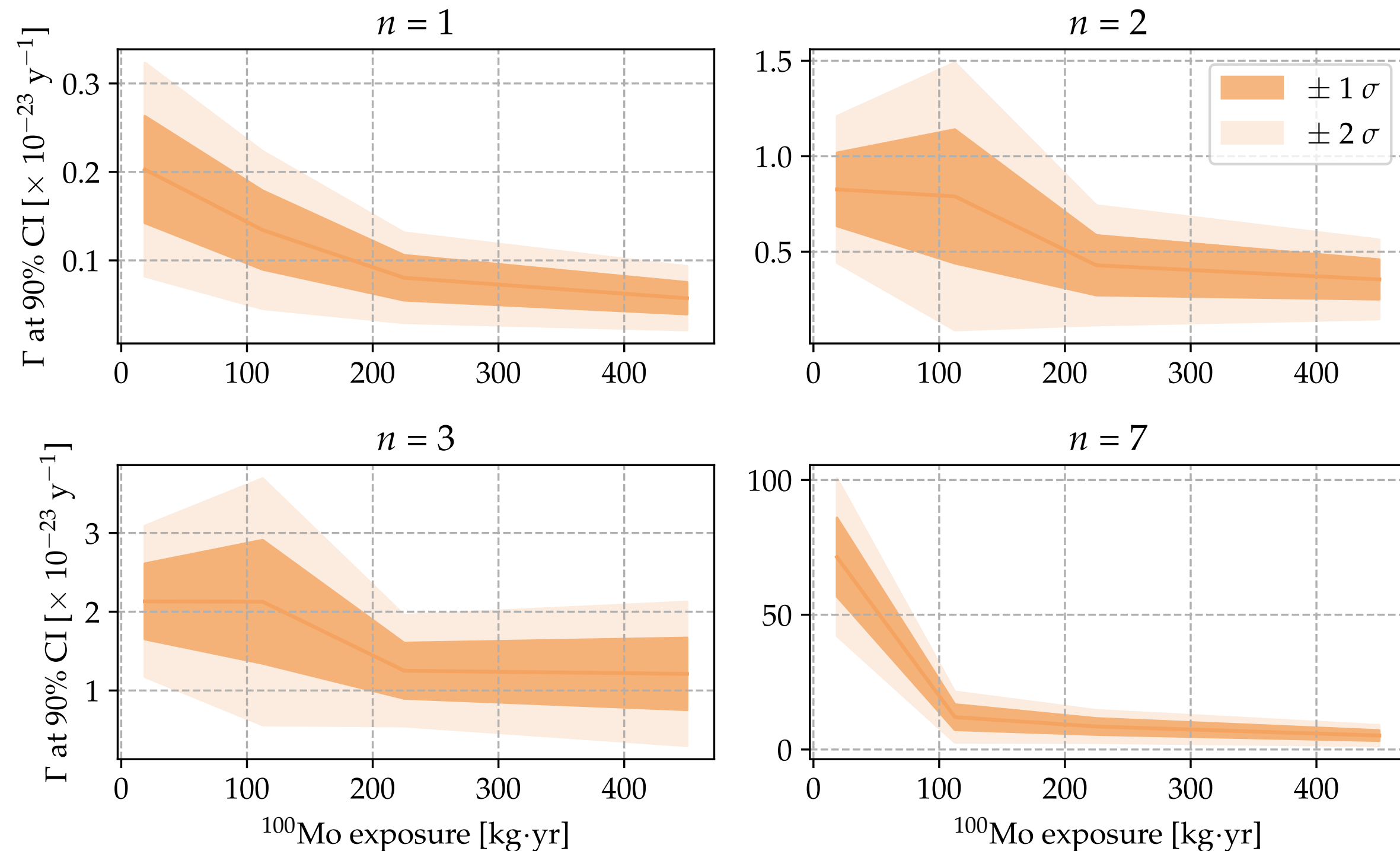
- ❖ The model of the spectral shape has been implemented in the background model fit and the value of $\xi_{31}^{2\nu}$ is kept as free parameter
- ❖ **First measurement** of the $\xi_{31}^{2\nu}$ parameter compatible with the SSD prediction:
 $\xi_{31}^{2\nu} = 0.45 \pm 0.03(\text{stat.}) \pm 0.05(\text{syst.})$

Systematic test	Uncert. $T_{1/2}[\%]$	Uncert. $\xi_{3,1} [\%]$
Source location	0.83	0.9
$^{90}\text{Sr}+^{90}\text{Y}$	$+1.0^a$	-4.9^a
Minimal model	0.24	7.7
Binning	0.37	1.4
Energy bias	$+0.11$ -0.16	$+3.5$ -3.7
Bremsstrahlung	$+0.13$ -0.22	$+6.0$ -6.8
MC statistics	0.11	1.4
Efficiency	1.2	-
Isotopic abundance	0.2	-

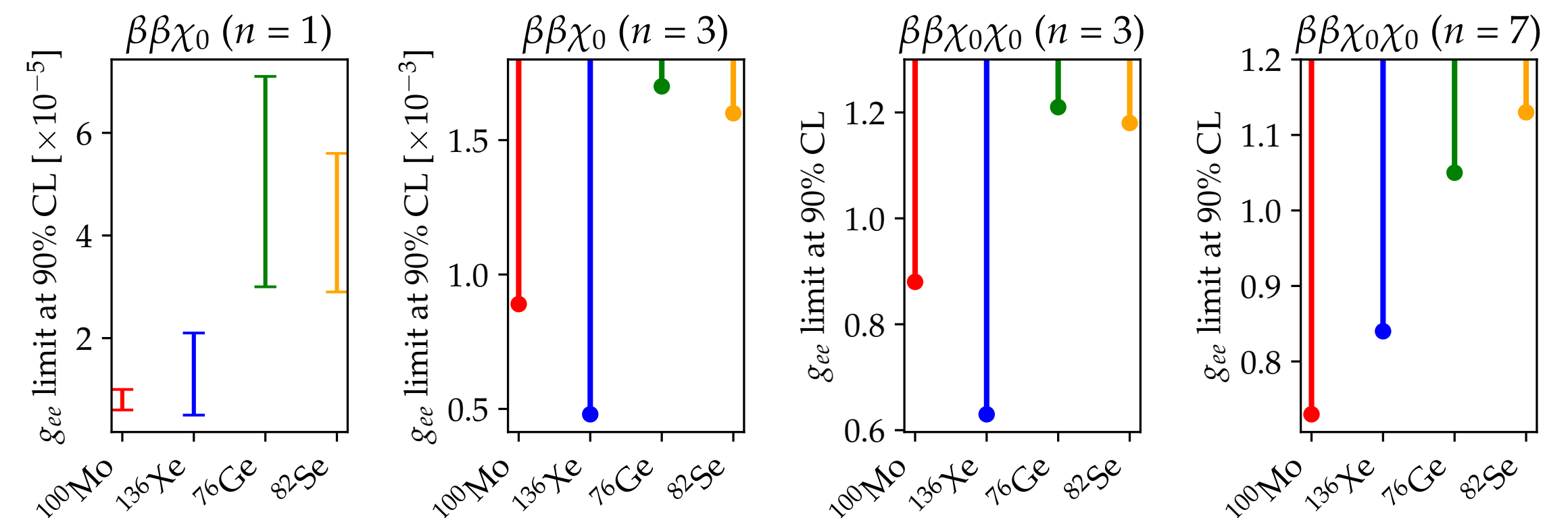


Sensitivity: Majoron decays

- ❖ Exposure scan corresponding to 1 month, 6 months, 1 year and 2 years of data taking (about 19, 112, 225, and 450 kg·yr of ^{100}Mo)
- ❖ With 450 kg·yr of ^{100}Mo the CUPID median exclusion sensitivity on the neutrino-Majoron coupling will be competitive with the limits obtained with ^{136}Xe



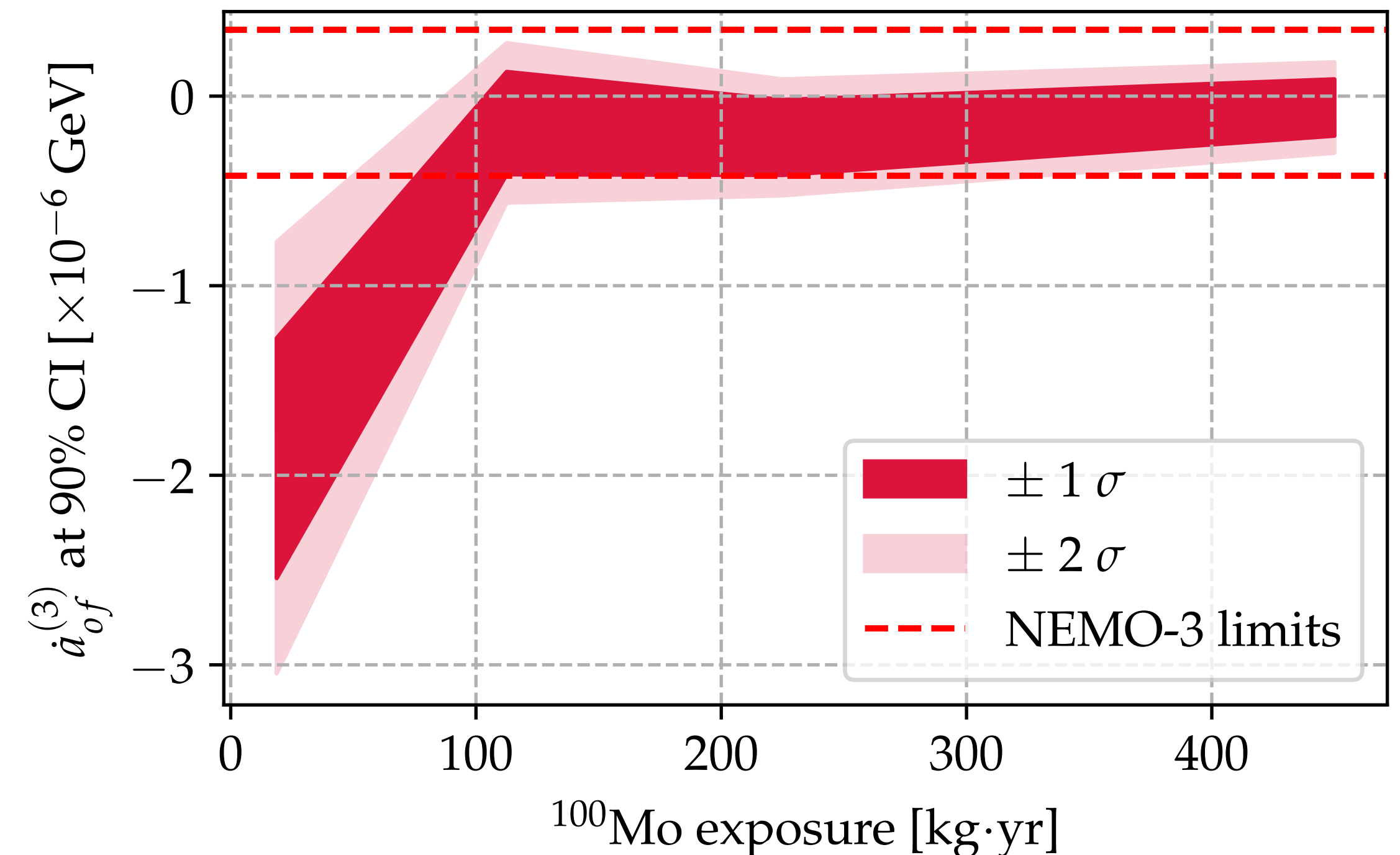
Decay mode	CUPID exclusion sensitivity		NEMO-3 [46, 135]	
	$T_{1/2}$ [yr]	g_{ee}^M	$T_{1/2}$ [yr]	g_{ee}^M
$\beta\beta\chi_0$ ($n=1$)	1.2×10^{24}	$(0.6 - 1.0) \times 10^{-5}$	4.4×10^{22}	$(3.0 - 5.1) \times 10^{-5}$
$\beta\beta\chi_0$ ($n=2$)	2.0×10^{23}	-	9.9×10^{21}	-
$\beta\beta\chi_0$ ($n=3$)	7.5×10^{22}	0.0089	4.4×10^{21}	0.023
$\beta\beta\chi_0\chi_0$ ($n=3$)	7.5×10^{22}	0.88	4.4×10^{21}	1.42
$\beta\beta\chi_0\chi_0$ ($n=7$)	1.9×10^{22}	0.73	1.2×10^{21}	1.15



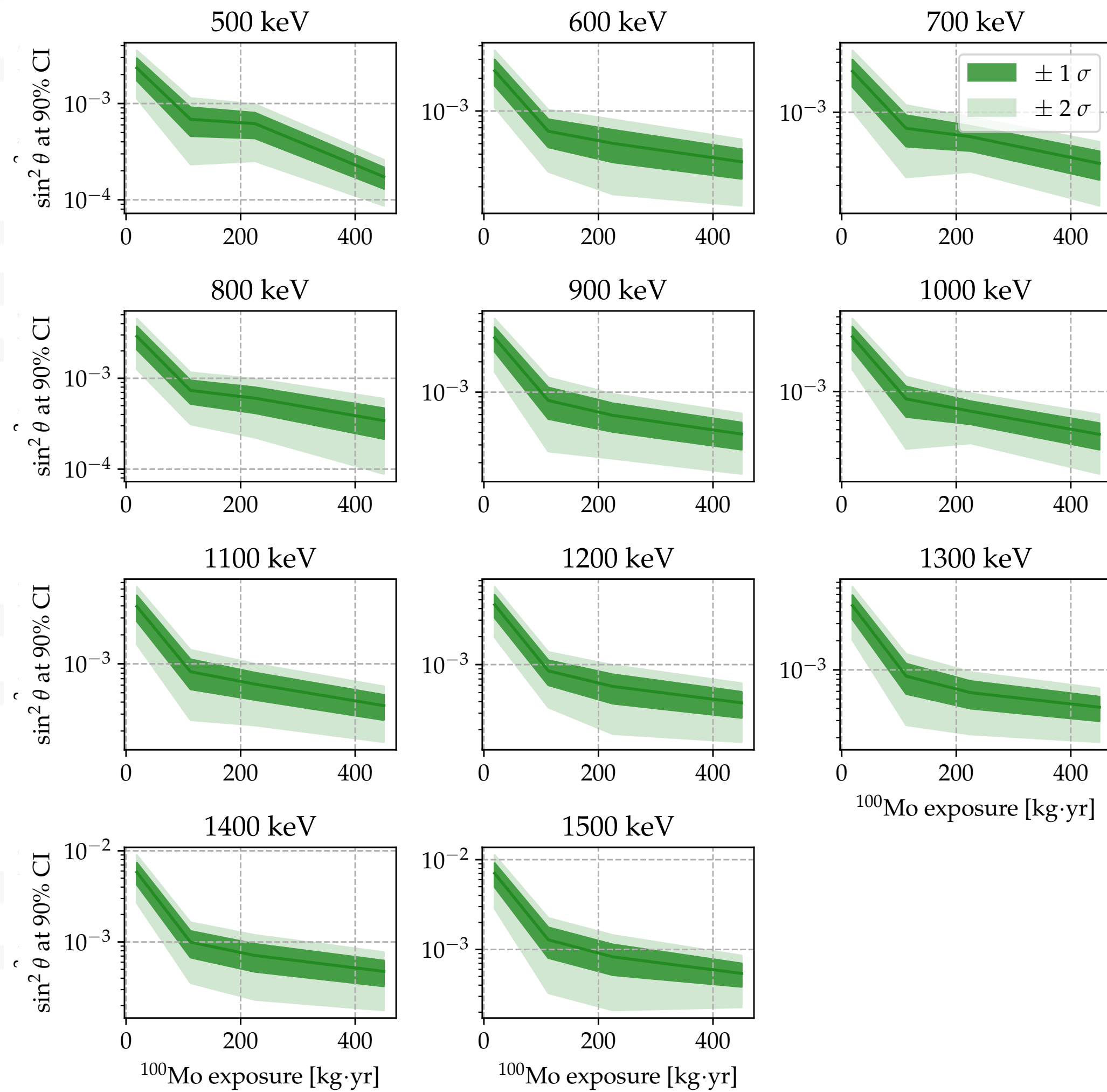
Sensitivity: Lorentz violation

- ❖ Negative fluctuations produce a bias when the background sources do not have enough statistic to be constrained in the fit.
- ❖ With 450 kg·yr of ^{100}Mo we expect to reach the most stringent limit on the countershaded operator among $0\nu\beta\beta$ experiments

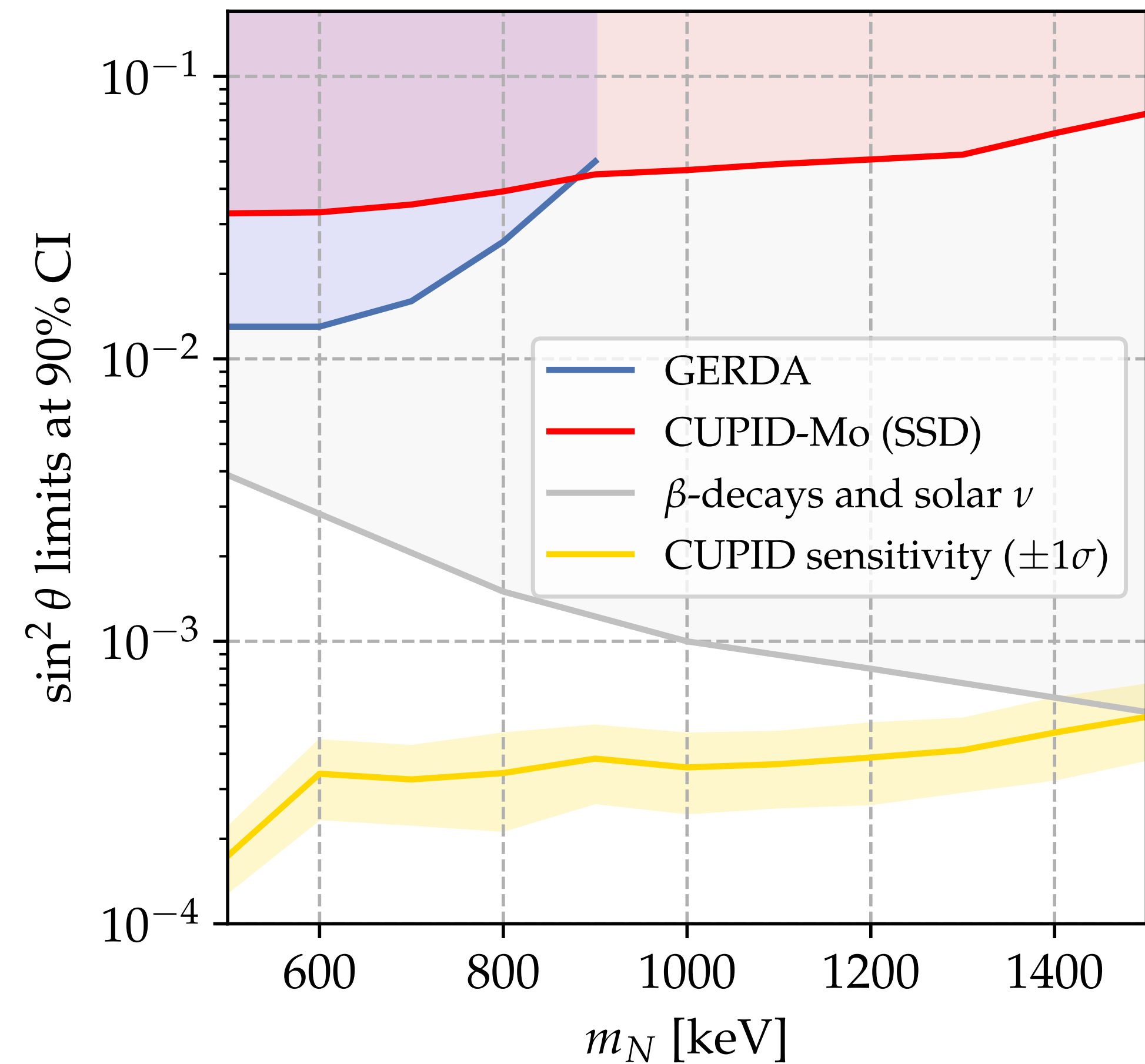
CUPID	$-2.2 \cdot 10^{-7} < \dot{a}_{of}^{(3)} < 7.5 \cdot 10^{-8}$
Isotope	Limit on $\dot{a}_{of}^{(3)}$ [GeV]
^{76}Ge	$(-2.7 < \dot{a}_{of}^{(3)} < 6.2) \cdot 10^{-6}$
^{82}Se	$\dot{a}_{of}^{(3)} < 4.1 \cdot 10^{-6}$
^{136}Xe	$-2.65 \cdot 10^{-5} < \dot{a}_{of}^{(3)} < 7.6 \cdot 10^{-6}$
^{116}Cd	$\dot{a}_{of}^{(3)} < 4.0 \cdot 10^{-6}$
^{100}Mo	$(-4.2 < \dot{a}_{of}^{(3)} < 3.5) \cdot 10^{-7}$
^3H	$ \dot{a}_{of}^{(3)} < 3.0 \cdot 10^{-8}$



Sensitivity: Sterile neutrino emission



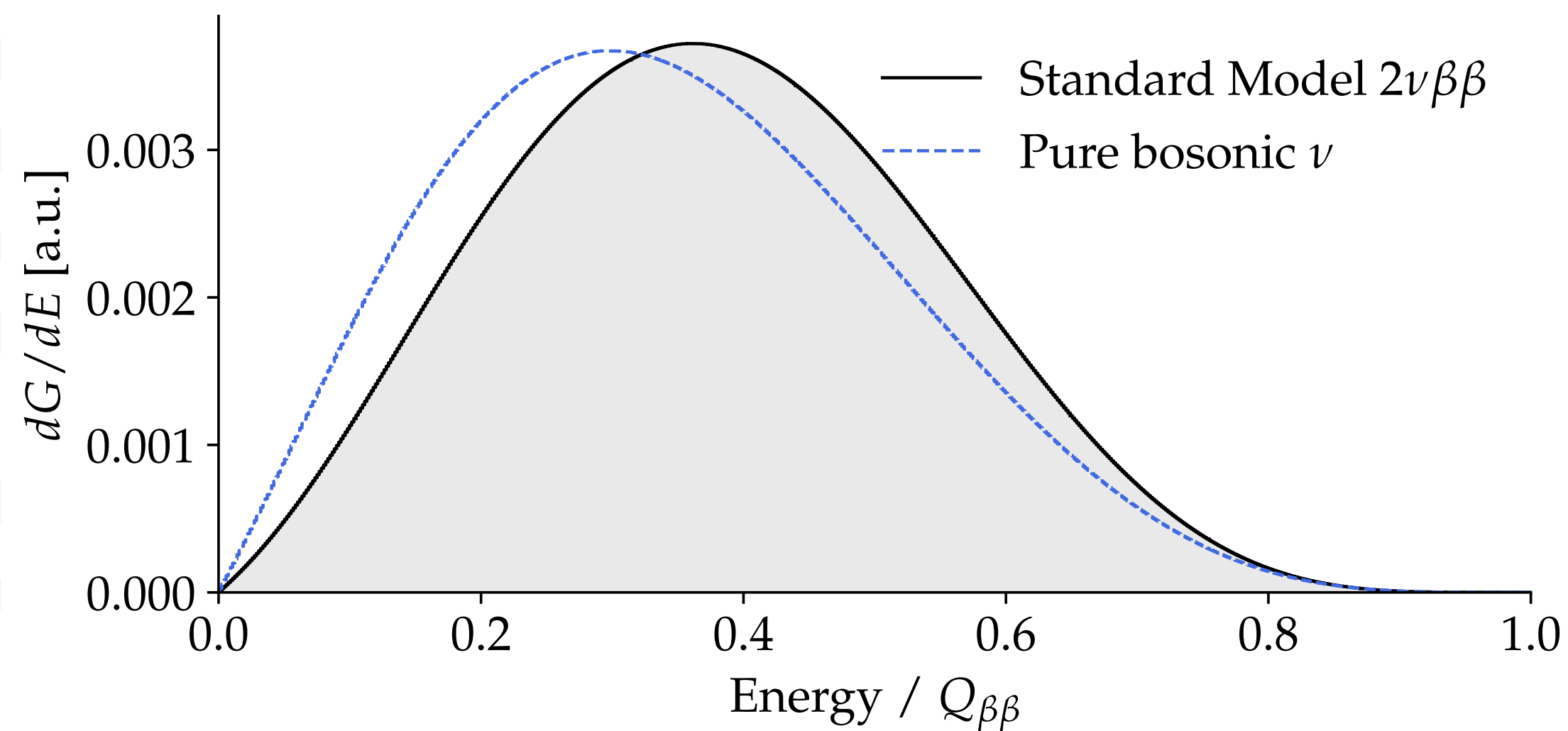
CUPID median exclusion sensitivity with 450 kg·yr of ^{100}Mo



Sensitivity: Bosonic neutrinos

$$\Gamma_{2\nu\beta\beta} = \cos^4 \chi \Gamma_f + \sin^4 \chi \Gamma_b$$

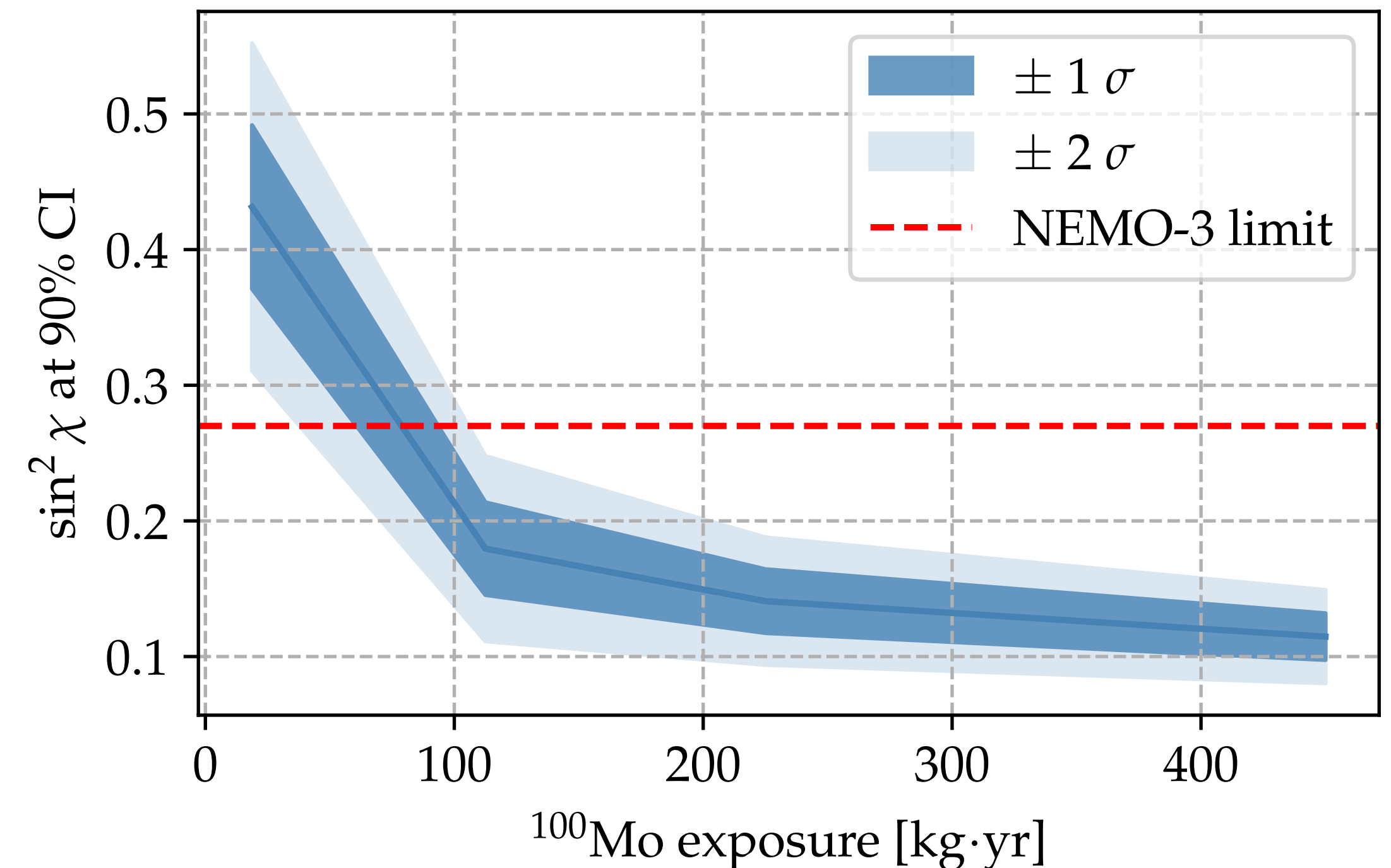
$\sin^4 \chi$ represents the bosonic fraction of the neutrino wave function, Γ_f and Γ_b are theoretically calculated (model dependent)



The actual limit from NEMO-3 is

$$\sin^2 \chi < 0.27$$

The mean exclusion sensitivity of CUPID with 450 kg·yr of ^{100}Mo is



Sensitivity: Bosonic neutrinos

$$\Gamma_{2\nu\beta\beta} = \cos^4 \chi \Gamma_f + \sin^4 \chi \Gamma_b$$

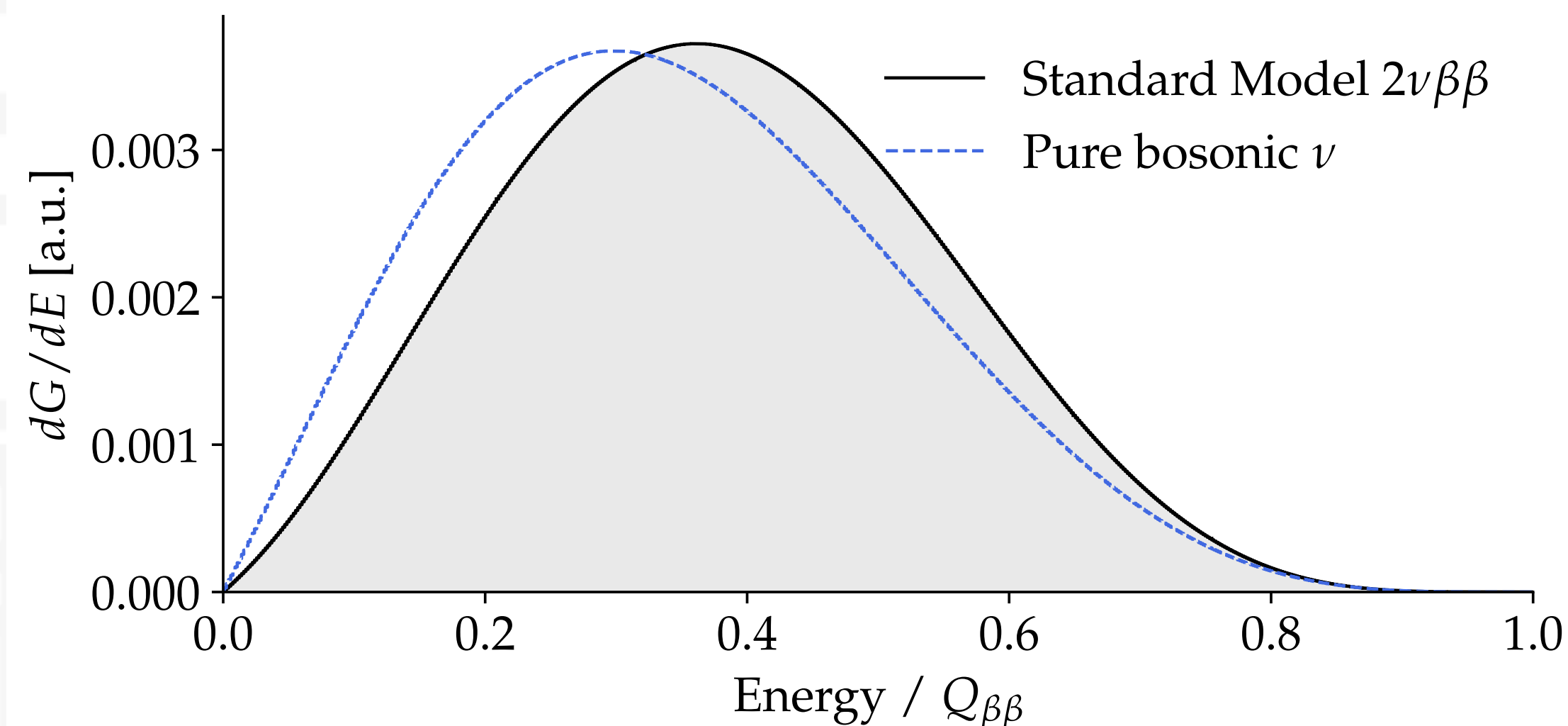
$\sin^4 \chi$ represents the bosonic fraction of the neutrino wave function, Γ_f and Γ_b are theoretically calculated (model dependent)

The actual limit from NEMO-3 is

$$\sin^2 \chi < 0.27 \text{ at 90\% CL}$$

The mean exclusion sensitivity of CUPID with 450 kg·yr of ^{100}Mo is

$$\sin^2 \chi < 0.11 \text{ at 90\% CI}$$



Background in the ROI for CUPID-Mo

- ❖ Radio purity of Li_2MoO_4 crystals sufficient to reach the goals of CUPID
- ❖ Higher contribution from cryostat copper components \rightarrow Cryostat not optimised for $0\nu\beta\beta$ searches

